



**Calhoun: The NPS Institutional Archive**  
**DSpace Repository**

---

Theses and Dissertations

1. Thesis and Dissertation Collection, all items

---

1973

## Performance analysis of digital radiometers.

Swett, Jorge Eduardo.

Monterey, California. Naval Postgraduate School

---

<http://hdl.handle.net/10945/16741>

---

*Downloaded from NPS Archive: Calhoun*



<http://www.nps.edu/library>

Calhoun is the Naval Postgraduate School's public access digital repository for research materials and institutional publications created by the NPS community. Calhoun is named for Professor of Mathematics Guy K. Calhoun, NPS's first appointed -- and published -- scholarly author.

**Dudley Knox Library / Naval Postgraduate School**  
**411 Dyer Road / 1 University Circle**  
**Monterey, California USA 93943**

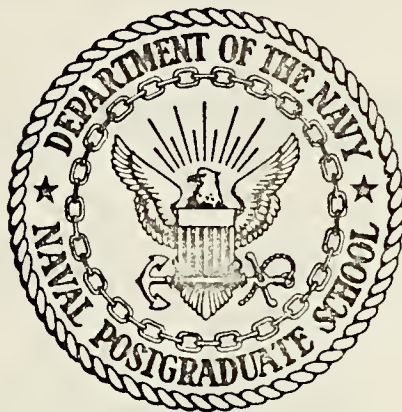
PERFORMANCE ANALYSIS OF  
DIGITAL RADIOMETERS

Jorge Eduardo Swett

Library  
Naval Postgraduate School  
Monterey, California 93940

# NAVAL POSTGRADUATE SCHOOL

Monterey, California



## THESIS

PERFORMANCE ANALYSIS  
OF  
DIGITAL RADIOMETERS

by

Jorge Eduardo Swett

Thesis Advisor:

J.E. Ohlson

March 1973

T 154583

*Approved for public release; distribution unlimited.*



Performance Analysis  
of  
Digital Radiometers

by

Jorge Eduardo Swett  
Lieutenant, Chilean Navy  
B.S., United States Naval Academy, 1966  
Ingeniero Naval Electronico, Academia  
Politecnica Naval, Chile, 1969

Submitted in partial fulfillment of the  
requirements for the degree of

ELECTRICAL ENGINEER

from the  
NAVAL POSTGRADUATE SCHOOL  
March 1973



### ABSTRACT

This work investigates the effects of digital processing in radiometers. It deals mainly with two digital versions of a total power radiometer. The first consists of RF, Mixer and IF sections followed by an analog to digital converter. All further processing is done in a digital computer. The second version consists of RF, Mixer and IF sections followed by a square law detector, RC filter and analog to digital converter. From this point on the processing is done by a digital computer. A figure of merit is defined based on the performance of an analog total power radiometer. Exact results are obtained for the figure of merit of the first digital version. For the second, an approximate solution is obtained. The effects of saturation and finite step size of the quantizer were taken into consideration for the above results. The performance of digital balanced-Dicke and noise-adding radiometers is investigated using the above results. The effects of digital filtering on the performance of a radiometer is considered.



## TABLE OF CONTENTS

I.	INTRODUCTION -----	8
II.	PERFORMANCE FIGURE OF A RADIOMETER. DEGRADATION FACTOR -----	12
III.	DEGRADATION FACTOR CALCULATION WITH NO QUANTIZER -----	17
	A. IF SAMPLING -----	17
	1. Ideal Filter -----	20
	2. Single Tuned Filter -----	23
	3. Gaussian Filter -----	25
	4. Butterworth Filter -----	26
	B. RC FILTERING THEN SAMPLING -----	28
IV.	TRANSFER CHARACTERISTICS OF A QUANTIZER WITH A ZERO MEAN GAUSSIAN INPUT PROCESS -----	31
	A. QUANTIZER ALONE -----	32
	B. QUANTIZER FOLLOWED BY SQUARE LAW DETECTOR -	46
V.	DEGRADATION FACTOR CALCULATION WITH A QUANTIZER -----	50
	A. IF SAMPLING -----	50
	1. Exact Solution -----	50
	a. Ideal Filter -----	56
	b. Single Tuned Filter -----	62
	c. Gaussian Filter -----	68
	d. Butterworth Filter -----	74
	2. An Approximation -----	54
	B. RC FILTERING AND THEN SAMPLING -----	84
	1. First Approximation -----	84



2. Second Approximation -----	102
VI. DYNAMIC RANGE AND LINEARITY OF A DIGITAL RADIOMETER -----	104
A. IF SAMPLING -----	104
B. RC FILTERING AND THEN SAMPLING -----	107
VII. APPLICATION TO SWITCHING RADIOMETERS -----	110
A. DICKE -----	110
B. NAR -----	113
VIII. DIGITAL FILTERING -----	119
IX. CONCLUSION -----	126
APPENDIX -----	128
LIST OF REFERENCES -----	154
INITIAL DISTRIBUTION LIST -----	156
FORM DD 1473 -----	157



## LIST OF FIGURES

### FIGURE

1	ANALOG TOTAL POWER RADIOMETER -----	9
2	IF SAMPLING DIGITAL TOTAL POWER RADIOMETER -----	10
3	RC FILTERING AND SAMPLING DIGITAL TOTAL POWER RADIOMETER -----	11
4	OUTPUT CHARACTERISTICS OF TYPICAL TOTAL POWER RADIOMETER -----	12
5	IDEAL BANDPASS FILTER CHARACTERISTICS -----	21
6	BLOCK DIAGRAM OF QUANTIZER AND QUANTIZER FOLLOWED BY SQUARE LAW DETECTOR -----	32
7	QUANTIZER CHARACTERISTICS -----	33
8 through 14	TRANSFER CHARACTERISTICS OF QUANTIZER -----	39
15	TRANSFER CHARACTERISTICS OF QUANTIZER FOLLOWED BY SQUARE LAW DETECTOR -----	49
16	CHANNEL OF IF SAMPLING TOTAL POWER RADIOMETER --	51
17	EXPECTED VALUE OF OUTPUT OF IF SAMPLING CASE ---	55
18 through 23	DEGRADATION FACTOR FOR IF SAMPLING CASE USING AN IDEAL BANDPASS INPUT FILTER -----	56
24 through 29	DEGRADATION FACTOR FOR IF SAMPLING CASE USING A SINGLE TUNED INPUT FILTER -----	62
30 through 35	DEGRADATION FACTOR FOR IF SAMPLING CASE USING A GAUSSIAN INPUT FILTER --	68
36 through 41	DEGRADATION FACTOR FOR IF SAMPLING CASE USING A BUTTERWORTH INPUT FILTER OF ORDER TWO -----	74
42	CHANNEL OF IF SAMPLING TOTAL POWER RADIOMETERS -	80
43	COMPARISON OF DEGRADATION FACTOR FOR IF SAMPLING CASE BETWEEN EXACT SOLUTION AND APPROXIMATION --	83



44	QUANTIZER CHARACTERISTICS -----	85
45	CHANNEL OF RC FILTERING AND SAMPLING CASE -----	86
46 through 51	DEGRADATION FACTOR FOR RC FILTERING AND SAMPLING. ZERO OFFSET -----	92
52	TRANSFER CHARACTERISTICS OF QUANTIZER WITH OFFSET -----	98
53	DEGRADATION FACTOR FOR RC FILTERING AND SAMPLING. QUANTIZER WITH OFFSET -----	99
54	COMPARISON OF DEGRADATION FACTOR FOR RC FILTERING AND SAMPLING FOR THE TWO APPROXIMATIONS USED -----	100
55	EXPECTED VALUE OF OUTPUT OF IF SAMPLING CASE ----	106
56	EXPECTED VALUE OF OUTPUT OF RC FILTERING AND SAMPLING CASE -----	108
57	DIGITAL BALANCED DICKE RADIOMETER, IF SAMPLING CASE -----	111
58	DIGITAL BALANCED DICKE RADIOMETER, RC FILTERING AND SAMPLING CASE -----	112
59	DIGITAL NAR, IF SAMPLING CASE -----	115
60	DIGITAL NAR, RC FILTERING AND SAMPLING CASE -----	116
61	EXPECTED VALUE OF OUTPUT, DIGITAL NAR, IF SAMPLING CASE -----	118
62	BLOCK DIAGRAM OF DIGITAL FILTER -----	120



### ACKNOWLEDGMENT

The author wishes to thank Professor John E. Ohlson of the Department of Electrical Engineering of the U.S. Naval Postgraduate School for his constant support, valuable ideas, comments and corrections made throughout this thesis.

To my wife and children, for their understanding and patience, I am deeply grateful.



## I. INTRODUCTION

A radiometer is basically a highly sensitive and stable noise receiver. The principle of operation lies in the fact that any object at temperatures above absolute zero radiates energy in the form of electromagnetic waves. Until some years ago, radiometers were used mainly as radio telescope receivers and constituted the main tool of Radio Astronomy [Ref. 1]. Lately, their use has expanded to many other areas. The measurement of atmospheric temperature [Refs. 2 and 3], detection of air turbulence in the Troposphere [Ref. 4], airborne mapping [Ref. 5], the measurement of absolute radiation from a projectile flow field [Ref. 6], and passive detection [Ref. 7] can be cited as examples.

The type of processing involved in a radiometer is especially fitted to digital methods. A number of institutions have integrated the radiometer with the digital computer in their applications. The purpose of this work is to investigate the effects of this integration, and to provide guidelines to the design of digital radiometers.

The main body of the investigation will deal with two digital versions of a total power radiometer (TPR) shown in Figure 1. The first one (Figure 2) consists of RF, Mixer, and IF sections, followed by an Analog to Digital Converter (ADC) section. All further processing is done in a digital computer. The second one (Figure 3) consists of RF, Mixer,



and IF sections followed by a square law detector, a low pass filter, and an ADC. From that point on, the processing is done by a digital computer.

The main difference of the two cases is the location of the ADC. The second version (Figure 3) is presently being used and its main advantages over the first version (Figure 2) is that it requires a much lower sampling rate.

The results obtained for a total power digital radiometer can be used to determine performance of other types of radiometers. Performance of digital Dicke and noise-adding radiometers will be considered.

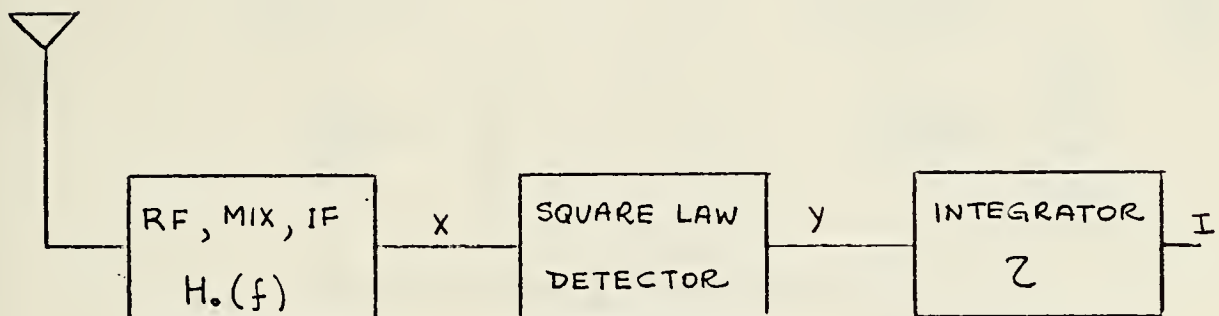


FIGURE 1



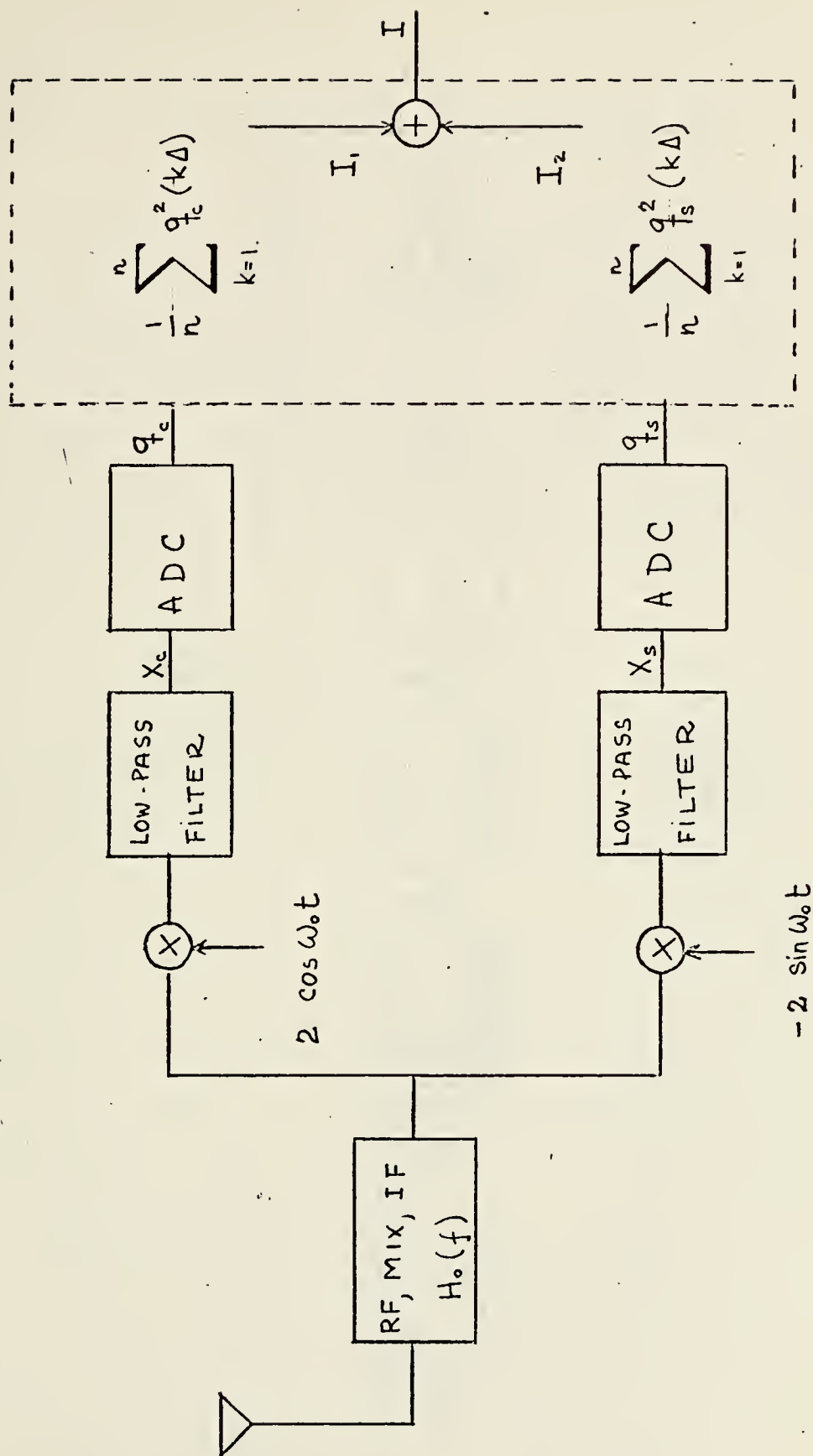


FIGURE 2



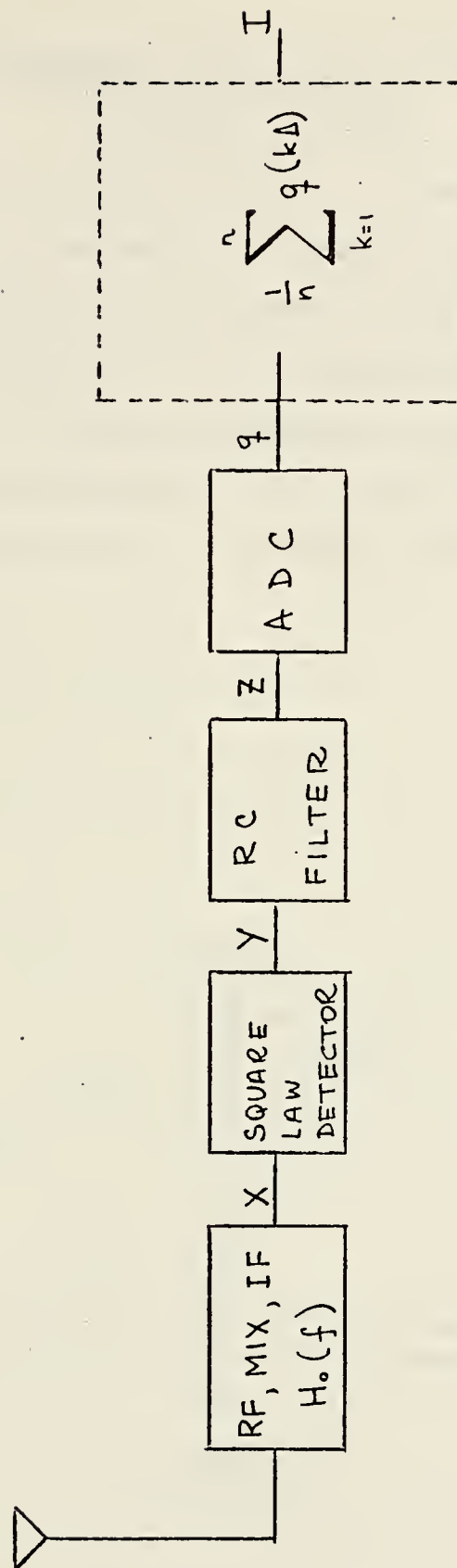


FIGURE 3



## II. PERFORMANCE FIGURE OF A RADIOMETER. DEGRADATION FACTOR

By definition, the sensitivity, or minimum detectable temperature, of a radiometer is taken as that change in operating temperature  $T$  that causes a change in the expected value of the output equal to one standard deviation of the output [Ref. 1]. Refer to Figure 4. It shows the expected value and the standard deviation of the output voltage as functions of temperature for a typical radiometer.

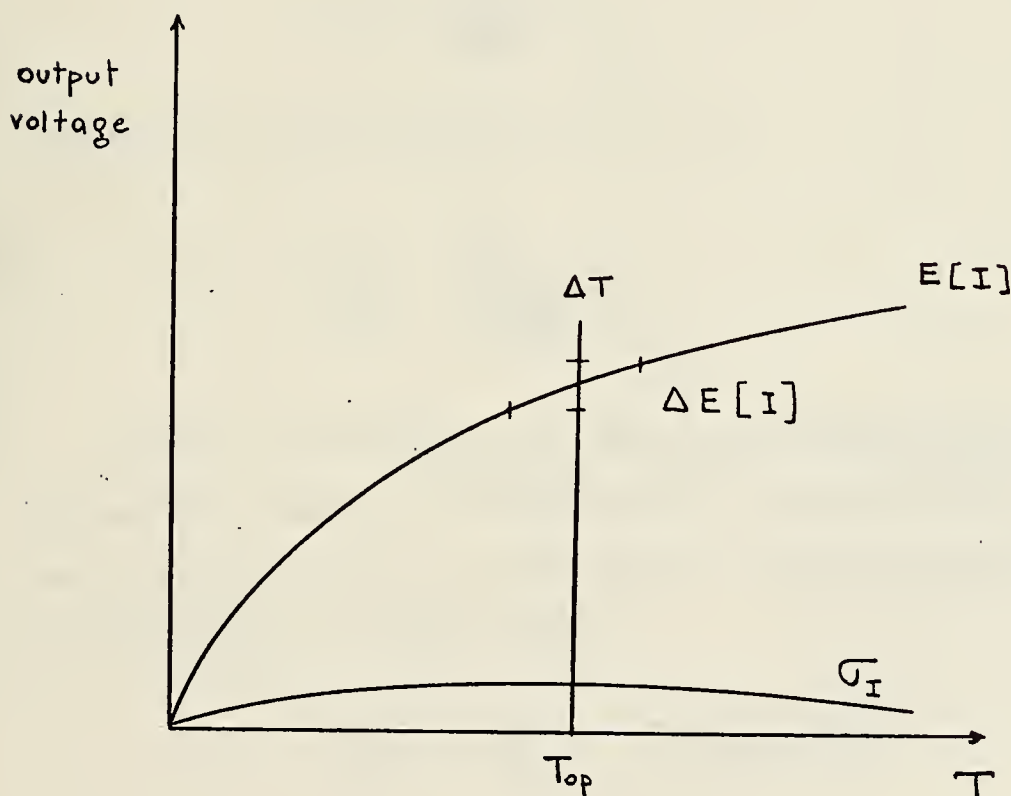


FIGURE 4



From Figure 4, it follows that (to first order)

$$\Delta E[I] = \left. \frac{dE[I]}{dT} \right|_{T_{op}} \cdot \Delta T \quad (1)$$

where  $E[\cdot]$  = Expected value of  $[\cdot]$ , and  $T_{op}$  is operating temperature. But by definition

$$\Delta E[I] = \sigma_I \Big|_{T_{op}} = \left. \frac{dE[I]}{dT} \right|_{T_{op}} \quad (2)$$

Therefore

$$\Delta T = \left. \frac{\sigma_I}{\frac{dE[I]}{dT}} \right|_{T_{op}} \quad (3)$$

A performance figure can be defined as,

$$\frac{\Delta T}{T_{op}} = \left. \frac{\frac{\sigma_I}{T_{op}}}{\frac{dE[I]}{dT}} \right|_{T_{op}} \quad (4)$$

It can be shown [Ref. 1] that for an analog total power radiometer (Figure 1), using the fact that the inverse of the integration time is much smaller than the bandwidth of the RF, Mixer, IF filter, that

$$E[I] = \tau k T_{op} \int_{-\infty}^{\infty} |H_o(f)|^2 df \quad (5)$$

$$\sigma_I^2 = 2 \tau k^2 T_{op}^2 \int_{-\infty}^{\infty} |H_o(f)|^4 df \quad (6)$$



where

$\tau$  = Integration time

$H_o(f)$  = Band-pass filter (RF,Mix,IF) frequency response

$k$  = Boltzmann's constant

Substituting into (4)

$$\frac{\Delta T}{T_{op}} = \frac{1}{(B_E \tau)^{\frac{1}{2}}} \quad (7)$$

where

$$B_E = \frac{\left( \int_0^{\infty} |H_o(f)|^2 df \right)^2}{\int_0^{\infty} |H_o(f)|^4 df} \quad (8)$$

The performance figure of the analog TPR, (7), will be used as a basis for evaluating the performance of a digital TPR. Hence, the Degradation Factor can be defined as

$$F = \frac{\text{Performance figure of Digital Radiometer}}{\text{Performance figure of Analog Radiometer}}$$

Intuitively,  $F$  should be equal or greater than one since as the sampling rate of the ADC goes to infinity and the step size of the quantizer goes to zero, both digital radiometers are reduced to an analog TPR.

Some comments are appropriate at this point. First, (5) and (6) show that for analog radiometers  $E[I]$  and  $\sigma_I$



are linear functions of temperature and go through the origin. Hence equation (4) reduces to

$$\frac{\Delta T}{T_{op}} = \frac{\sigma_I}{E[I]} \quad (9)$$

The addition of a quantizer, due to saturation, makes  $E[I]$  and  $\sigma_I$  nonlinear with respect to temperature, and the performance figure is thus temperature dependent. Therefore (4) must be used instead of the better-known (7). Secondly, the parameter  $T_{op}$  in equation (4) is not a convenient choice, since for a given  $T_{op}$ , different gain settings of the RF, Mixer, IF filter will change the performance of the radiometer. Referring to Figures 2 and 3 it is easily shown that

$$T = \alpha \sigma_{X_c}^2 \quad (\text{Figure 2}) \quad (10)$$

$$T = \beta \sigma_Z \quad (\text{Figure 3}) \quad (11)$$

where  $\alpha$  and  $\beta$  are proportionality constants. Using the parameters  $\sigma_{X_c}^2$  or  $\sigma_Z$  as appropriate, instead of  $T$ , normalizes the problem of gain setting out of the performance figure.



Then, for the radiometer of Figure 2

$$\frac{\Delta T}{T_{op}} = \frac{\frac{\sigma_I}{\sigma_{X_c}^2}}{\frac{dE[I]}{d\sigma_{X_c}^2}} \bigg|_{\sigma_{X_c}^2 \text{ at } T_{op}} \quad (12)$$

and for the radiometer of Figure 3

$$\frac{\Delta T}{T_{op}} = \frac{\frac{\sigma_I}{\sigma_Z}}{\frac{dE[I]}{d\sigma_Z}} \bigg|_{\sigma_Z \text{ at } T_{op}} \quad (13)$$



### III. DEGRADATION FACTOR CALCULATION WITH NO QUANTIZER

An ADC performs two basic operations on a signal. One is sampling, and the other is amplitude quantization. In this chapter the effects of sampling alone are considered. Hence it is assumed that each sample can be represented without any error.

#### A. IF SAMPLING

Refer to Figure 2. Assume that at the antenna white gaussian noise is present with double-sided power spectral density  $N_0/2$  watts/hertz. Then  $X(t)$  is a Narrow Band Gaussian Process with known power spectral density, and can be represented as

$$X(t) = X_c(t)\cos 2\pi f_o t - X_s(t)\sin 2\pi f_o t \quad (14)$$

where  $X_s(t)$  and  $X_c(t)$  are baseband Gaussian processes and  $f_o$  is the IF center frequency of the radiometer. It can be shown [Ref. 8] that if  $X(t)$ ,  $X_c(t)$  and  $X_s(t)$  are to be wide sense stationary, then

$$R_{X_c}(\mu) = R_{X_s}(\mu) \quad (15)$$

$$R_X(\mu) = R_{X_c}(\mu)\cos 2\pi f_o \mu + R_{X_s X_c}(\mu)\sin 2\pi f_o \mu \quad (16)$$



where  $R_X(\mu)$  is the autocorrelation function of the process  $X(t)$  and  $R_{X_S X_c}(\mu)$  is the crosscorrelation function of the processes  $X_c(t)$  and  $X_s(t)$ .

Furthermore if  $H_o(f)$  is symmetrical about  $f_o$  (this is the only case considered in this work), then

$$R_{X_c X_s}(\mu) = 0 \quad (17)$$

and  $R_{X_c}(\mu)$  is given by

$$R_{X_c}(\mu) = 2 \int_0^{\infty} S_X(f) \cos[2\pi(f-f_o)\mu] df \quad (18)$$

and  $S_{X_c}(f)$ , the power spectral density of  $X_c(t)$ , is the Fourier Transform of equation (18).

Physically, for the case of interest (i.e.  $X(t)$ ,  $X_c(t)$  and  $X_s(t)$  wide sense stationary, and  $H_o(f)$  symmetrical about  $f_o$ ),  $S_{X_c}(f)$  is just twice the low pass version of  $S_X(f)$ . Referring to Figure 2, the low pass filters filter out the double-frequency terms coming out of the multipliers. Then

$$I = I_1 + I_2 \quad (19)$$

$$I_1 = \frac{1}{n} \sum_{k=1}^n X_c^2(k\Delta) \quad (20)$$

since  $X_c(k\Delta) = q_c(k\Delta)$  and



$$I_2 = \frac{1}{n} \sum_{k=1}^n X_s^2(k\Delta) \quad (21)$$

since  $X_s(k\Delta) = q_s(k\Delta)$ .

Using the fact that for Gaussian random variables

$$E[X_1 X_2 X_3 X_4] = E[X_1 X_2]E[X_3 X_4] + E[X_1 X_3]E[X_2 X_4] + E[X_1 X_4]E[X_2 X_3] \quad (22)$$

and expanding the double summation, it follows that

$$\sigma_{I_1}^2 = \frac{2\sigma_{X_c}^4}{n} + \frac{4}{n} \sum_{k=1}^{n-1} \left(1 - \frac{k}{n}\right) R_{X_c}^2(k\Delta) \quad (23)$$

and

$$E[I_1] = \sigma_{X_c}^2 \quad (24)$$

For the random variable  $I_2$  the same results are obtained since  $R_{X_c}(\mu) = R_{X_s}(\mu)$

Then

$$E[I_2] = \sigma_{X_c}^2 \quad (25)$$

and

$$\sigma_I^2 = \sigma_{I_1}^2 + \sigma_{I_2}^2 + 2E[I_1 I_2] - 2E[I_1]E[I_2] \quad (26)$$



Expanding  $E[I_1 I_2]$  and using the fact that  $R_{X_c X_s}(\mu) = 0$ , the last two terms of (26) cancel out.

Using equations (25) and (26) in (12) it follows that

$$\left(\frac{\Delta T}{T_{op}}\right)^2 = \frac{1}{n} + \frac{2}{n\sigma_{X_c}^2} \sum_{k=1}^{n-1} \left(1 - \frac{k}{n}\right) R_{X_c}^2(k\Delta) \quad (27)$$

or

$$\left(\frac{\Delta T}{T_{op}}\right)^2 = \frac{\Delta}{\tau} + \frac{2\Delta}{\tau\sigma_{X_c}^2} \sum_{k=1}^{n-1} \left(1 - \frac{k}{n}\right) R_{X_c}^2(k\Delta) \quad (28)$$

where

$$\tau = n\Delta \quad (29)$$

The degradation factor squared is

$$F^2 = B_E \Delta + \frac{2B_E \Delta}{\sigma_{X_c}^2} \sum_{k=1}^{n-1} \left(1 - \frac{k\Delta}{\tau}\right) R_{X_c}^2(k\Delta) \quad (30)$$

$R_{X_c}(\mu)$  is a function of  $H_o(f)$ , therefore (30) will be used with four different frequency characteristics.

### 1. Ideal Bandpass Filter

Refer to Figure 5

$$R_{X_c}(\mu) = \frac{N_o B \sin \pi B \mu}{\pi B \mu} \quad (31)$$



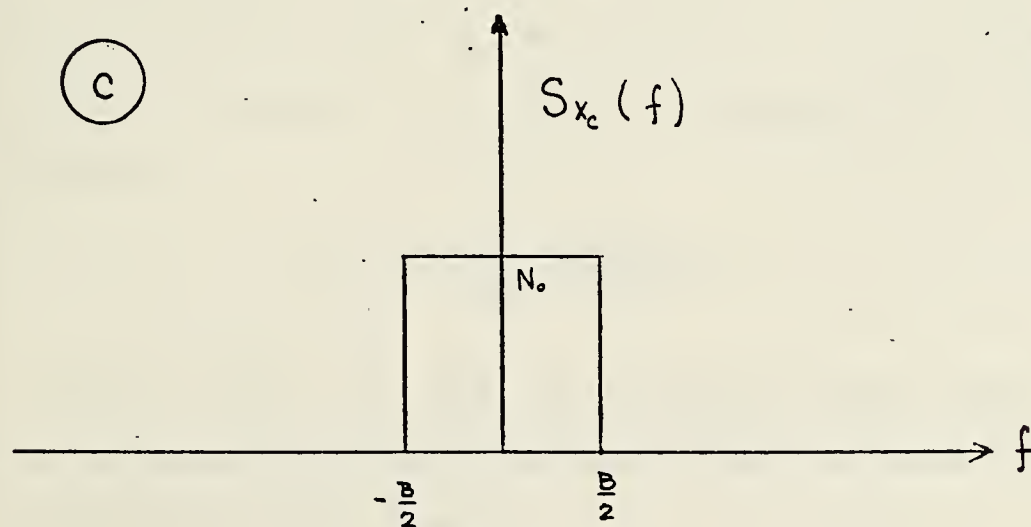
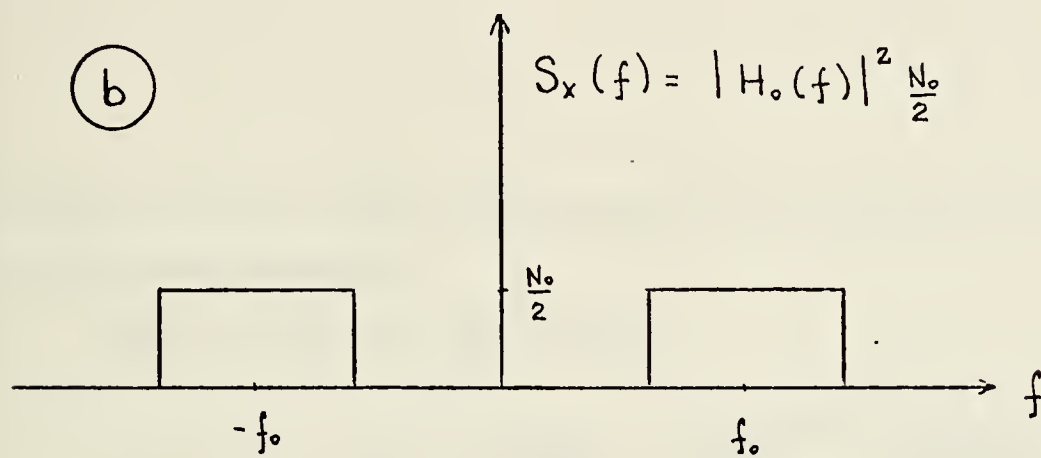
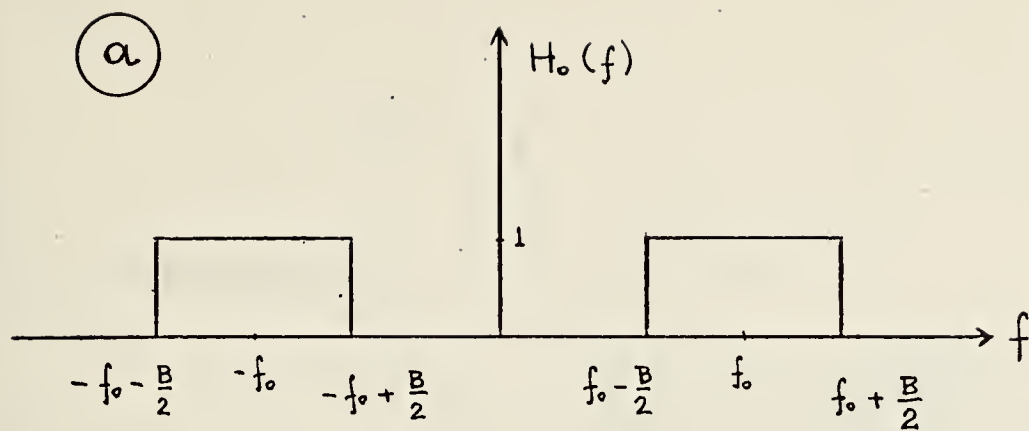


FIGURE 5



and

$$\sigma_{X_c}^2 = N_o B \quad (32)$$

Substituting (31) and (32) into (30)

$$F^2 = B_E \Delta + 2B_E \Delta \sum_{k=1}^{n-1} \left(1 - \frac{k\Delta}{\tau}\right) \frac{\sin^2 \pi k \Delta B}{(\pi k \Delta B)^2} \quad (33)$$

But

$$B_E = B = W \quad (34)$$

where  $B_E$  is the equivalent bandwidth from (8) and  $W$  is the half-power bandwidth.

Then (33) can be rewritten as

$$F^2 = W\Delta + 2W\Delta \sum_{k=1}^{n-1} \frac{\sin^2 \pi kW}{(\pi kW\Delta)^2} - \frac{2(W\Delta)^2}{\tau W} \sum_{k=1}^{n-1} \frac{k \sin^2 \pi kW}{(\pi kW\Delta)^2} \quad (35)$$

Since  $\tau \gg \Delta$ , it can be shown that the third term of (35) is much smaller than the second and thus can be ignored. Letting  $\Delta$  approach zero (sampling infinitely fast), (35) becomes

$$F^2 = 2W \int_0^{\tau} \frac{\sin^2 \pi Wt}{(\pi Wt)^2} dt \quad (36)$$

and then since  $\tau$  is large, the integral's upper limit can be replaced by infinity, and the integral reduces to one, giving the correct result.



Actually, by including the third term as  $\Delta$  goes to zero,  $F$  will be slightly less than one. The reason for this is that in calculating the performance figure of an analog TPR in (7) the fact that  $\frac{1}{T} \ll B$  was used to get (5) and (6). Had this fact not been used, as  $\Delta$  approached zero,  $F$  would approach one exactly.

$F$  will be plotted as a function of  $W\Delta$ . Hence, for this case the Nyquist sampling rate (twice the highest frequency) corresponds to  $W\Delta = 1$ .

The analysis done in this chapter is just a special case of the analysis that will be done in Chapter V, hence all results will be plotted in the figures of that chapter. The results obtained from (35) for an ideal bandpass filter are plotted in Figures 18 through 23. It is of interest to note that for  $W$  less than one (sampling faster than the Nyquist rate),  $F$  is exactly equal to one, an intuitively satisfying result.

## 2. Single Tuned Filter

For a Single Tuned Filter

$$|H_o(f)|^2 = \frac{1}{1 + 4\left(\frac{f+f_o}{W}\right)^2} + \frac{1}{1 + 4\left(\frac{f-f_o}{W}\right)^2} \quad (37)$$

where  $W$  is the half power bandwidth and  $W$  is much less than  $f_o$ . It follows that

$$S_X(f) = \frac{N_o}{2} |H_o(f)|^2 \quad (38)$$



and

$$S_{X_c}(f) = \frac{N_o}{1 + 4\left(\frac{f}{W}\right)^2} \quad (39)$$

From (39), using the Inverse Fourier Transform

$$R_{X_c}(\mu) = \frac{N_o W}{4} e^{-\pi W |\mu|} \quad (40)$$

and

$$\frac{\Delta T}{T_{op}} = \frac{\Delta}{\tau} + \frac{2\Delta}{\tau} \sum_{k=1}^{n-1} \left(1 - \frac{k\Delta}{\tau}\right) e^{-2\pi k W \Delta} \quad (41)$$

Equation (41) can be put in closed form by letting

$$A = e^{-2\pi W \Delta} \quad (42)$$

Using the fact that [Ref. 9]

$$\sum_{k=1}^{n-1} A^k = \frac{A - A^n}{1 - A} \quad (43)$$

and

$$\sum_{k=1}^{n-1} k A^k = \frac{A - n A^n + (n-1) A^{n+1}}{(1-A)^2} \quad (44)$$

and after some tedious but straightforward manipulations, it follows that

$$\left(\frac{\Delta T}{T_{op}}\right)^2 = \frac{\Delta}{\tau} (\coth \pi W \Delta) - \frac{\Delta^2}{2\tau} (\operatorname{cosech}^2 \pi W \Delta) (1 - e^{-2\pi W \tau}) \quad (45)$$

and

$$F^2 = \Delta B_E (\coth \pi W \Delta) - \frac{(\Delta B_E)^2}{2\tau B_E} (\operatorname{cosech}^2 \pi W \Delta) (1 - e^{-2\pi W \tau}) \quad (46)$$



It can be shown that the equivalent bandwidth of a single tuned filter is [Ref. 1]

$$B_E = \pi W \quad (47)$$

where  $W$  is the half-power bandwidth. Furthermore, since  $\tau \gg \Delta$ , the second term is negligible with respect to the first, hence

$$F^2 = \pi W \Delta (\coth \pi W \Delta) \quad (48)$$

To compare with the analog case, let  $\Delta$  go to zero. Then  $F$  would become one, which is the correct result. Figures 24 through 29 show the results obtained for this filter.

### 3. Gaussian Filter

For a Gaussian Filter

$$[H_0(f)]^2 = e^{-v(\frac{f-f_0}{W})^2} + e^{-v(\frac{f+f_0}{W})^2} \quad (49)$$

where  $v = 4 \ln 2 = 2.773$ ,  $W$  is the half-power bandwidth, and  $W$  is much less than  $f_0$ .

It follows that

$$S_{X_c}(f) = N_0 e^{-v(\frac{f}{W})^2} \quad (50)$$

and

$$R_{X_c}(\mu) = N_0 W \left(\frac{\pi}{v}\right)^{\frac{1}{2}} e^{-\frac{\pi^2}{v}(W\mu)^2} \quad (51)$$



Replacing equation (51) into (30) and using the fact that for this filter

$$B_E = \left(\frac{2\pi}{v}\right)^{\frac{1}{2}} W = 1.505 W \quad (52)$$

it follows that

$$F^2 = 1.505 W \Delta + 3.01 W \Delta \sum_{k=1}^{n-1} \left(1 - \frac{k\Delta}{\tau}\right) e^{-\frac{2}{v}(\pi k W \Delta)^2} \quad (53)$$

Using the same argument as before ( $\Delta \ll \tau$ ), (53) becomes

$$F^2 = 1.505 W \Delta + 3.01 W \sum_{k=1}^{n-1} e^{-\frac{2}{v}(\pi k W \Delta)^2} \quad (54)$$

To compare to the analog case let  $\Delta$  approach zero. Then (54) becomes

$$F^2 = 3.01 W \int_0^{\tau} e^{-\frac{2}{v}(\pi k W \Delta)^2} \quad (55)$$

and since  $\tau$  is large, the integral's upper limit can be replaced by infinity, and the integral reduces to one, as it should. The numerical results are plotted in Figures 30 through 35.

#### 4. Butterworth Filter

The last filter to be considered is a Butterworth Filter of order two. For this case

$$[H_o(f)]^2 = \frac{1}{1 + 16\left(\frac{f-f_o}{W}\right)^4} + \frac{1}{1 + 16\left(\frac{f-f_o}{W}\right)^4} \quad (56)$$

where  $W$  is the half-power bandwidth, and  $W$  is much less than  $f_o$ .



Then

$$S_{X_c}(f) = \frac{N_o}{1 + 16\left(\frac{f}{W}\right)^4} \quad (57)$$

and

$$R_{X_c}(\mu) = \frac{N_o \pi W}{2} e^{-|\mu| \frac{\pi W}{(2)^{\frac{1}{2}}}} \cos\left(\frac{|\mu| \pi W}{(2)} - \frac{\pi}{4}\right) \quad (58)$$

For this filter, it can be shown that

$$B_E = \frac{(2)^{\frac{1}{2}}}{3} \pi W = 1.48W \quad (59)$$

Substituting (58) and (59) into (30) it follows, after some effort that

$$F^2 = 1.48W\Delta + 2.96W\Delta \sum_{k=1}^{n-1} e^{-k\pi(2)^{\frac{1}{2}}W\Delta} [1 + \sin(k\pi(2)^{\frac{1}{2}}W\Delta)] \\ - \frac{2.96(\Delta W)^2}{\tau W} \sum_{k=1}^{n-1} k e^{-k\pi(2)^{\frac{1}{2}}W\Delta} [1 + \sin(k\pi(2)^{\frac{1}{2}}W\Delta)] \quad (60)$$

Again it can be argued that the third term is negligible, therefore

$$F^2 = 1.48W\Delta + 2.96W\Delta \sum_{k=1}^{n-1} e^{-k\pi(2)^{\frac{1}{2}}W\Delta} [1 + \sin(k\pi(2)^{\frac{1}{2}}W\Delta)] \quad (61)$$

Comparing to the analog case by letting  $\Delta$  approach zero, (61) becomes

$$F^2 = 2.96W\Delta \int_0^{\tau} e^{-\pi(2)^{\frac{1}{2}}Wt} [1 + \sin(\pi(2)^{\frac{1}{2}}Wt)] dt \quad (62)$$



Since  $\tau$  is large, the integral's upper limit can be replaced by infinity, and it reduces as it should to one.

The numerical results for this filter are plotted in Figures 36 through 41.

#### B. RC FILTERING AND THEN SAMPLING

Refer to Figure 3. This type of digital TPR was studied by Ohlson [Ref. 10] for the case where no quantizer is present. Only the results and its implications are presented here.

It can be shown that

$$E[Z] = g \frac{N_o}{2} \quad (63)$$

and

$$\sigma_Z^2 = g^2 \left(\frac{N_o}{2}\right)^2 \frac{1}{2B_E t_{RC}} \quad (64)$$

where  $g$  is a system gain parameter,  $N_o$  is as defined on page 17, and  $t_{RC}$  is the time constant of the RC filter.

Also

$$E[I] = E[Z] \quad (65)$$

and

$$\sigma_I^2 = \frac{\sigma_Z^2}{n} + \frac{2\Delta}{\tau} \sum_{k=1}^{n-1} \left(1 - \frac{k\Delta}{\tau}\right) [R_Z(k\Delta) - E^2[Z]] \quad (66)$$

where  $R_Z(\mu)$  is the autocorrelation function of the process  $Z(t)$ .



Substituting (65) and (66) into (13), we have

$$\left(\frac{\Delta T}{T_{op}}\right)^2 = \frac{1}{2B_E t_{RC}} \left[ \frac{1}{n} + \frac{2\Delta}{\tau} \sum_{k=1}^{n-1} \left(1 - \frac{k\Delta}{\tau}\right) e^{-\frac{k\Delta}{t_{RC}}} \right] \quad (67)$$

Defining

$$A = e^{-\Delta/t_{RC}} \quad (68)$$

and using equations (43) and (44) it can be shown that

$$F^2 = \frac{\Delta}{2t_{RC}} \coth \frac{\Delta}{2t_{RC}} - \frac{(1 - e^{-\tau/t_{RC}}) \left(\frac{\Delta}{2t_{RC}} \operatorname{csch} \frac{\Delta}{2t_{RC}}\right)^2}{(\tau/t_{RC})} \quad (69)$$

Equation (69) is of the same form as equation (47).

Note that in that case it was argued that the second term was negligible since  $\tau W$  was large (on the order of  $10^8$ ).

Here the same assumption can not be made since  $\frac{1}{t_{RC}} \ll W$  (i.e. the RC filter bandwidth is much smaller than the bandwidth of the RF, Mixer, IF filter). The first term of equation (69) reduces to one as  $\Delta$  approaches zero. The second term however, contributes negatively. Therefore  $F$  can be less than one. The reason for this lies in the addition of an RC filter to the radiometer, which has the effect of lengthening the integration time  $\tau$ . As  $\Delta$  approaches zero, a comparison is being made of two TPR, one with an RC filter after the square law detector and the other without one. The one with the RC filter will have greater sensitivity (smaller  $\Delta T$ ) due to a longer effective integration time. Therefore  $F$  can be less than one.



However, if the effects of sampling only are of interest (not the effect of the addition of the RC filter), the second term must be disregarded by assuming that  $\tau/t_{RC} = \infty$ . This implies that all the filtering is done by the integrator and none by the RC filter.

As explained in part A of this chapter, the results are presented in Chapter V. Refer to Figures 46 through 51.

In summary, the effects of an ideal ADC (i.e. no saturation and step size equal to zero) was studied in this chapter. Its main importance is the fact that it provides a lower bound for the Degradation Factor and, that under certain conditions, a correction can be added to these results to account for the finite step size of the quantizer.



#### IV. TRANSFER CHARACTERISTICS OF A QUANTIZER WITH A ZERO MEAN GAUSSIAN INPUT PROCESS

In this chapter the effects of a quantizer on a zero mean Gaussian input process are analyzed. Two cases are investigated. Refer to Figure 6. It is desired to find the autocorrelation function at point 2 given the autocorrelation function of  $X(t)$  and the knowledge that it is Gaussian and has zero mean. Several approaches have been explored for the case of a quantizer alone. The one suggested by Kellog [Ref.11] was used since it can be easily extended for the case of a quantizer followed by a square law detector, and also the equations that it leads to are in a form suitable for computer programming. Figure 7 shows two quantizers, one with even number of levels and the other with odd number of levels.

Let  $N$  be the number of levels of the quantizer. Then

$$x_i = \frac{2L(1 - N/2)}{N-1} \quad (70)$$

and

$$q_i = \frac{2L[1 - (N+1)/2]}{N-1} \quad (71)$$



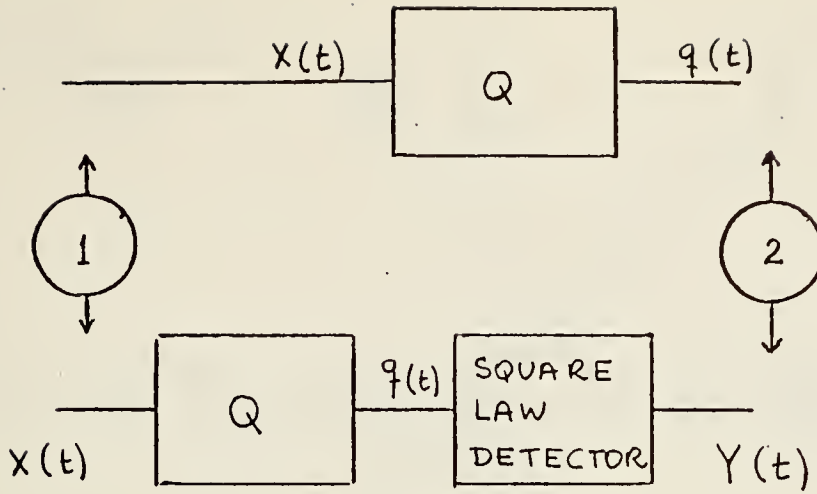


FIGURE 6

#### A. QUANTIZER ALONE

The autocorrelation function of  $q(t)$  is

$$R_q(\mu) = E\{Q[X(t)]Q[X(t+\mu)]\} \quad (72)$$

Let

$$X(t) = \zeta_1 \quad (73)$$

and

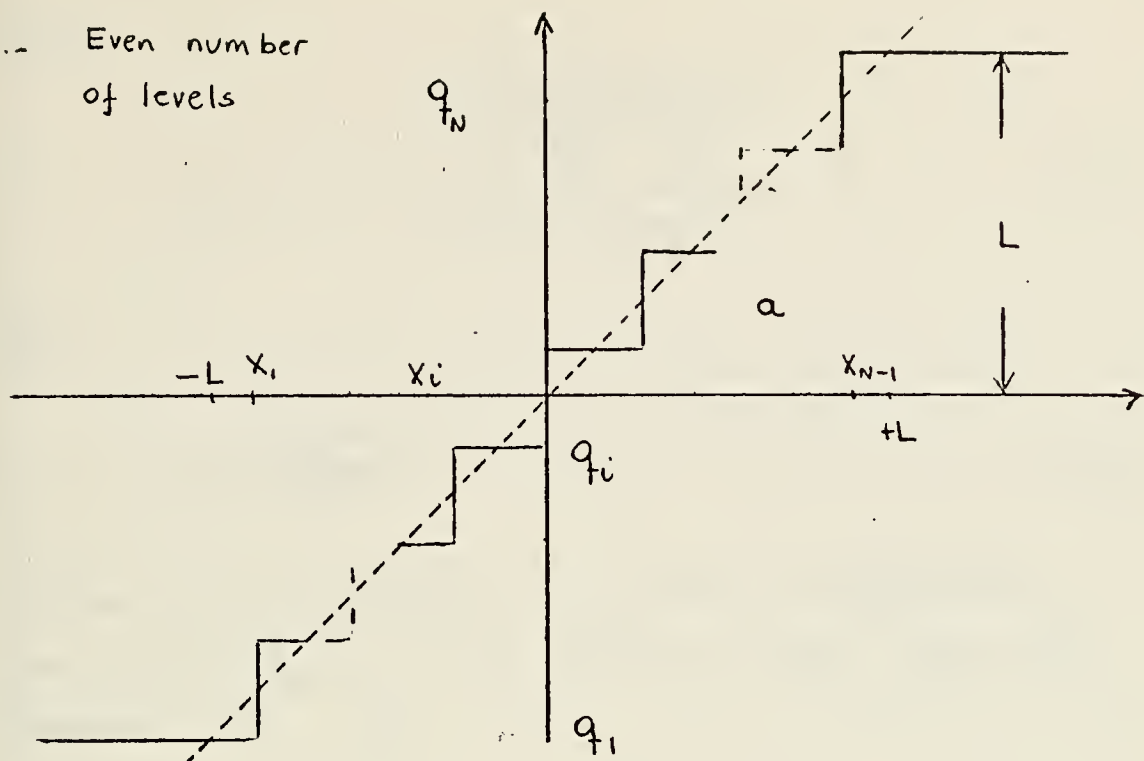
$$X(t+\mu) = \zeta_2 \quad (74)$$

Then

$$R_q(\mu) = \int_{-\infty}^{\infty} \int_{-\infty}^{\infty} Q(\zeta_1)Q(\zeta_2)f(\zeta_1, \zeta_2; \mu) d\zeta_1 d\zeta_2 \quad (75)$$



a. Even number of levels



b. Odd number of levels

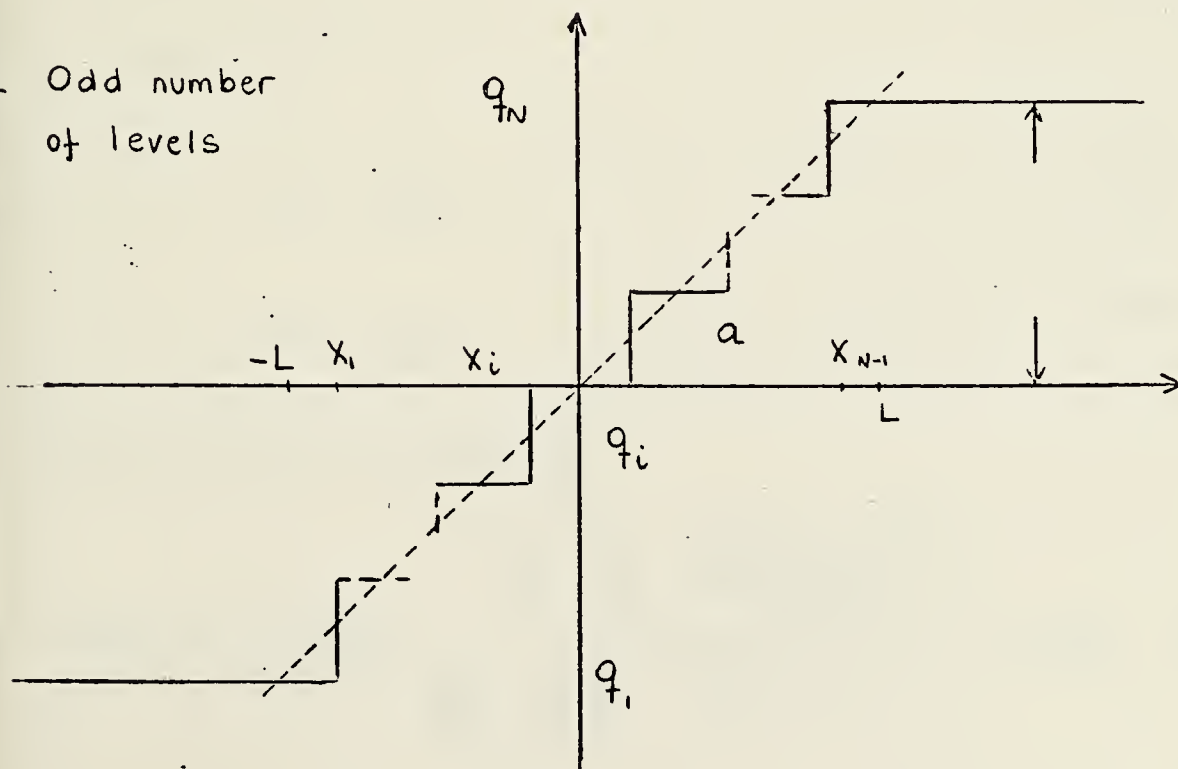


FIGURE 7



where

$$f(\zeta_1, \zeta_2; \mu) = \frac{e^{-\frac{(\zeta_1^2 - 2\rho_X \zeta_1 \zeta_2 + \zeta_2^2)}{(1-\rho_X^2) 2\sigma_X^2}}}{\sigma_X^2 2\pi (1-\rho_X^2)^{\frac{1}{2}}} \quad (76)$$

and

$$\rho_X = \frac{R_X(\mu)}{R_X(0)} \quad (77)$$

Noting that the dependence of  $R_q$  upon  $\mu$  is only via  $\rho_X$ , the notation  $R_q(\rho_X)$  will be used for brevity. Then (75) becomes

$$R_q(\rho_X) = \sum_{i=1}^N \sum_{j=1}^N q_i q_j \int_{X_{i-1}}^{X_i} \int_{X_{j-1}}^{X_j} f(\zeta_1, \zeta_2; \rho_X) d\zeta_1 d\zeta_2 \quad (78)$$

Let

$$\beta_1 = \zeta_1 / \sigma_X \quad (79)$$

$$\beta_2 = \zeta_2 / \sigma_X \quad (80)$$

then (78) can be written as

$$R_q(\rho_X) = \sum_{i=1}^N \sum_{j=1}^N q_i q_j \int_{\frac{X_{i-1}}{\sigma_X}}^{\frac{X_i}{\sigma_X}} \int_{\frac{X_{j-1}}{\sigma_X}}^{\frac{X_j}{\sigma_X}} \frac{e^{-\frac{(\beta_1^2 - 2\rho_X \beta_1 \beta_2 + \beta_2^2)}{2(1-\rho_X^2)}}}{2(1-\rho_X^2)^{\frac{1}{2}}} d\beta_1 d\beta_2 \quad (81)$$



but

$$\beta_1^2 - 2\beta_1\beta_2\rho_X + \beta_2^2 = (\beta_2 - \rho_X\beta_1)^2 + \beta_1^2(1 - \rho_X^2) \quad (82)$$

Therefore

$$- \left[ \frac{\beta_1^2 - 2\rho_X\beta_1\beta_2 + \beta_2^2}{2(1 - \rho_X^2)} \right] = \frac{-(\beta_2 - \rho_X\beta_1)^2}{2(1 - \rho_X^2)} - \frac{\beta_1^2}{2} \quad (83)$$

and (81) becomes

$$R_q(\rho_X) = \sum_{i=1}^N \sum_{j=1}^N q_i q_j \int_{\frac{X_{i-1}}{\sigma_X}}^{\frac{X_i}{\sigma_X}} \frac{1}{2\pi} e^{\beta_1^2/2} \int_{\frac{X_{j-1}}{\sigma_X}}^{\frac{X_j}{\sigma_X}} \frac{e^{\frac{-(\beta_2 - \rho_X\beta_1)^2}{2(1-\rho_X^2)}}}{[2\pi(1-\rho_X^2)]^{1/2}} d\beta_2 d\beta_1 \quad (84)$$

Now let

$$\frac{\beta_2 - \rho_X\beta_1}{[2(1-\rho_X^2)]^{1/2}} = \alpha \quad (85)$$

It follows that the second integral can be written as

$$\frac{1}{2} \left\{ \operatorname{erf} \left[ \frac{X_j/\sigma_X - \rho_X\beta_1}{[2(1-\rho_X^2)]^{1/2}} \right] - \operatorname{erf} \left[ \frac{X_{j-1}/\sigma_X - \rho_X\beta_1}{[2(1-\rho_X^2)]^{1/2}} \right] \right\} \quad (86)$$

where

$$\operatorname{erf}(\alpha) = \frac{2}{\pi^{1/2}} \int_0^\alpha e^{-v^2} dv \quad (87)$$



If a new function is defined as

$$\psi(\rho_X, \beta_1) = \sum_{j=1}^N \frac{q_j}{2} \left\{ \operatorname{erf} \left[ \frac{X_j/\sigma_X - \rho_X \beta_1}{[2(1-\rho_X^2)]^{1/2}} \right] - \operatorname{erf} \left[ \frac{X_{j-1}/\sigma_X - \rho_X \beta_1}{[2(1-\rho_X^2)]^{1/2}} \right] \right\} \quad (88)$$

then (84) can be written as

$$R_q(\rho_X) = \frac{1}{(2\pi)^{1/2}} \sum_{i=1}^N q_i \int_{\frac{X_{i-1}}{\sigma_X}}^{\frac{X_i}{\sigma_X}} \psi(\rho_X, \beta_1) e^{-\frac{\beta_1^2}{2}} d\beta_1 \quad (89)$$

Dividing both sides of (89) by  $\sigma_X^2$  and substituting the expressions for  $X_i$  and  $q_i$ , it is found that a new parameter appears, namely  $\sigma_X/L$ . This parameter together with  $N$  and  $\rho_X$  will be the independent variables of (89). Note that with the introduction of  $\sigma_X/L$ , the dynamic range of the quantizer,  $L$ , is no longer an independent factor.

By letting

$$q'_i = q_i/L \quad (90)$$

$$X'_i = X_i/L \quad (91)$$

and

$$\sigma'_X = \sigma_X/L \quad (92)$$

it follows that

$$\frac{R_q(\rho_X)}{\sigma_X^2} = \frac{1}{(2\pi)^{1/2}} \sum_{i=1}^n \frac{q'_i}{\sigma'_X} \int_{\frac{X'_{i-1}}{\sigma'_X}}^{\frac{X'_i}{\sigma'_X}} \psi'(\rho_X, \beta_1) e^{-\frac{\beta_1^2}{2}} d\beta_1 \quad (93)$$

and



$$\psi'(\rho_X, \beta_1) = \sum_{j=1}^N \frac{q_j'}{2\sigma_X'} \left\{ \operatorname{erf} \left[ \frac{X_j'/\sigma_X' - \rho_X \beta_1}{[2(1-\rho_X^2)]^{1/2}} \right] - \operatorname{erf} \left[ \frac{X_{j-1}'/\sigma_X' - \rho_X \beta_1}{[2(1-\rho_X^2)]^{1/2}} \right] \right\} \quad (94)$$

It can be shown, following a similar procedure, that for  $\rho_X$  equal to one, (93) becomes

$$\frac{R_q(1)}{\sigma_X'^2} = \frac{\sigma_q^2}{\sigma_X'^2} = \frac{1}{2} \sum_{i=1}^N \left( \frac{q_i'}{\sigma_X'} \right)^2 \left\{ \operatorname{erf} \left[ \frac{X_i'/\sigma_X'}{(2)^{1/2}} \right] - \operatorname{erf} \left[ \frac{X_{i-1}'/\sigma_X'}{(2)^{1/2}} \right] \right\} \quad (95)$$

This gives us  $\sigma_q^2$  numerically so we can get the normalized autocorrelation of  $q$ . Equations (93) through (95) allow the computation of the autocorrelation function of the output of a quantizer of  $N$  steps and saturation level  $L$  given that the input is Gaussian, zero mean, and of known autocorrelation function. The procedure would be as follows. First, calculate  $\sigma_X'$ ,  $X_i'$  and  $q_i'$  for the given quantizer and input process. Second, find a value of  $\rho_X$  for a particular  $\mu$  (Equation (76)). Third, form the function  $\psi'(\rho_X, \beta_1)$  for the particular value of  $\rho_X$  determined in the second step. Fourth, replace the function  $\psi'(\rho_X, \beta_1)$  into (93) and perform the integration. This procedure will map one point of the input autocorrelation function into one point of the output autocorrelation function.

A program was written to solve (93) through (95) for the case of symmetrical quantizers (See Appendix under Transfer Characteristics of Odd level Quantizer, and Transfer Characteristics of Even level Quantizer) and the results are



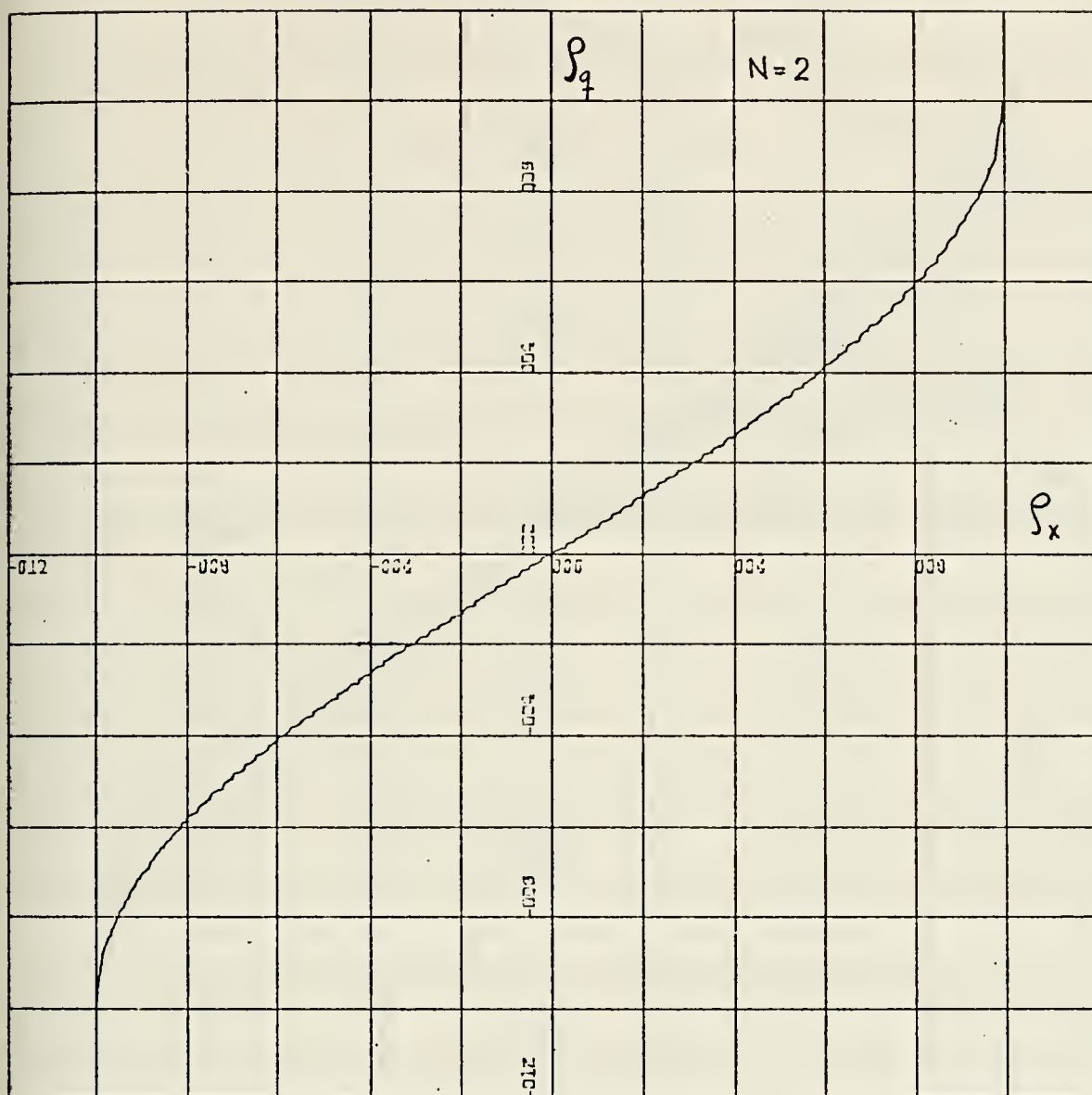
plotted in Figures 8 through 14 as a function of  $\rho_X$ . The ordinate axis is  $\frac{R_q(\mu)}{\sigma_q^2} = \rho_q$ . In other words, for a given  $\rho_X$ ,  $\rho_q$  is obtained. The advantage of plotting it this way is that the curves are independent of the input autocorrelation function (as long as the input process is Gaussian and zero mean).

In general, the curves are a function of  $\sigma_X/L$  (except for the special case of  $N=2$ ). Note that for  $N=2$  the result is the well-known relationship [Ref. 7]

$$\frac{R_q(\rho_X)}{\sigma_q^2} = \frac{2}{\pi} \arcsin \rho_X \quad (96)$$

It is of interest to note the behavior of these curves as  $\sigma_X/L$  approaches extreme values. For a quantizer with odd number of levels, as  $\sigma_X/L$  gets very large, the quantizer will appear as a hard limiter, hence the curves will approach that of Figure 8. As  $\sigma_X/L$  approaches zero the quantizer will appear as a three step quantizer (eventually it will become an open circuit) and the curves will show a behavior similar to those shown in Figure 9. For a quantizer with an even number of levels, the behavior of the curves as  $\sigma_X/L$  becomes large is also as described above. When  $\sigma_X/L$  approaches zero, however, the quantizer will appear again as a hard limiter, therefore the curves will approach that of Figure 8.

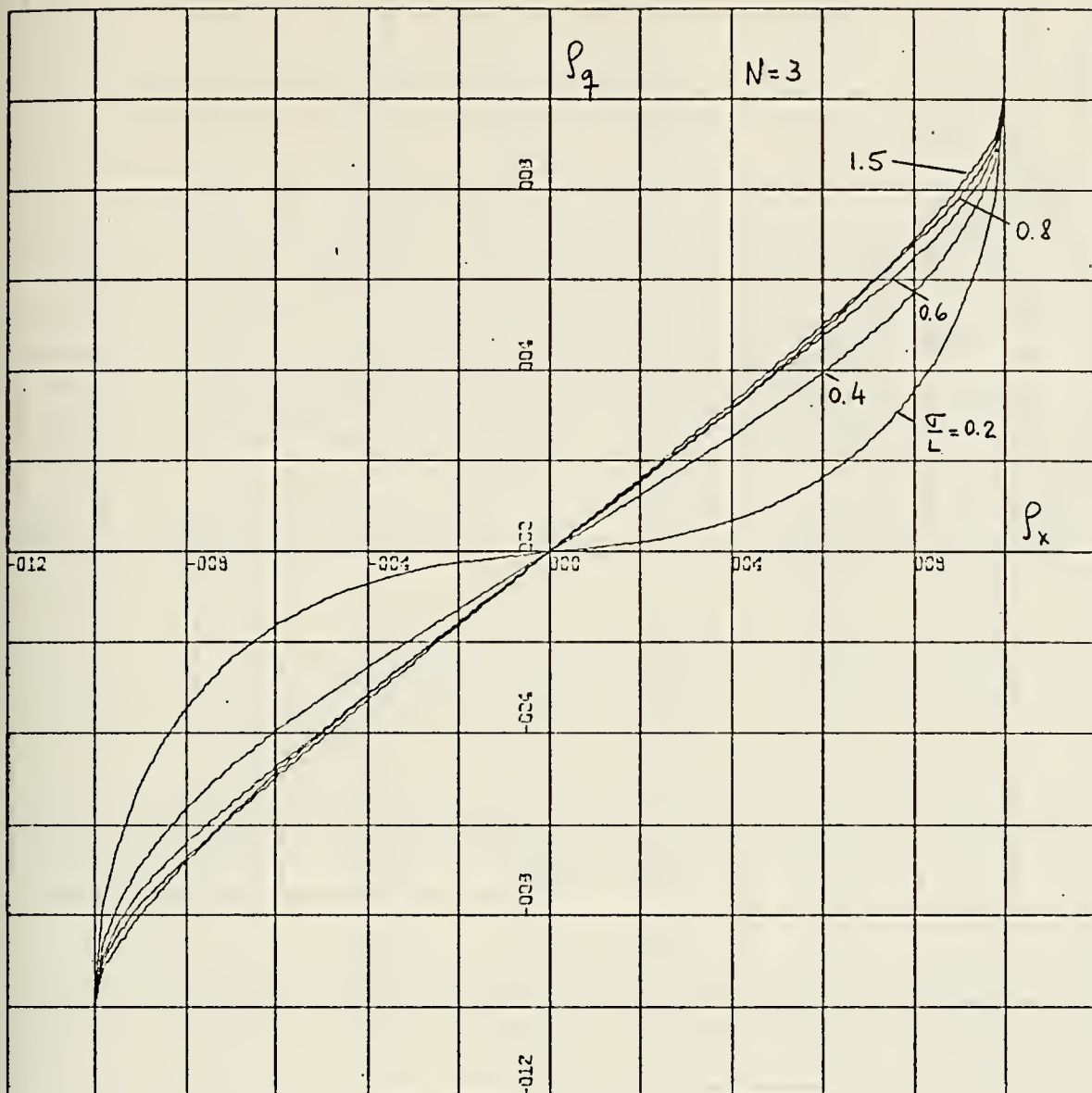




X-SCALE=4.00E-01 UNITS INCH.  
Y-SCALE=4.00E-01 UNITS INCH.

FIGURE 8

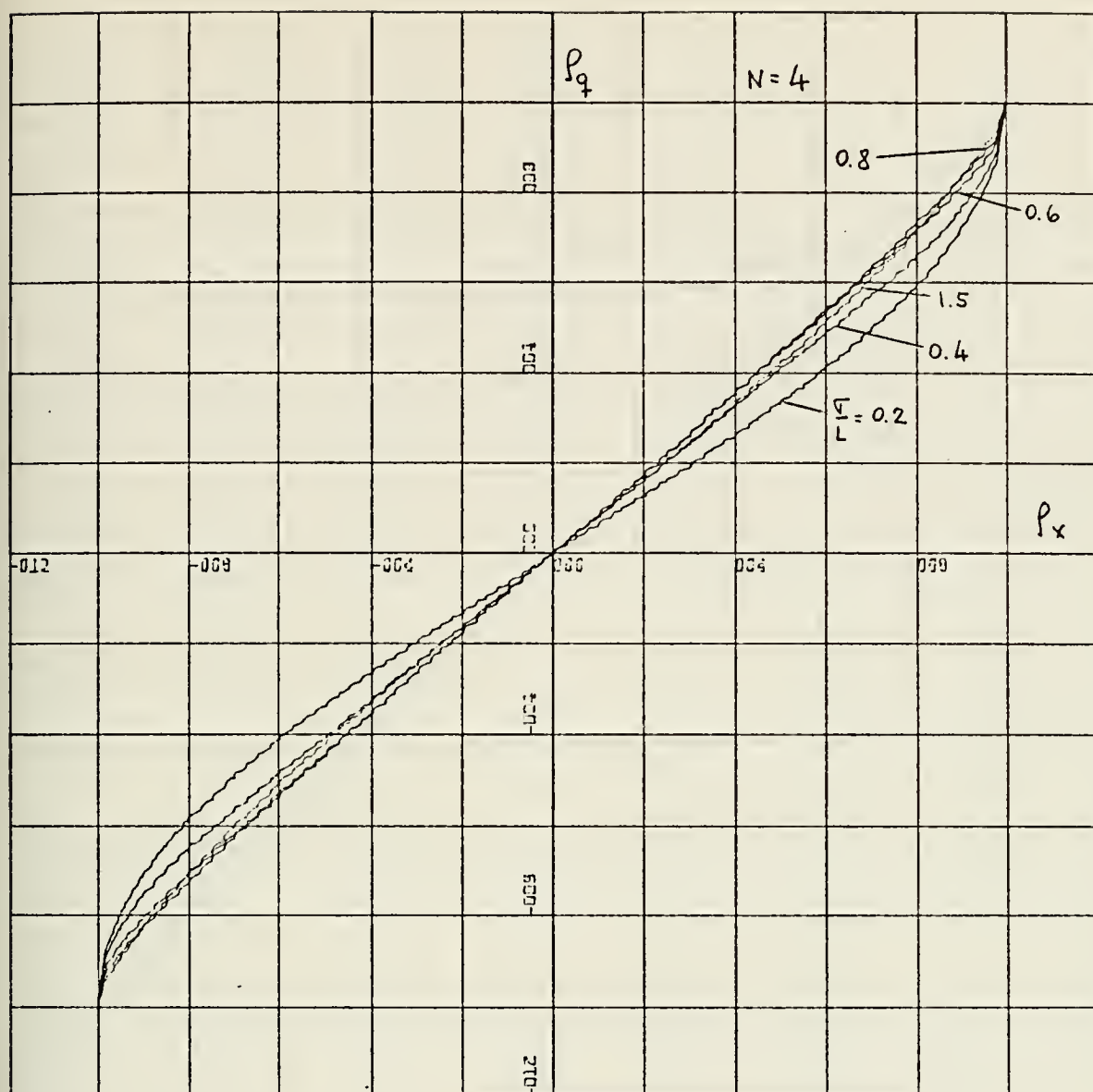




X-SCALE=4.00E-01 UNITS INCH.  
Y-SCALE=4.00E-01 UNITS INCH.

FIGURE 9

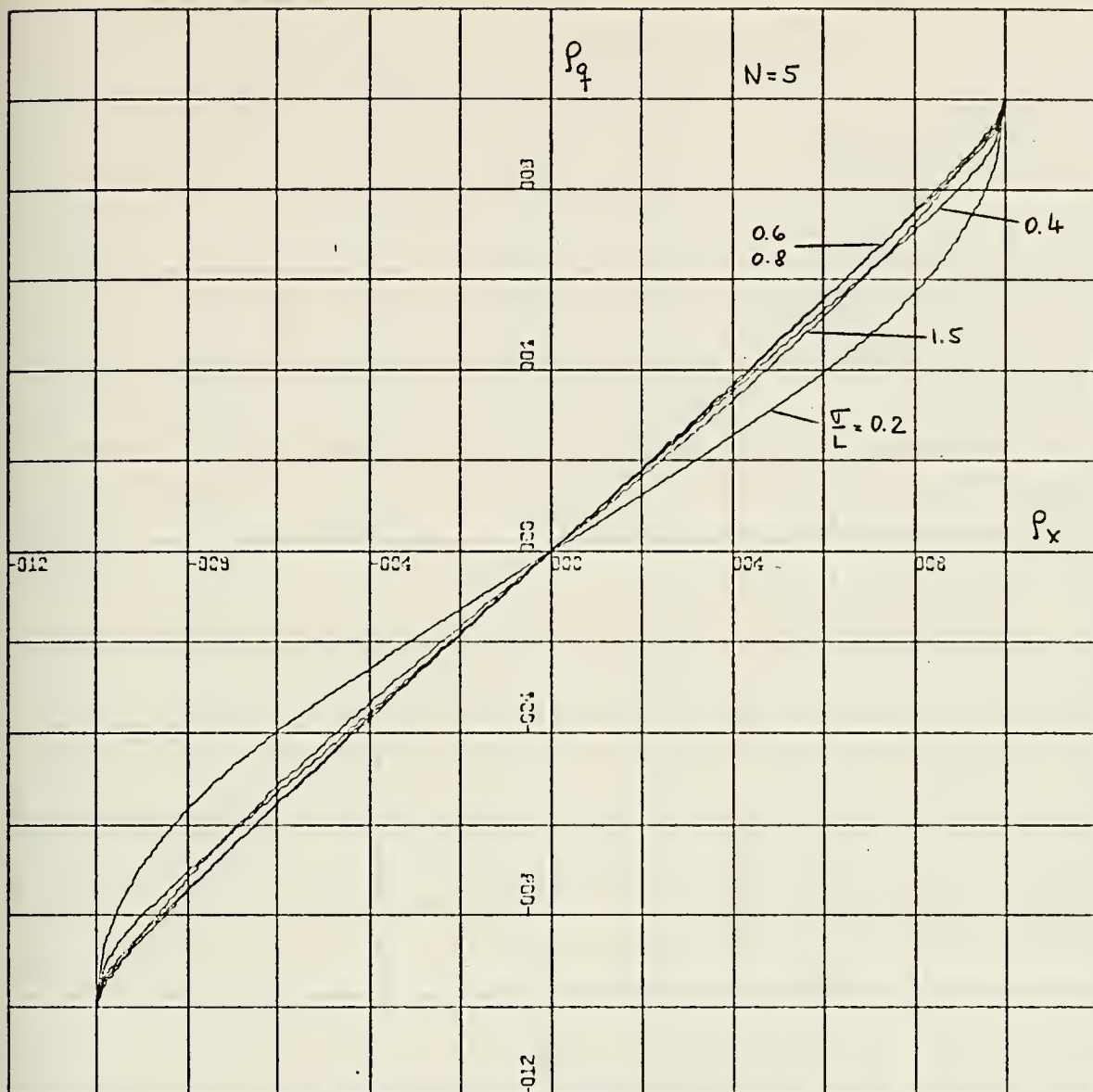




X-SCALE=4.00E-01 UNITS INCH.  
Y-SCALE=4.00E-01 UNITS INCH.

FIGURE 10

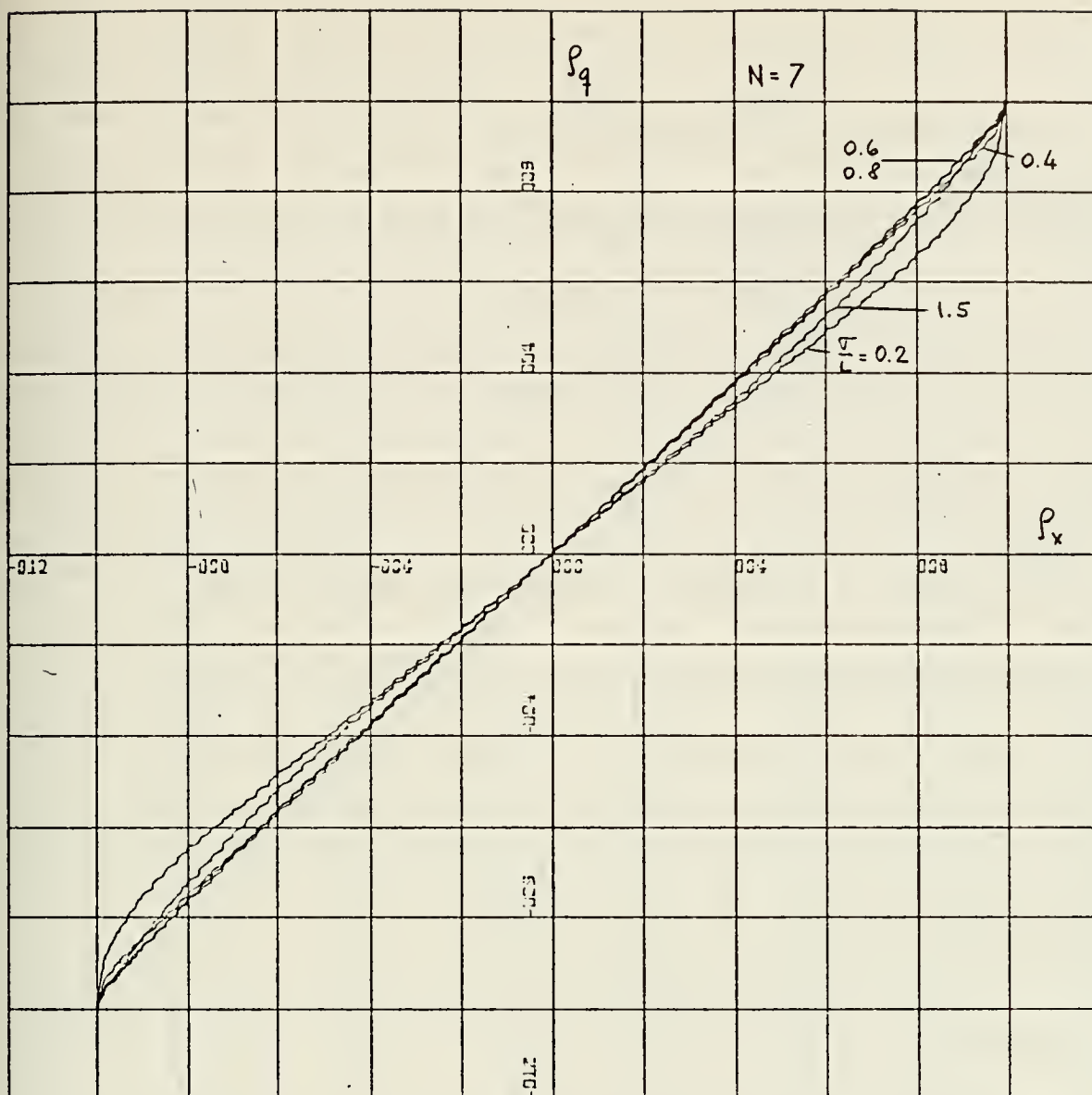




X-SCALE=4.00E-01 UNITS INCH.  
Y-SCALE=4.00E-01 UNITS INCH.

FIGURE 11



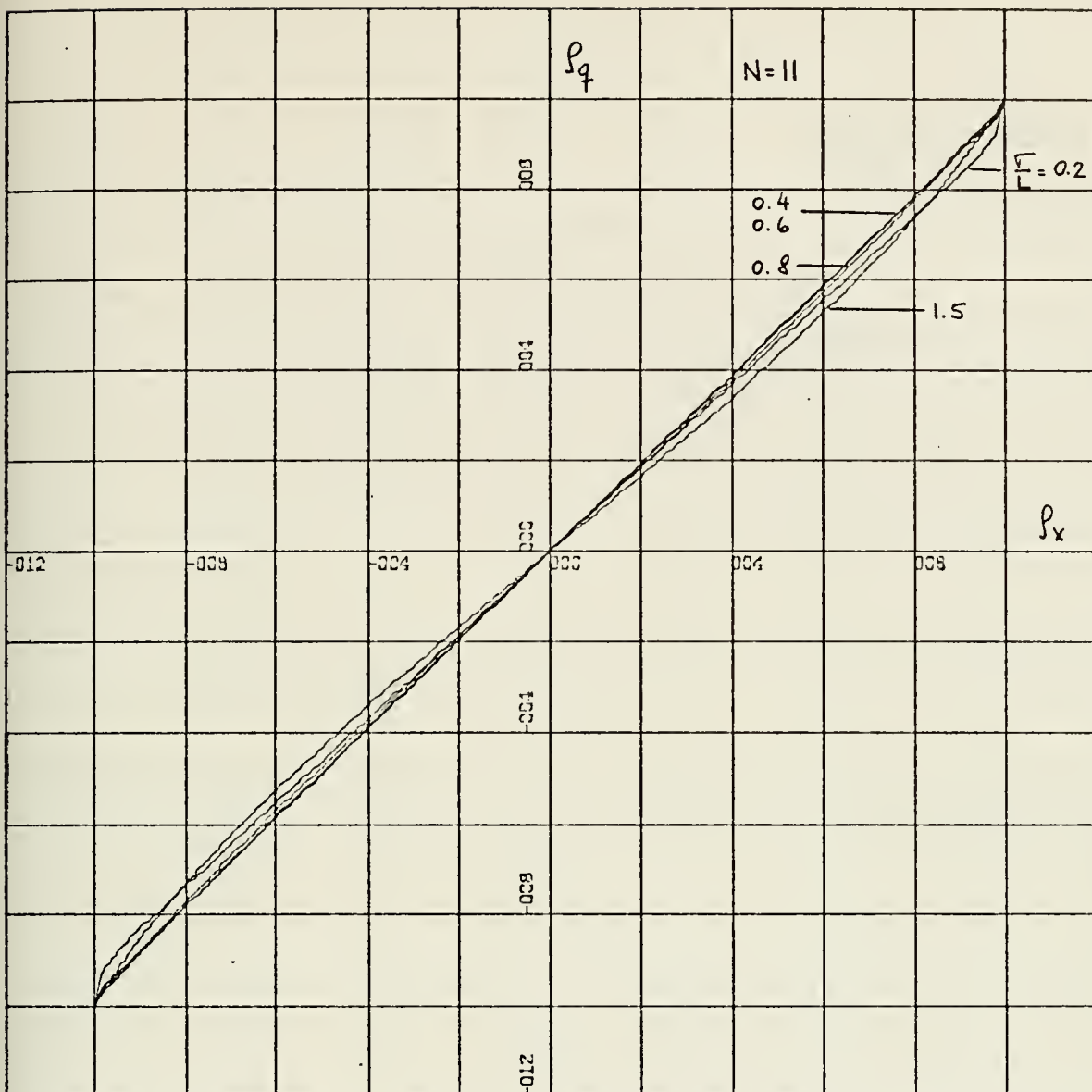


X-SCALE=4.00E-01 UNITS INCH.

Y-SCALE=4.00E-01 UNITS INCH.

FIGURE 12

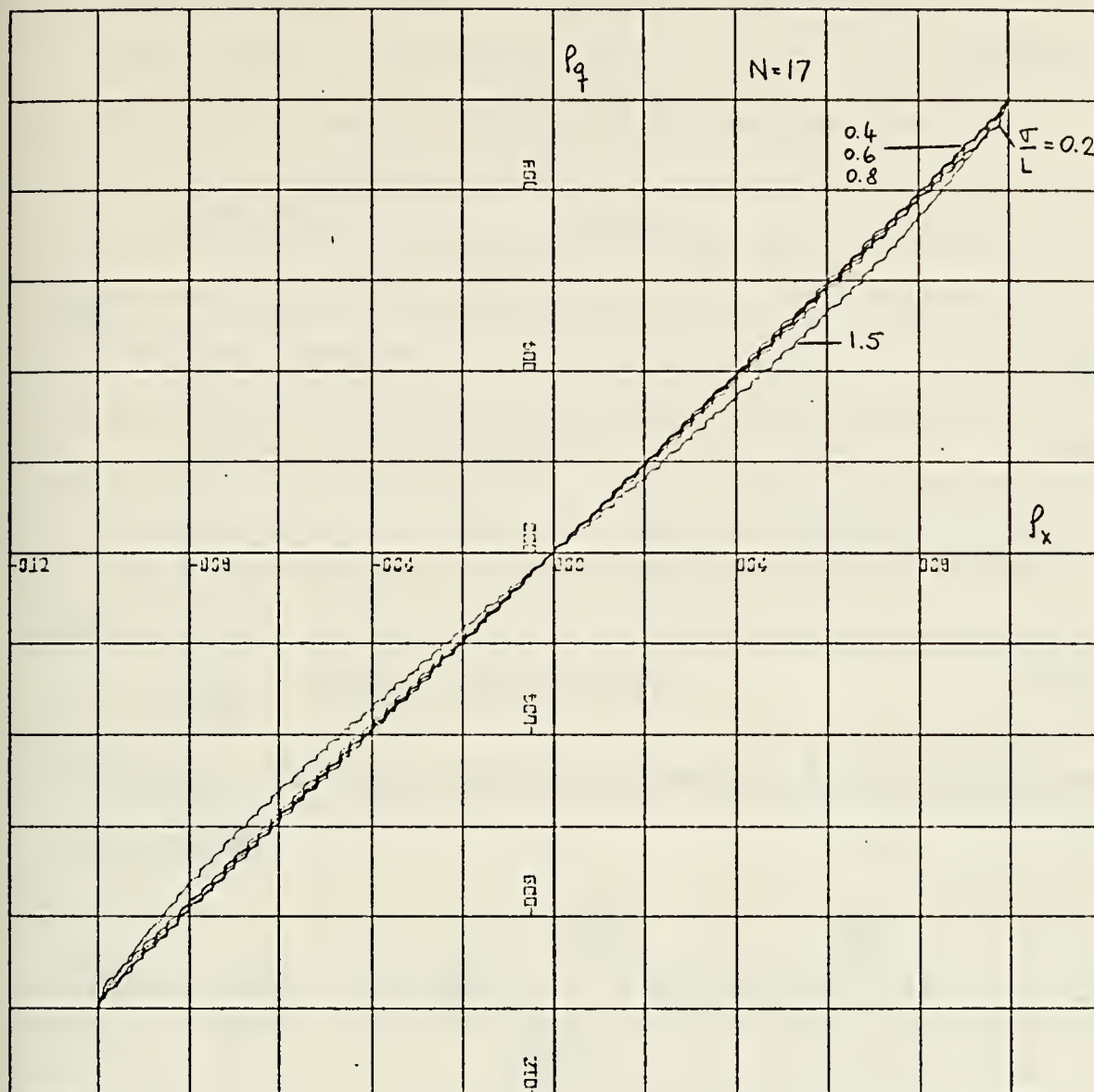




X-SCALE=4.00E-01 UNITS INCH.  
Y-SCALE=4.00E-01 UNITS INCH.

FIGURE 13





X-SCALE=4.00E-01 UNITS INCH.

Y-SCALE=4.00E-01 UNITS INCH.

FIGURE 14



## B. QUANTIZER FOLLOWED BY A SQUARE LAW DETECTOR

The reason for analyzing this case will become apparent in Chapter V. Refer to Figure 6 and observe that

$$Y(t) = q^2(t) \quad (97)$$

and

$$q(t) = Q[X(t)] \quad (98)$$

$$R_Y(\mu) = E[Y(t)Y(t+\mu)] \quad (99)$$

Upon substituting (97) and (98) into (99) it follows that

$$R_Y(\mu) = E\{Q^2[X(t)]Q^2[X(t+\mu)]\} \quad (100)$$

Following a similar procedure as done for the previous case, (100) becomes

$$\frac{R_Y(\rho_X)}{\sigma_X^4} = \frac{1}{(2\pi)^{\frac{1}{2}}} \sum_{i=1}^N \left(\frac{q'_i}{\sigma'_X}\right)^2 \int_{\frac{X'_{i-1}}{\sigma'_X}}^{\frac{X'_i}{\sigma'_X}} \Lambda(\rho_X, \beta_1) e^{-\frac{\beta_1^2}{2}} d\beta_1 \quad (101)$$

and

$$\Lambda(\rho_X, \beta_1) = \frac{1}{2} \sum_{j=1}^N \left(\frac{q'_j}{\sigma'_X}\right)^2 \left\{ \operatorname{erf}\left[ \frac{X'_j/\sigma'_X - \rho_X \beta_1}{[2(1-\rho_X^2)]^{\frac{1}{2}}} \right] - \operatorname{erf}\left[ \frac{X'_{j-1}/\sigma'_X - \rho_X \beta_1}{[2(1-\rho_X^2)]^{\frac{1}{2}}} \right] \right\} \quad (102)$$

For  $\rho_X=1$  it can be shown that

$$\frac{E[Y^2]}{\sigma_X^4} = \frac{1}{2} \sum_{i=1}^N \left(\frac{q'_i}{\sigma'_X}\right)^4 \left[ \operatorname{erf}\left( \frac{X'_i}{\sigma'_X(2)^{\frac{1}{2}}} \right) - \operatorname{erf}\left( \frac{X'_{i-1}}{\sigma'_X(2)^{\frac{1}{2}}} \right) \right] \quad (103)$$



$x'_1$ ,  $q'_1$ ,  $\sigma'_X$ , and  $\rho_X$  were defined in (90), (91), (92) and (77) respectively.

A computer program was written for this case when the quantizer is symmetrical (See Appendix under "Transfer Characteristics of Odd Quantizer Followed by a Square Law Detector" and "Transfer Characteristics of Even Quantizer Followed by a Square Law Detector"). The same comments as in the previous section apply for the plots of this case except that now the ordinate axis is  $\frac{R_Y(\mu)}{R_Y(0)}$  instead of  $\rho_Y$  since  $Y(t)$  is not zero mean. The results are shown on Figure 15 for  $N$  equal to five and eleven.

It can be shown that for the case of no quantizer  $\frac{R_Y(\mu)}{R_Y(0)}$  is given by

$$\frac{R_Y(\mu)}{R_Y(0)} = \frac{1 + 2\rho_X^2}{3} \quad (104)$$

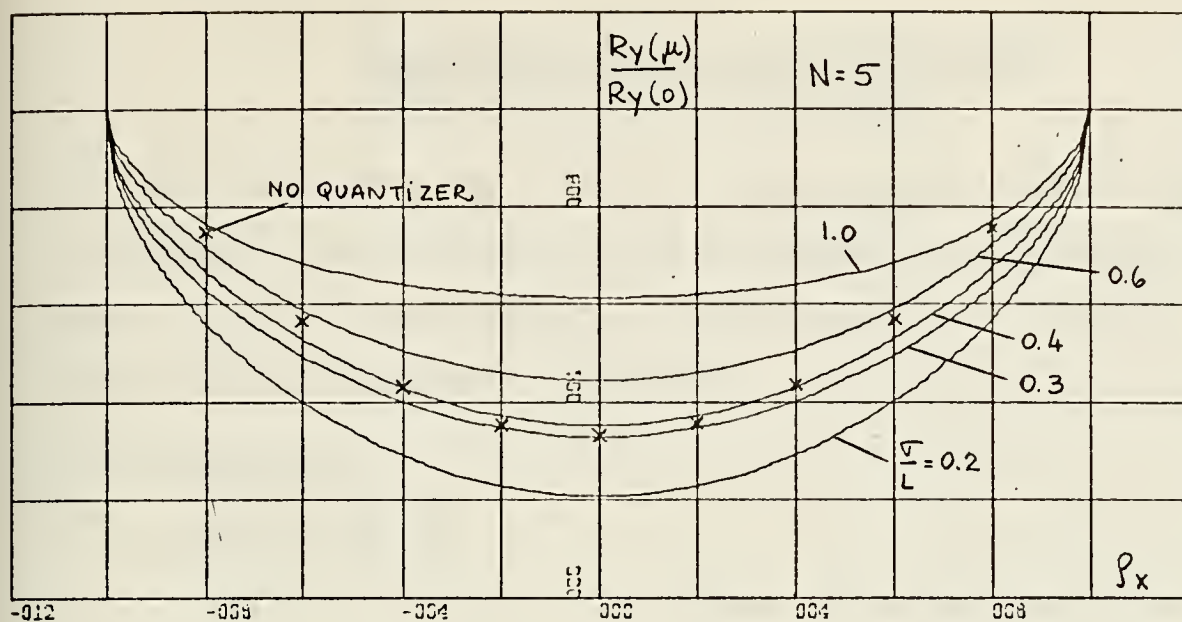
Note how the curves of Figure 15 depart from the curve given by (104) due to the effects of the quantizer.

In summary, in this chapter an algorithm has been developed suitable for computer programming in order to find the autocorrelation function of the output of a quantizer (or quantizer and a square law detector) given that the input process is Gaussian and zero mean, and with known autocorrelation function. What it basically does (for both cases) is to reduce a double integral (75) and (100) into a single integral by using the error function which is available in most computer libraries.

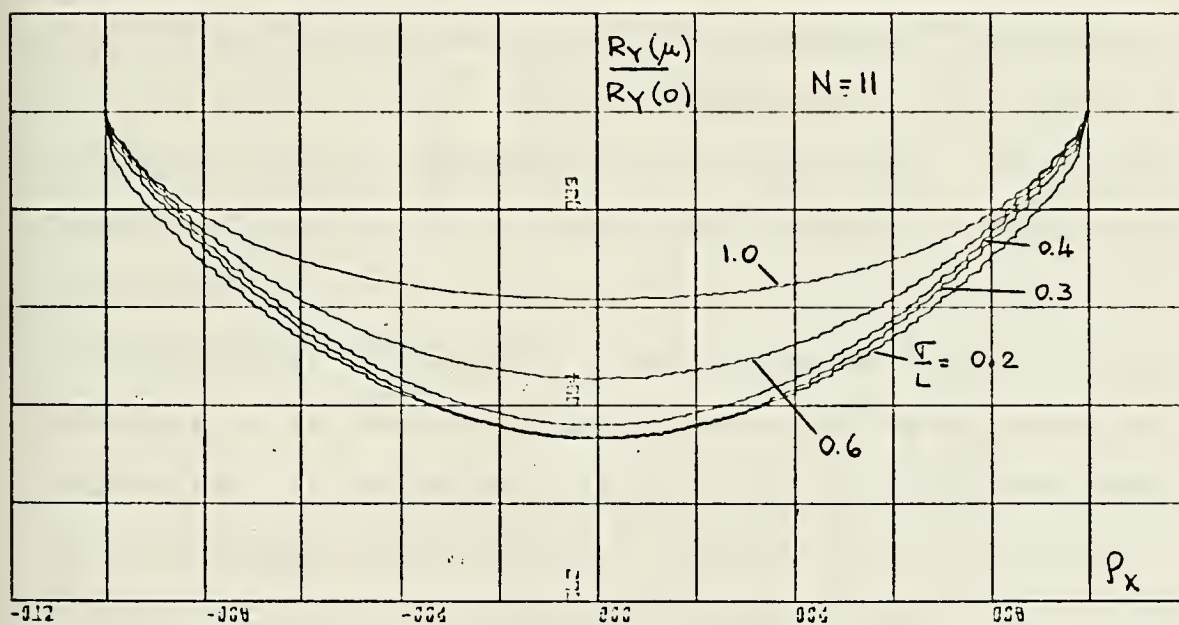


The transfer curves for both cases, shown on Figures 8 through 14 and 15 are independent of the input process providing it is Gaussian and has zero mean. These results will be used in Chapter V.





(a)



(b)

X-SCALE=4.00E-01 UNITS INCH.  
Y-SCALE=4.00E-01 UNITS INCH.

FIGURE 15



## V. DEGRADATION FACTOR CALCULATION WITH BOTH SAMPLING AND QUANTIZATION

In this chapter the effects of sampling and quantization on the performance figure of the two digital radiometers under study are investigated. As in Chapter III, the two cases will be considered separately.

### A. IF SAMPLING

#### 1. Exact Results

Refer to Figure 2. In Chapter III an expression was developed for the degradation factor for the case where there was no quantizer — see (30). Those results cannot be applied directly to this case since in order to obtain (30) it was assumed that  $q_c(k\Delta)$  and  $q_s(k\Delta)$  were samples of Gaussian processes — see (22). With the addition of a quantizer it is clear that this assumption no longer holds. Hence we must start again with a more general approach. This can be accomplished by concentrating first on the top channel of the radiometer of Figure 2. The processing that the ADC and computer do to the signal can be drawn sequentially as in Figure 16. It is argued that the order in which the signal  $q_c(t)$  is sampled and squared is immaterial as far as the random variable  $I_1$  is concerned. Hence Figure 16 is a valid model of a channel of the radiometer of Figure 2.

Referring to Figure 16 it follows that [Ref. 12]

$$\sigma_{I_1}^2 = \frac{\sigma_Y^2}{n} + \frac{2}{n} \sum_{k=1}^{n-1} \left(1 - \frac{k}{n}\right) [R_Y(k\Delta) - E^2[Y]] \quad (105)$$



$R_Y(k)$  is the  $k^{\text{th}}$  sample of the autocorrelation function of  $Y(t)$

and

$$E[I_1] = E[Y(t)] = \sigma_{q_c}^2 \quad (106)$$

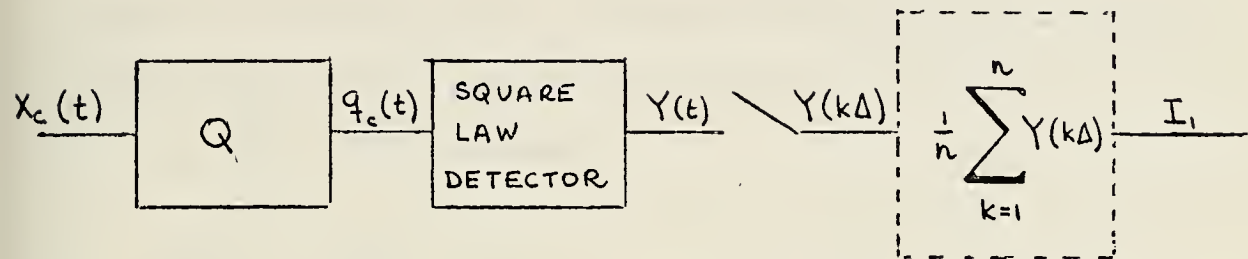


FIGURE 16

Using (26) and the fact that for the case of Figure 2 the RF, Mixer, IF filter is symmetrical about  $f_o$ , then

$$\sigma_I^2 = 2 \sigma_{I_1}^2 \quad (107)$$

and

$$E[I] = 2E[I_1] = 2 \sigma_{q_c}^2 \quad (108)$$

Applying the definition of degradation factor it follows that

$$F^2 = \frac{\frac{2\sigma_Y^2}{4} B_E \Delta + \frac{4B_E \Delta}{\sigma_{X_c}^2} \sum_{k=1}^{n-1} \left(1 - \frac{k\Delta}{\tau}\right) [R_Y(k\Delta) - \sigma_q^4]}{\left[ \frac{dE[I]}{d\sigma_{X_c}^2} \right]^2} \bigg|_{\sigma_{X_c}^2 \text{ at } T_{op}} \quad (109)$$



Using the same argument as in Chapter III ( $\Delta \ll \tau$ ) it can be shown that the term

$$\frac{4B_E \Delta}{\sigma_{X_c}^4} \sum_{k=1}^{n-1} \frac{k\Delta}{\tau} [R_Y(k\Delta) - \sigma_{q_c}^4] \quad (110)$$

can be disregarded due to its small value compared with the other terms in the numerator of (110).

Then (109) becomes

$$F^2 = \frac{\frac{2\sigma_Y^2}{\sigma_{X_c}^4} B_E \Delta + \frac{4B_E \Delta}{\sigma_{X_c}^4} \sum_{k=1}^{n-1} [R_Y(k\Delta) - \sigma_{q_c}^4]}{\left[ \frac{dE[I]}{d\sigma_{X_c}^2} \right]^2} \bigg|_{\sigma_{X_c}^2 \text{ at } T_{op}} \quad (111)$$

Looking at (111) term by term, it is noted that in the numerator, the first term can be obtained from (103) and (95). The second term can be obtained from the corresponding value of  $\frac{R_{X_c}(k\Delta)}{R_{X_c}(0)}$  and the transfer characteristics of a quantizer followed by a square law detector (Figure 15). Actually, a scale factor of  $\sigma_Y^2/\sigma_{X_c}^4$  will appear because of the way the curves were normalized. The denominator can be obtained from (95). Note however that Equations (93), (95) and the transfer characteristics developed in Chapter IV have  $\sigma_X/L$  as a parameter and not  $\sigma_{X_c}$ . This is due to the choice of  $\sigma_X/L$  as a parameter since it was found in that chapter that the ratio of  $\sigma_X$  and  $L$  was of importance and not their



absolute magnitudes. Therefore it makes sense to have (111) be a function of  $\sigma_{X_c}/L$  at  $T_{op}$  instead of  $\sigma_{X_c}$ .  $\sigma_{X_c}/L$  can be thought of as a normalized standard deviation of  $X_c(t)$  and its value can be related to temperature in the same form as Equations (10) and (11).

A plot of  $E[I]/L^2$  versus  $\sigma_{X_c}^2/L^2$  is shown in Figure 17 for different values of  $N$ . The effects of saturation of the quantizer can be observed as temperature (equivalent to  $\sigma_{X_c}^2/L^2$ ) is increased.

The four filters previously considered for this case were used again and the results are shown in Figures 18 through 41. The bottom curve for each figure represents the case investigated in Chapter III where there is no quantizer. The programs used to evaluate (111) are included in the Appendix. It should be pointed out that the programs used to calculate the transfer characteristics of Chapter IV did not provide a continuous function as it is shown on the plots of that chapter. Since in order to solve (111) the transfer curves must be known at every point, a least-mean-squared-error polynomial fit was done to the data obtained from the programs of Chapter IV.

Looking at Figures 18 through 41 it is noted that in each case there is a reasonable optimum value of  $\sigma_{X_c}/L$  where the degradation factor is lowest. Physically this can be explained by the fact that for small  $\sigma_{X_c}/L$ , the step size degrades the performance of the system, hence increasing  $\sigma_{X_c}/L$  will tend to minimize this effect. However a point is



reached where saturation effects start dominating and the further increase of  $\sigma_{X_c}/L$  causes an increase of the degradation factor. For  $N > 4$ ,  $\sigma_{X_c}/L$  optimum is around 0.35 regardless of the sampling rate. This would imply that for a given  $T_{op}$ , the gain setting of the RF, Mixer IF filter should be set at a value such that  $\sigma_{X_c}/L$  is equal to 0.35 for optimum performance. Note that this optimality is for small source temperatures. For large signals, dynamic range is a problem. See Chapter VI.

## 2. An Approximation

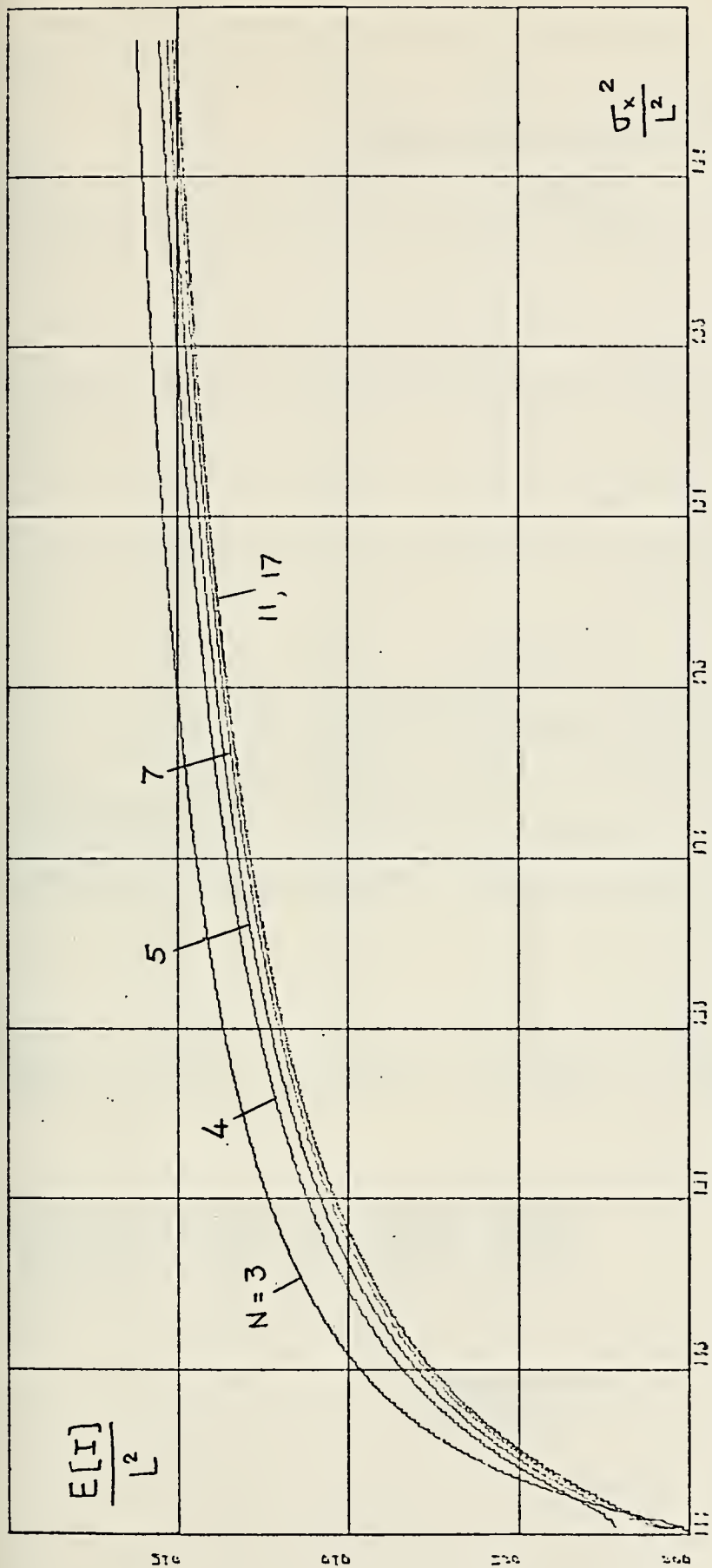
The evaluation of (111) for the exact value of the degradation factor requires extensive computer time. For a quantizer of five bits or greater the computation time per case is very long (on the order of hours). Therefore it is of interest to investigate an approximate solution for the degradation factor and to compare the results with the exact values already obtained.

Figure 42 shows one of the channels of the radiometer of Figure 2. Assume that the sampling rate is not too fast, the step size of the quantizer is small with respect to the standard deviation of the process  $X_c(t)$  and no saturation takes place in the quantizer. Then

$$q_c(k\Delta) = X_c(k\Delta) + e_k \quad (112)$$

where  $X_c(k\Delta)$  is the  $k^{th}$  sample of  $X_c(t)$  and  $e_k$  is a uniformly distributed random variable that accounts for the error introduced by the quantizer. The probability density

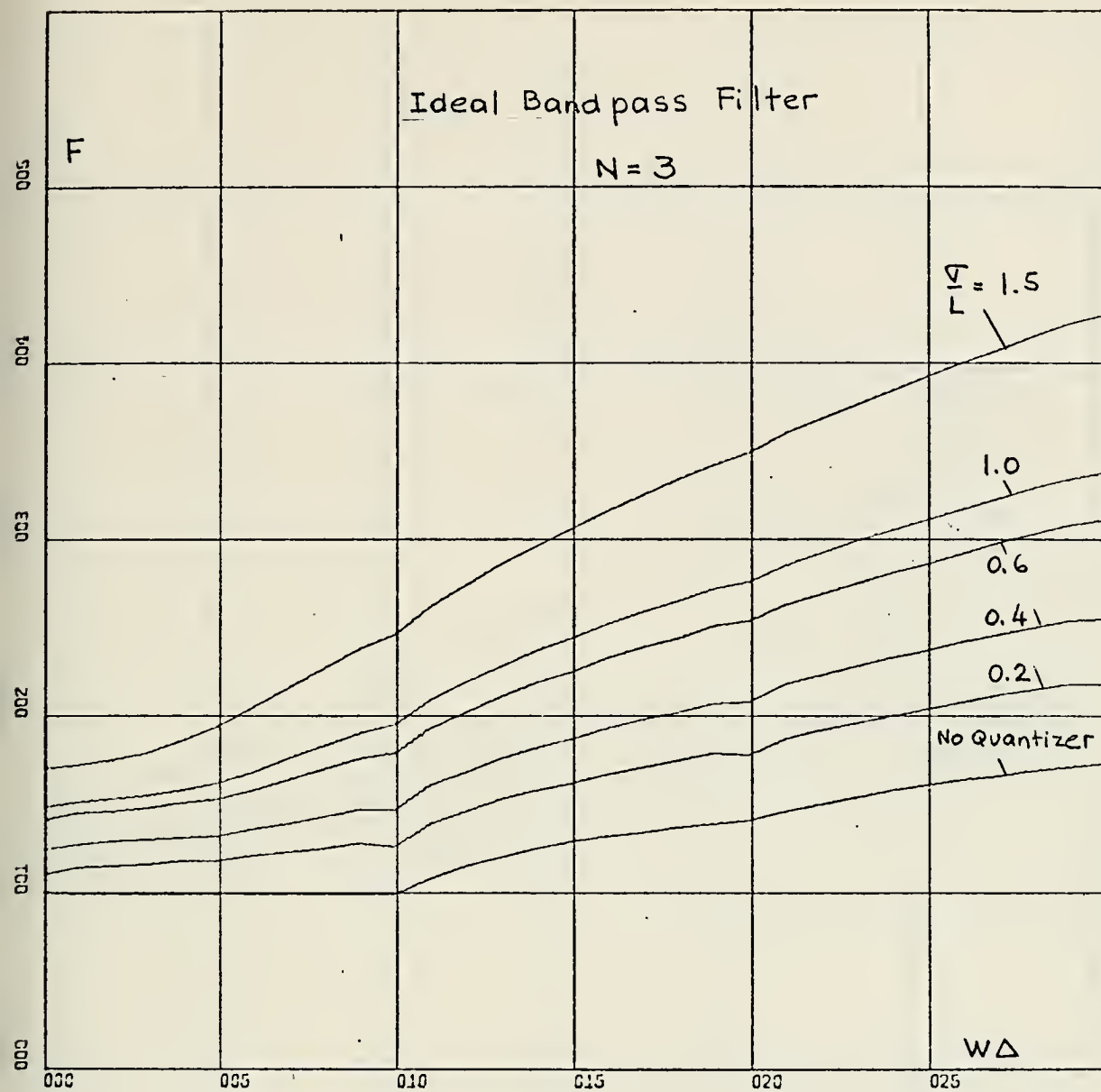




X-SCALE=5.00E-01 UNITS INCH.  
Y-SCALE=5.00E-01 UNITS INCH.

FIGURE 17

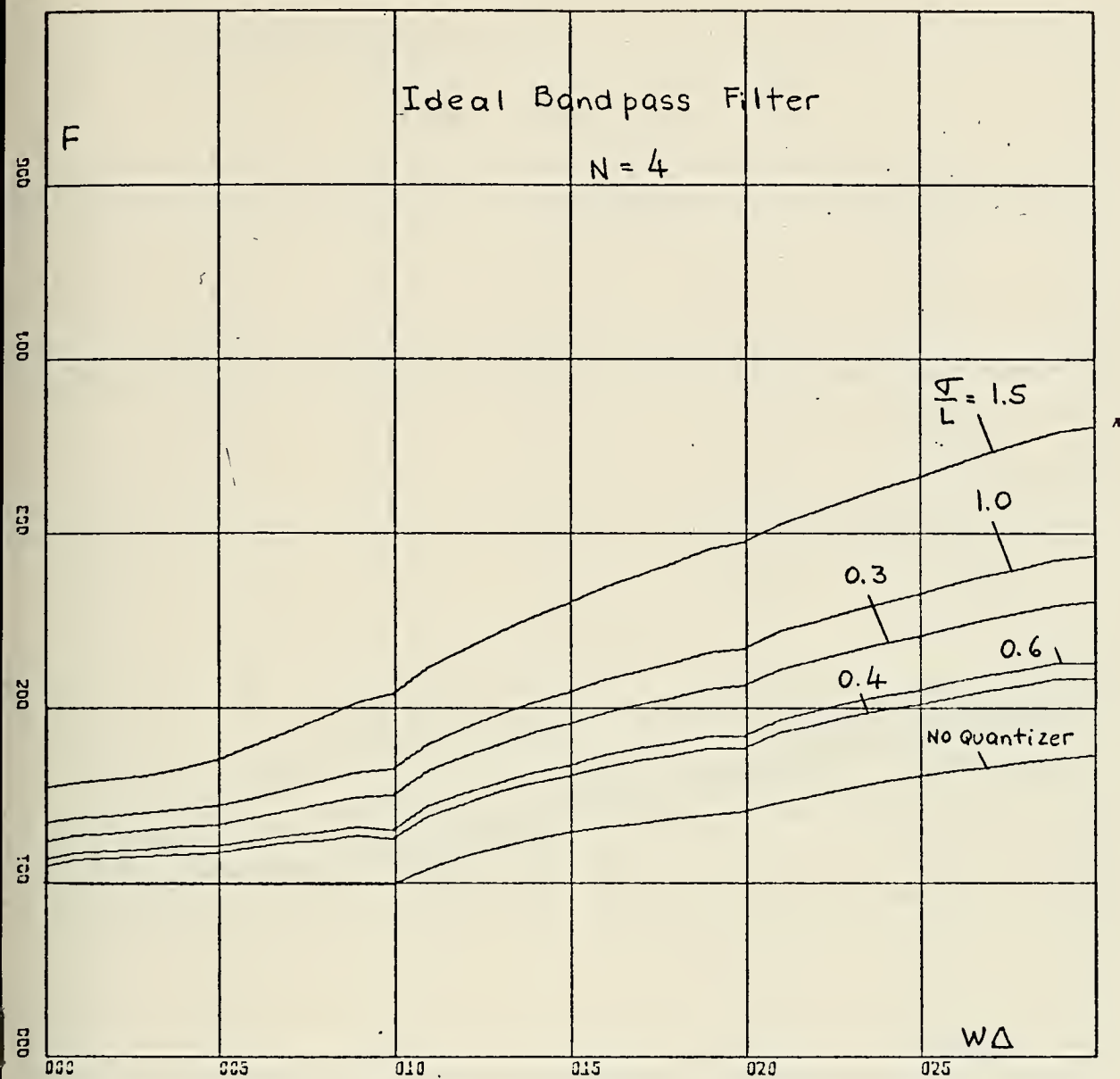




X-SCALE= $5.00E-01$  UNITS INCH.  
Y-SCALE= $1.00E+00$  UNITS INCH.

FIGURE 18

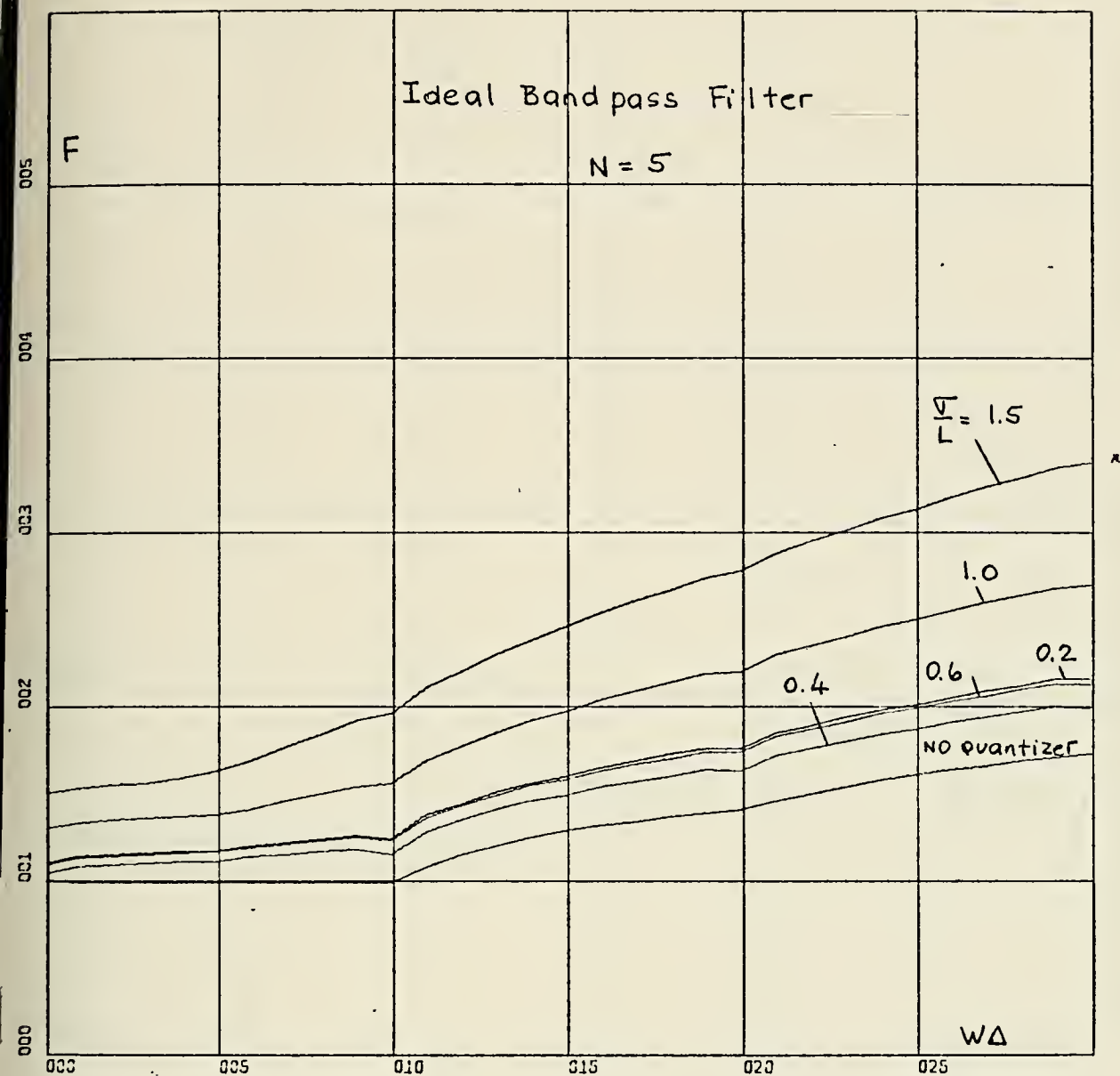




X-SCALE=5.00E-01 UNITS INCH.  
 Y-SCALE=1.00E+00 UNITS INCH.

FIGURE 19



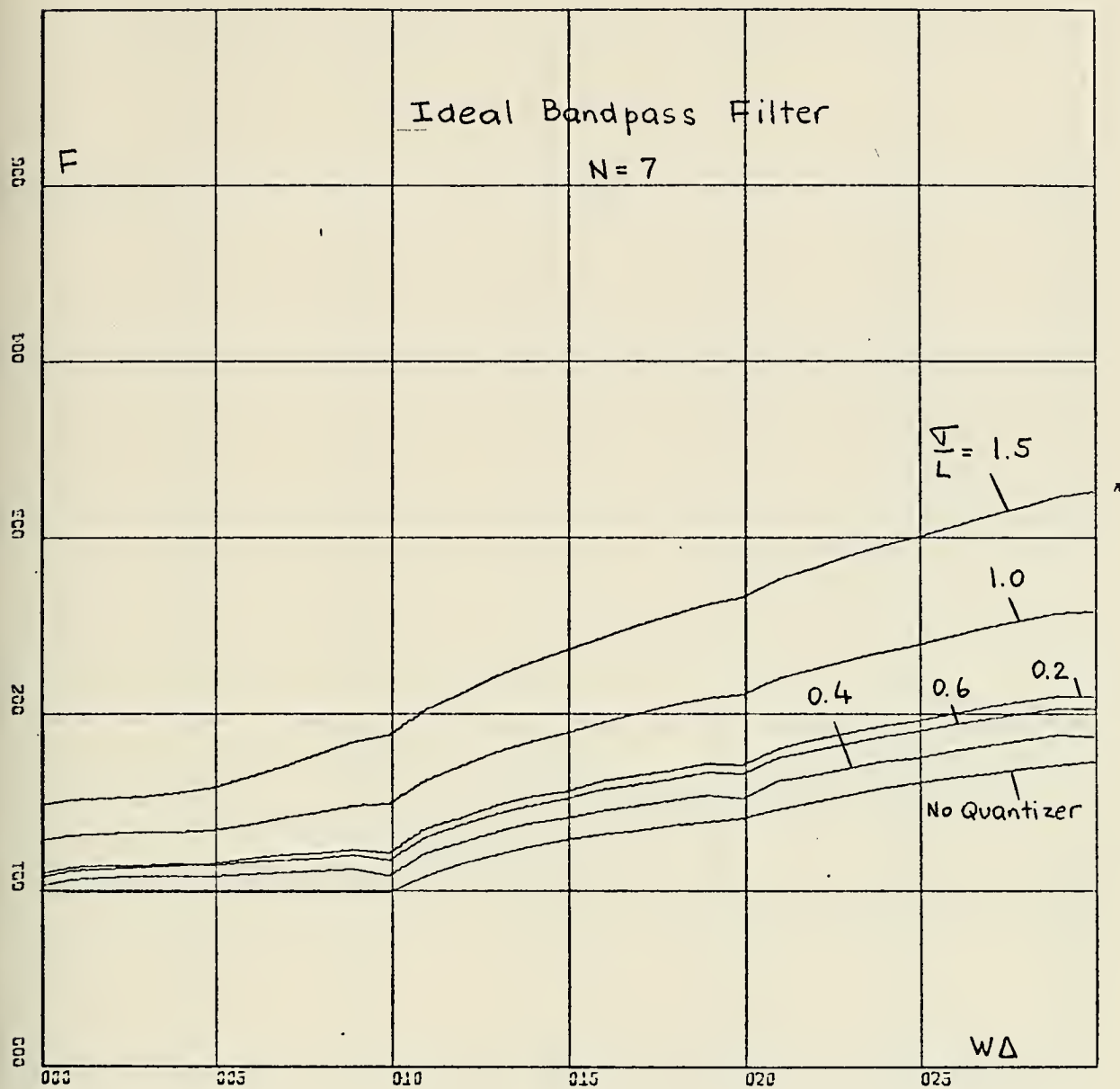


X-SCALE=5.00E-01 UNITS INCH.

Y-SCALE=1.00E+00 UNITS INCH.

FIGURE 20

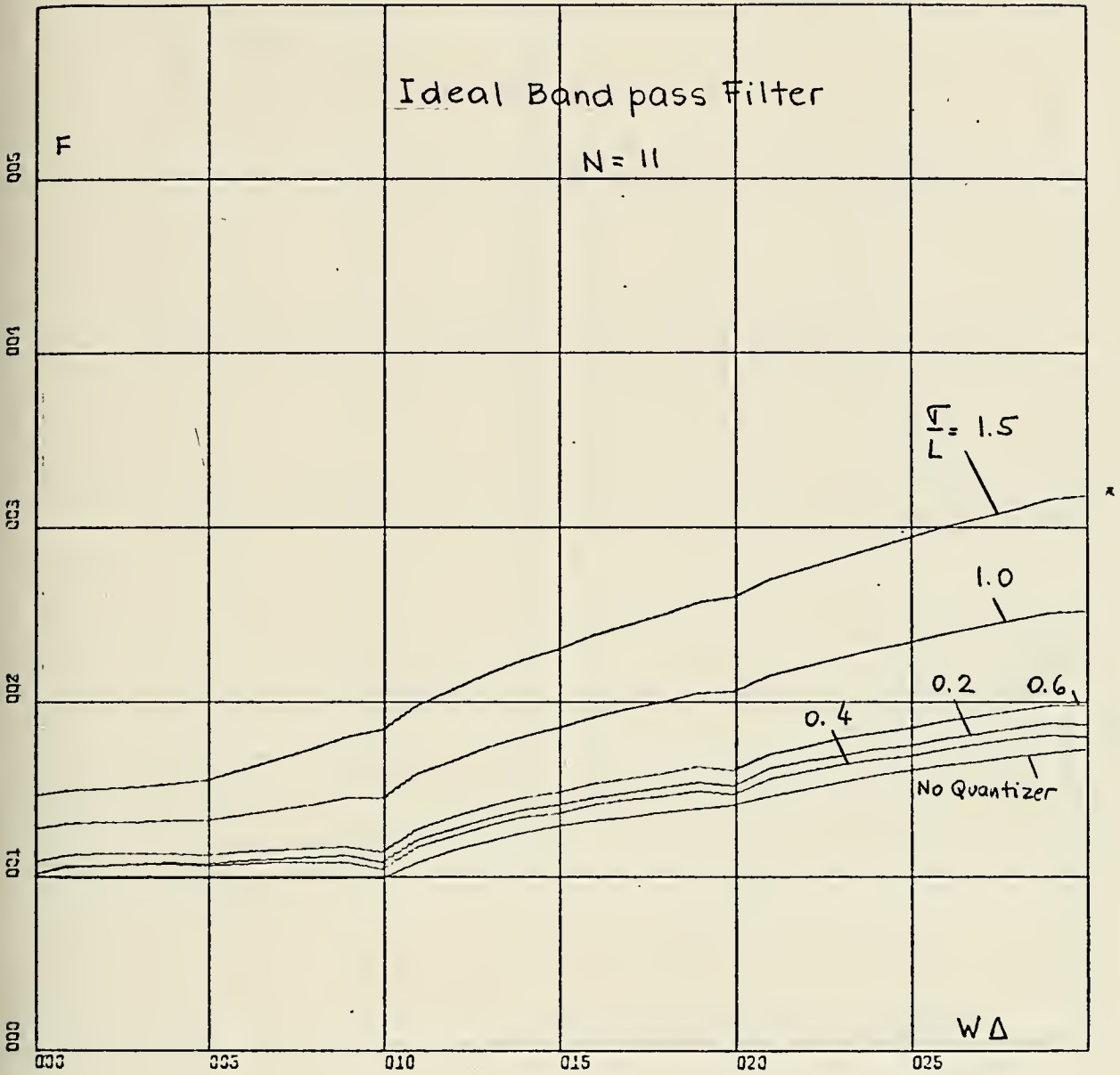




X-SCALE=5.00E-01 UNITS INCH.  
 Y-SCALE=1.00E+00 UNITS INCH.

FIGURE 21

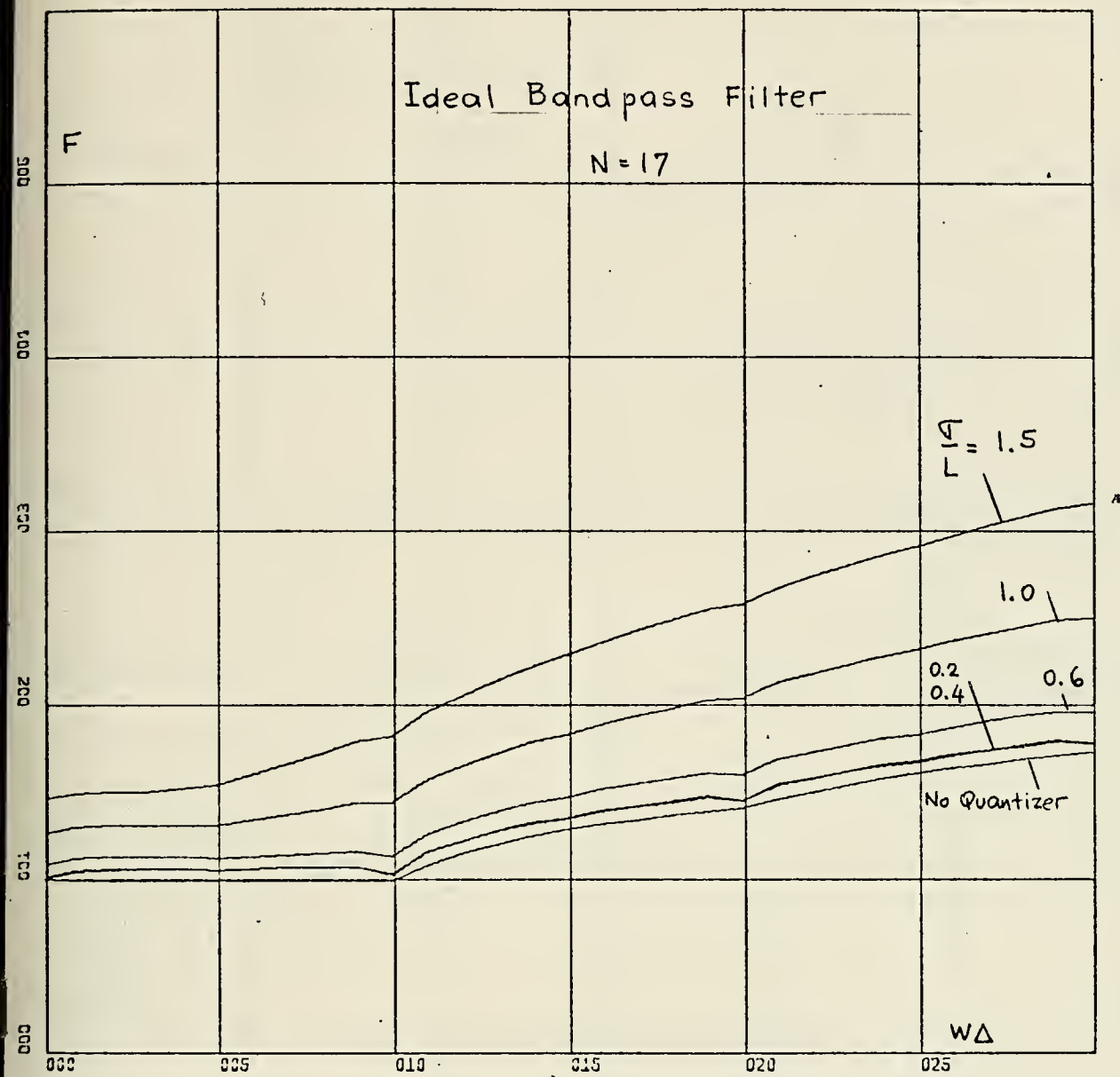




X-SCALE=5.00E-01 UNITS INCH.  
Y-SCALE=1.00E+00 UNITS INCH.

FIGURE 22



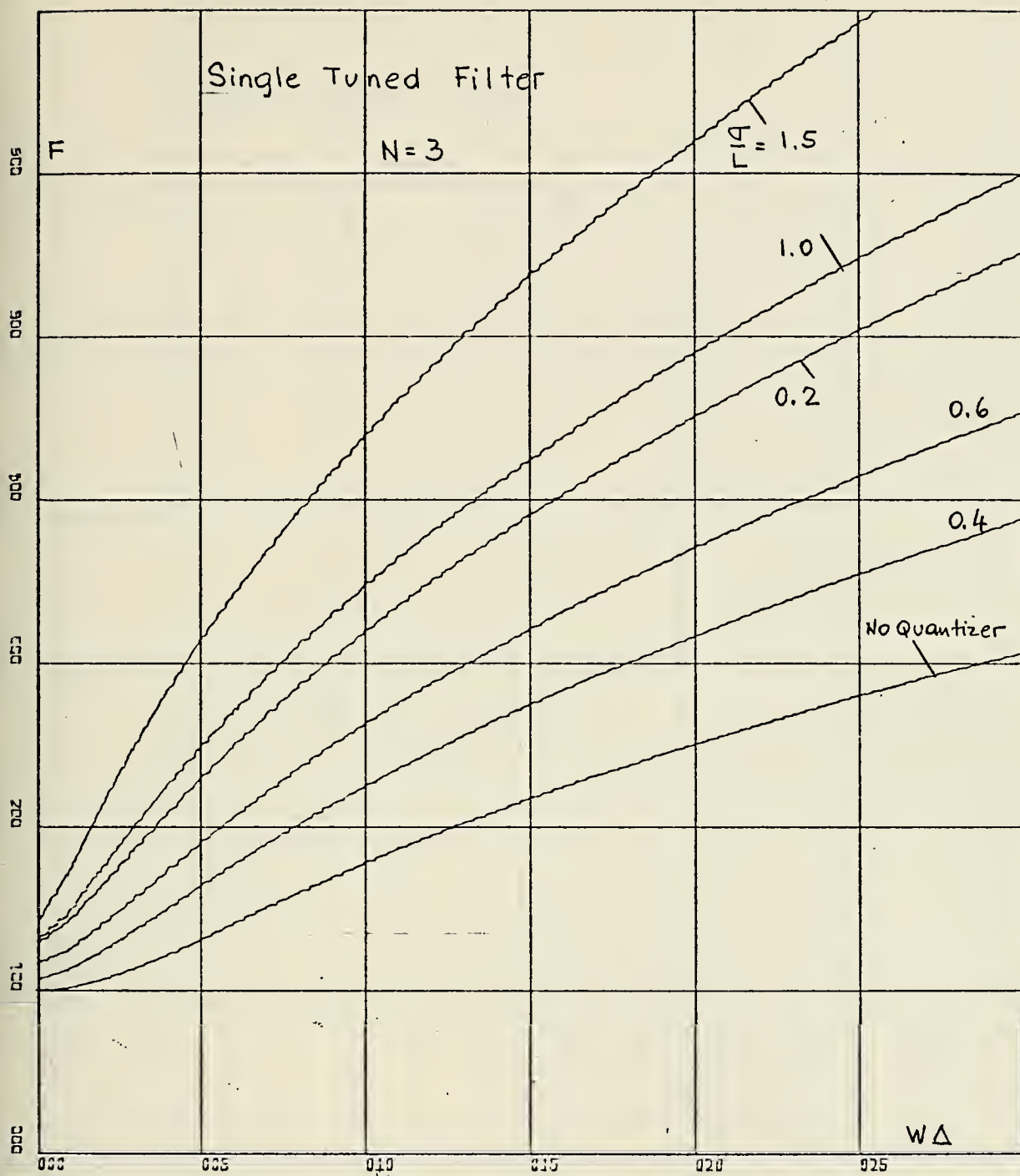


X-SCALE=5.00E-01 UNITS INCH.

Y-SCALE=1.00E+00 UNITS INCH.

FIGURE 23

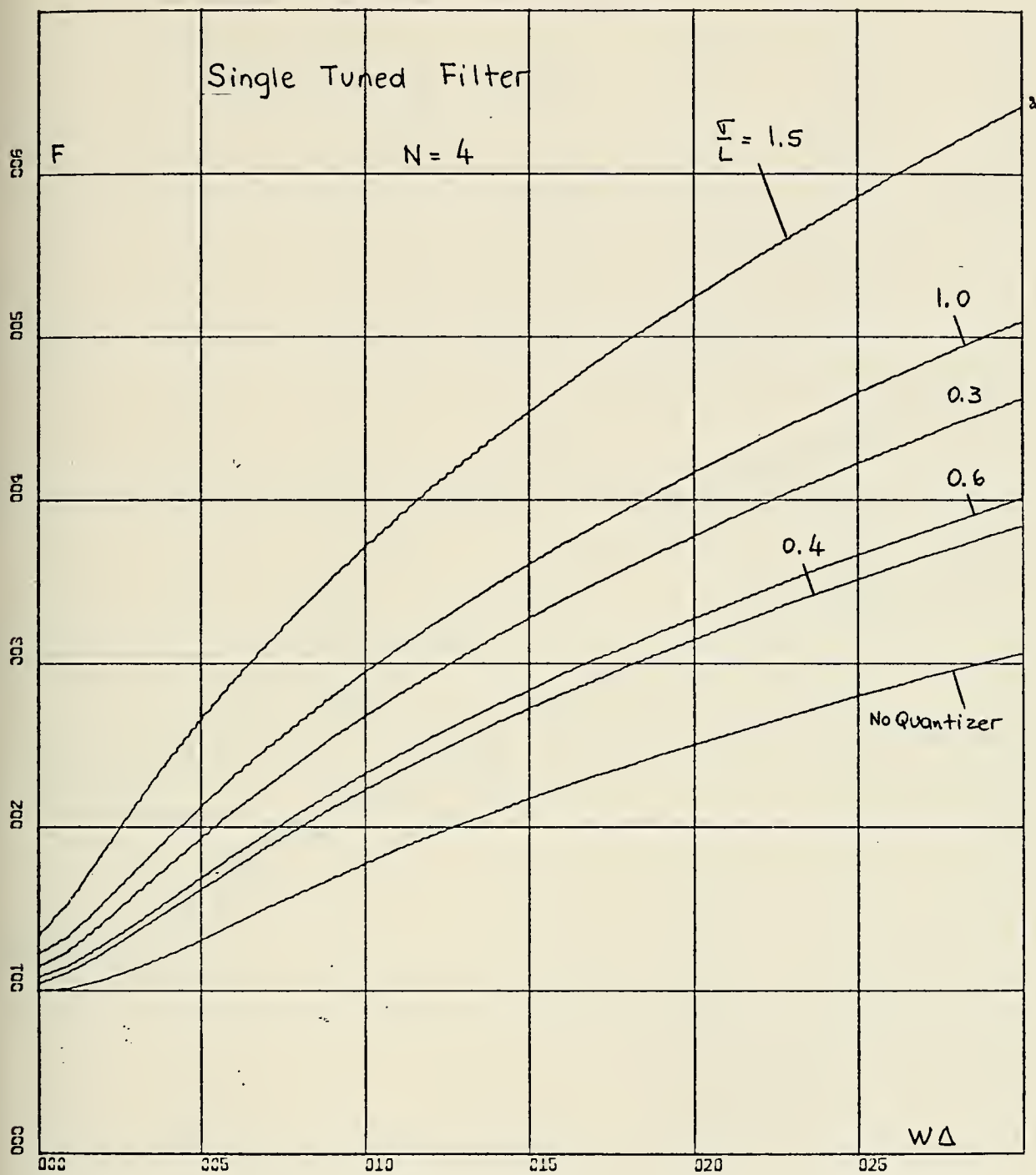




X-SCALE=5.00E-01 UNITS INCH.  
Y-SCALE=1.00E+00 UNITS INCH.

FIGURE 24



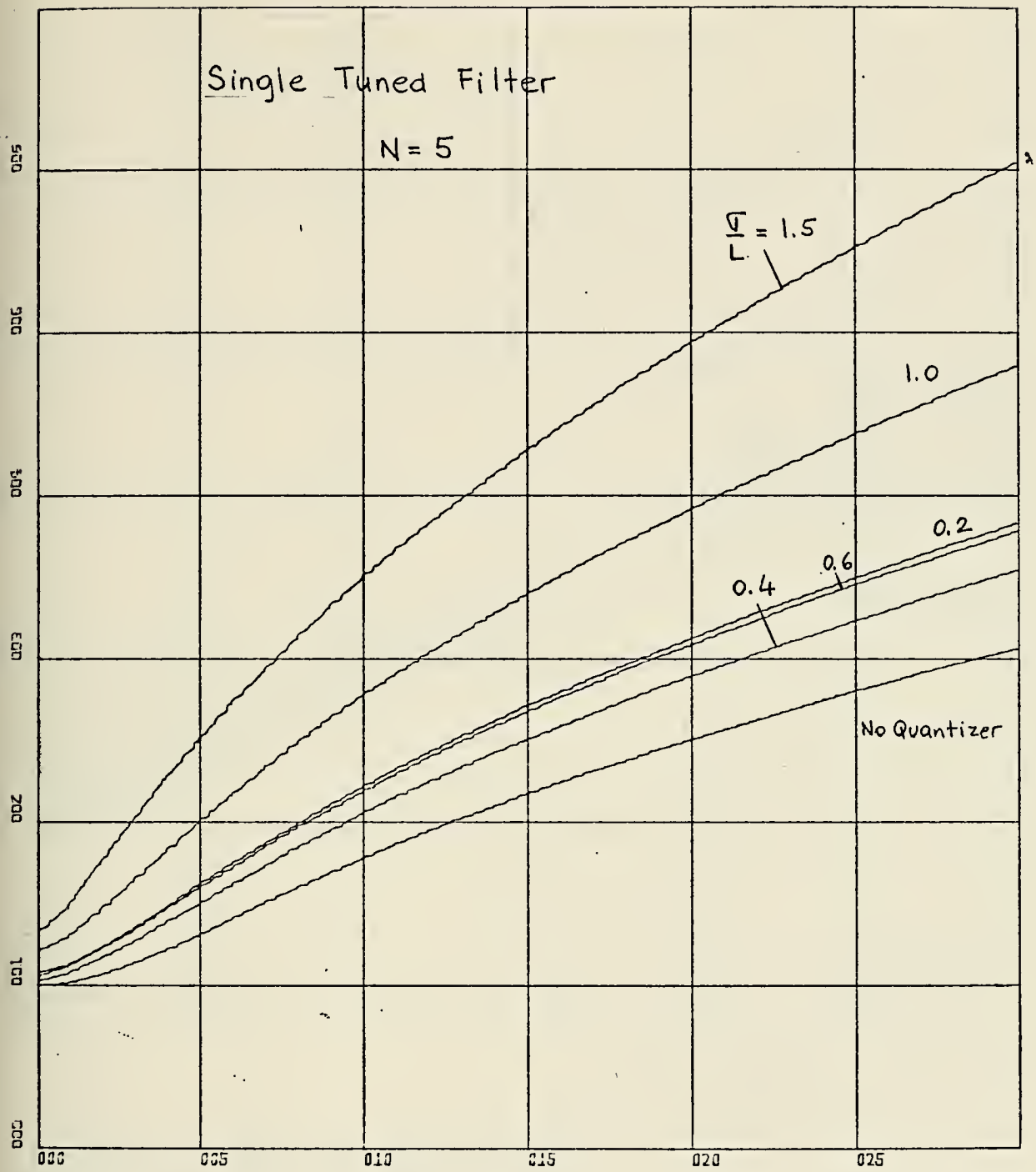


X-SCALE=5.00E-01 UNITS INCH.

Y-SCALE=1.00E+00 UNITS INCH.

FIGURE 25

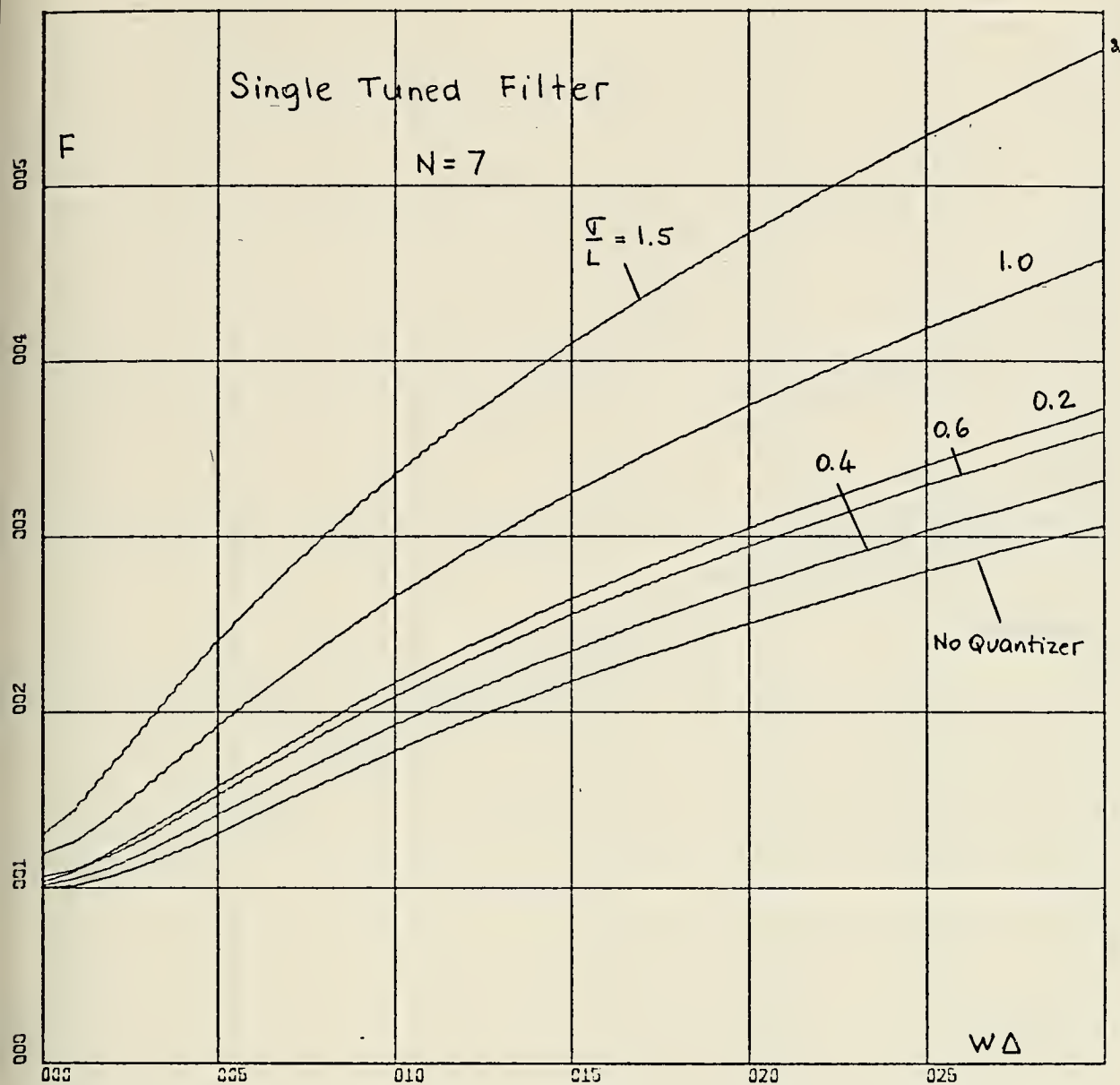




X-SCALE=5.00E-01 UNITS INCH.  
Y-SCALE=1.00E+00 UNITS INCH.

FIGURE 26

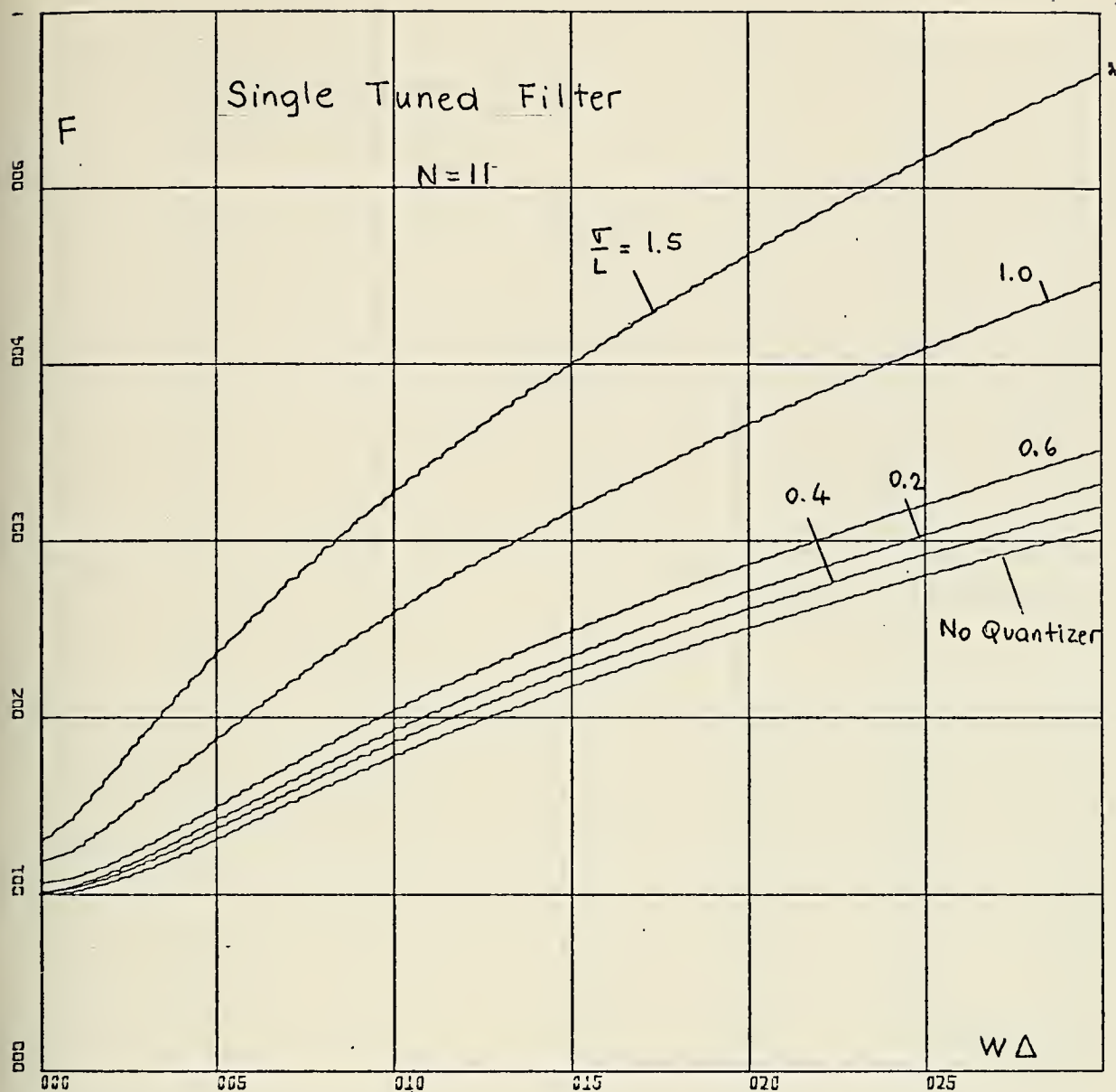




X-SCALE=5.00E-01 UNITS INCH.  
Y-SCALE=1.00E+00 UNITS INCH.

FIGURE 27



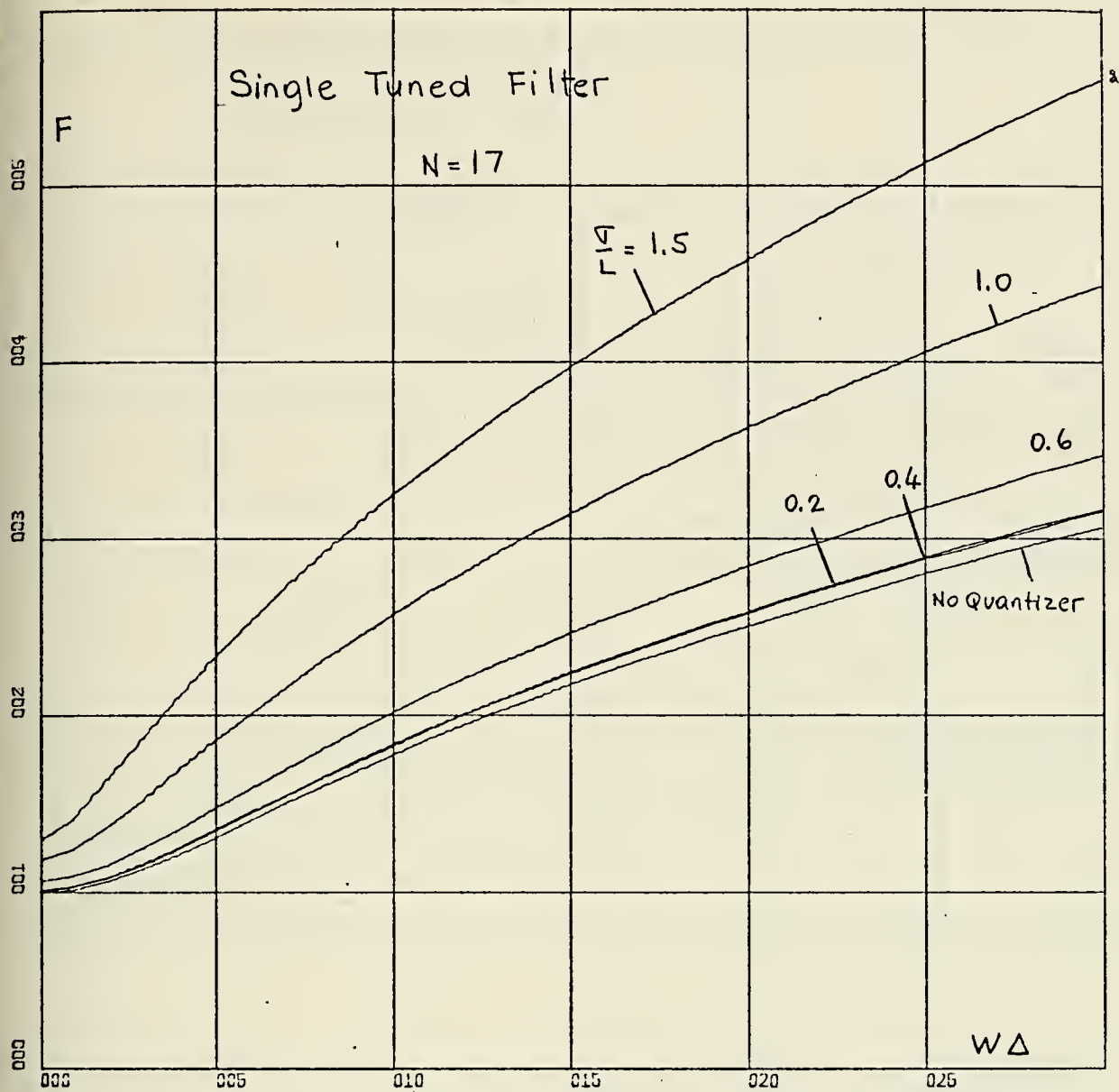


X-SCALE=5.00E-01 UNITS INCH.

Y-SCALE=1.00E+00 UNITS INCH.

FIGURE 28

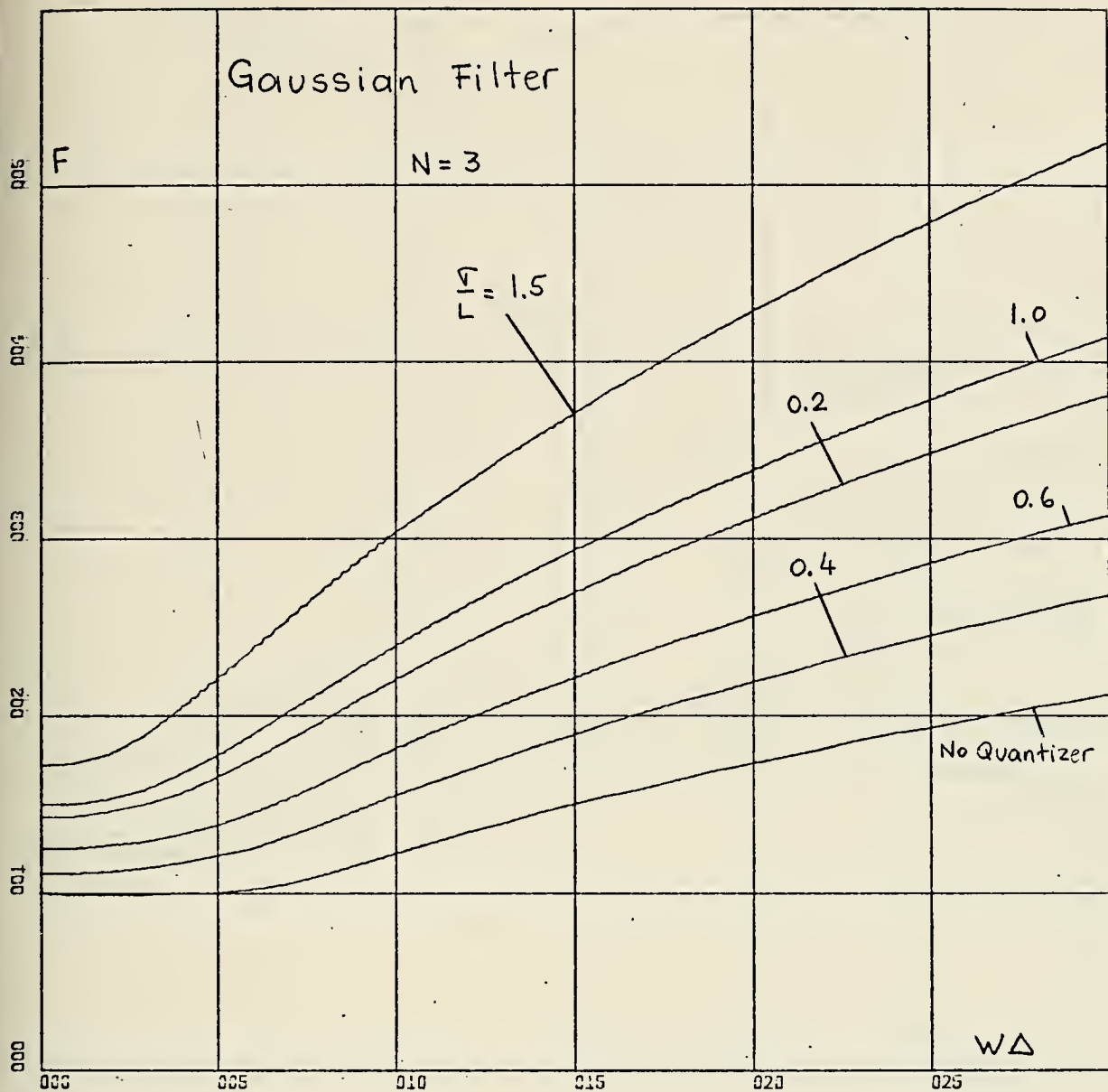




X-SCALE=5.00E-01 UNITS INCH.  
Y-SCALE=1.00E+00 UNITS INCH.

FIGURE 29



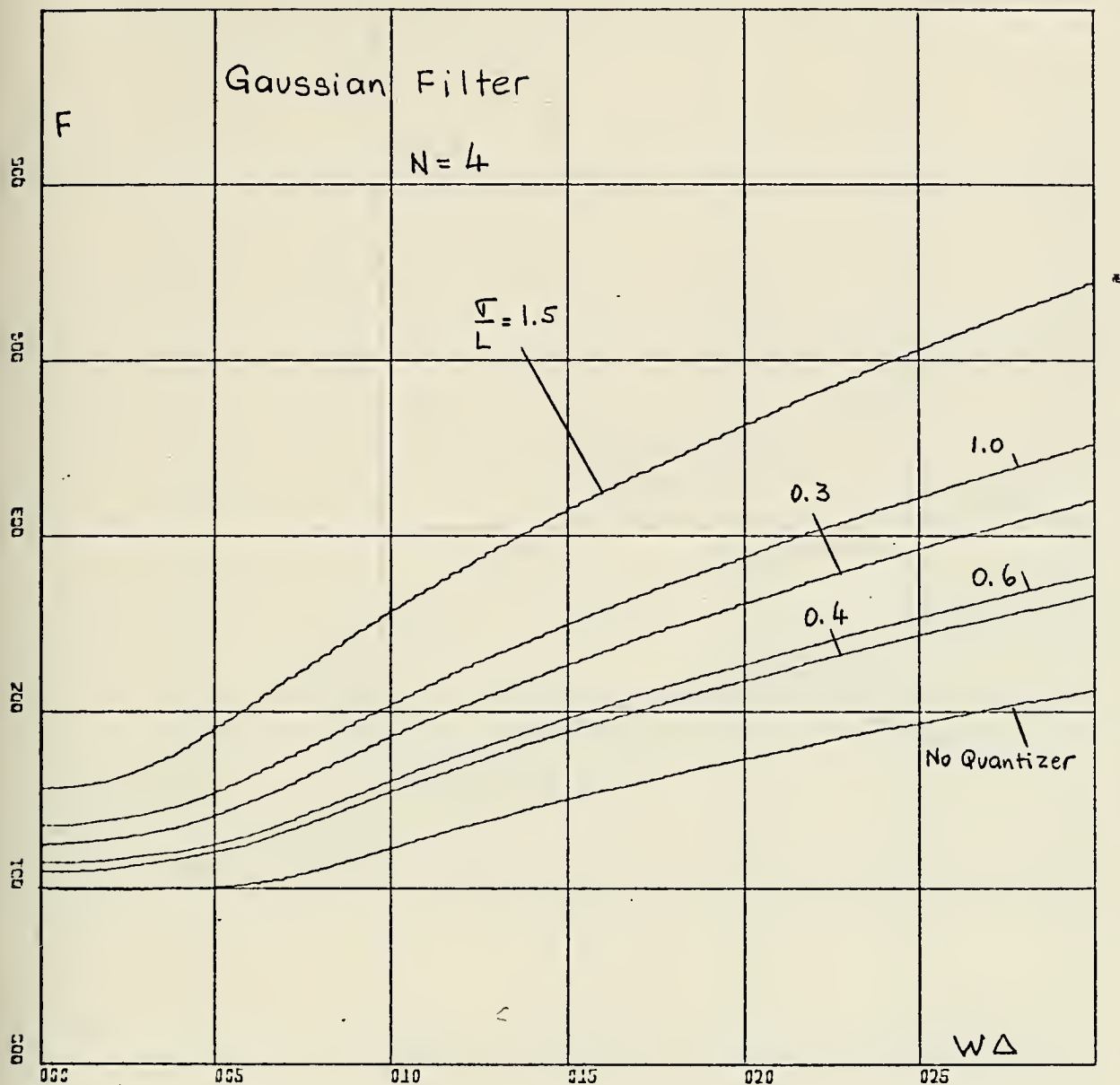


X-SCALE=5.00E-01 UNITS INCH.

Y-SCALE=1.00E+00 UNITS INCH.

FIGURE 30



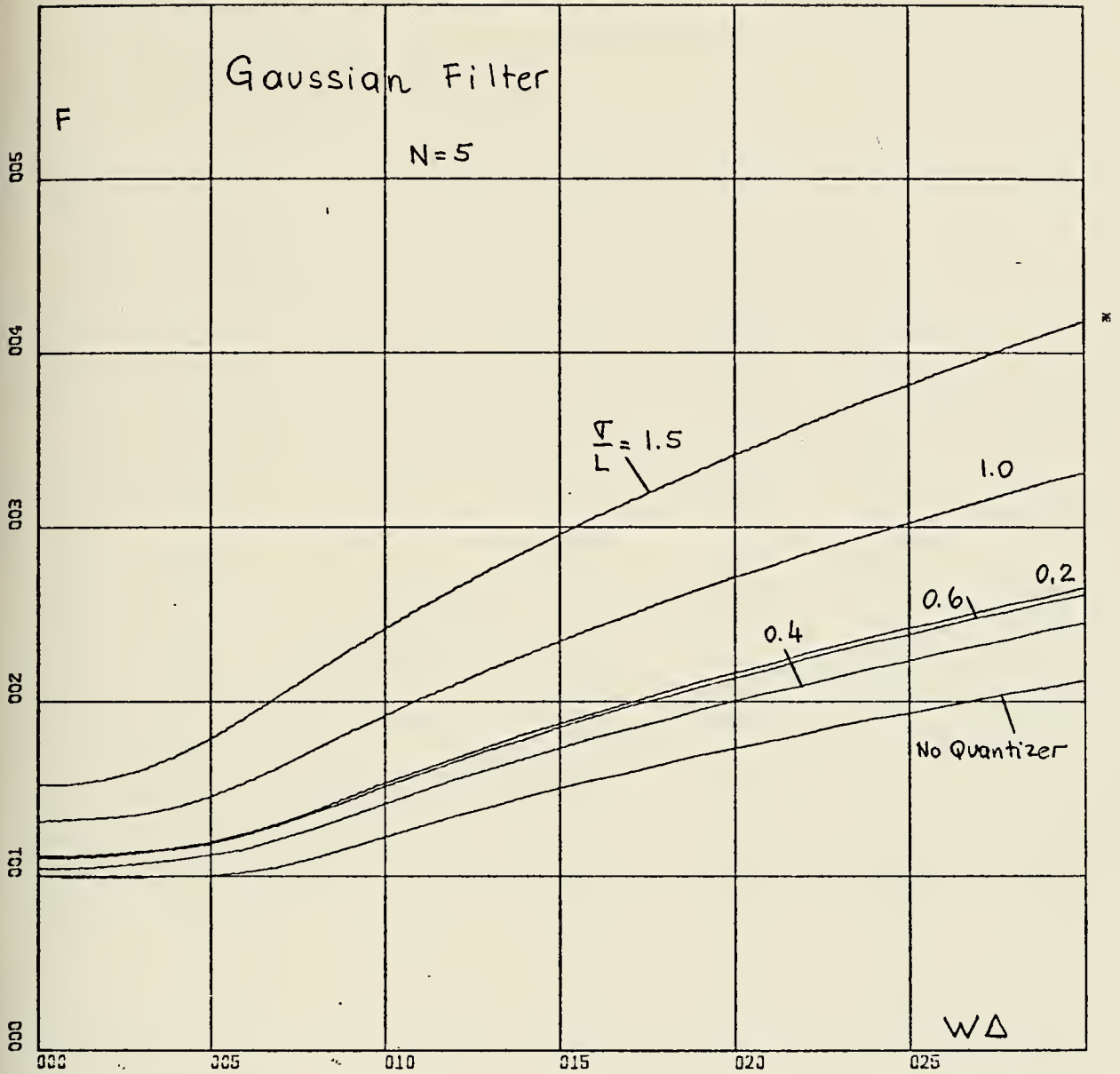


X-SCALE=5.00E-01 UNITS INCH.

Y-SCALE=1.00E+00 UNITS INCH.

FIGURE 31



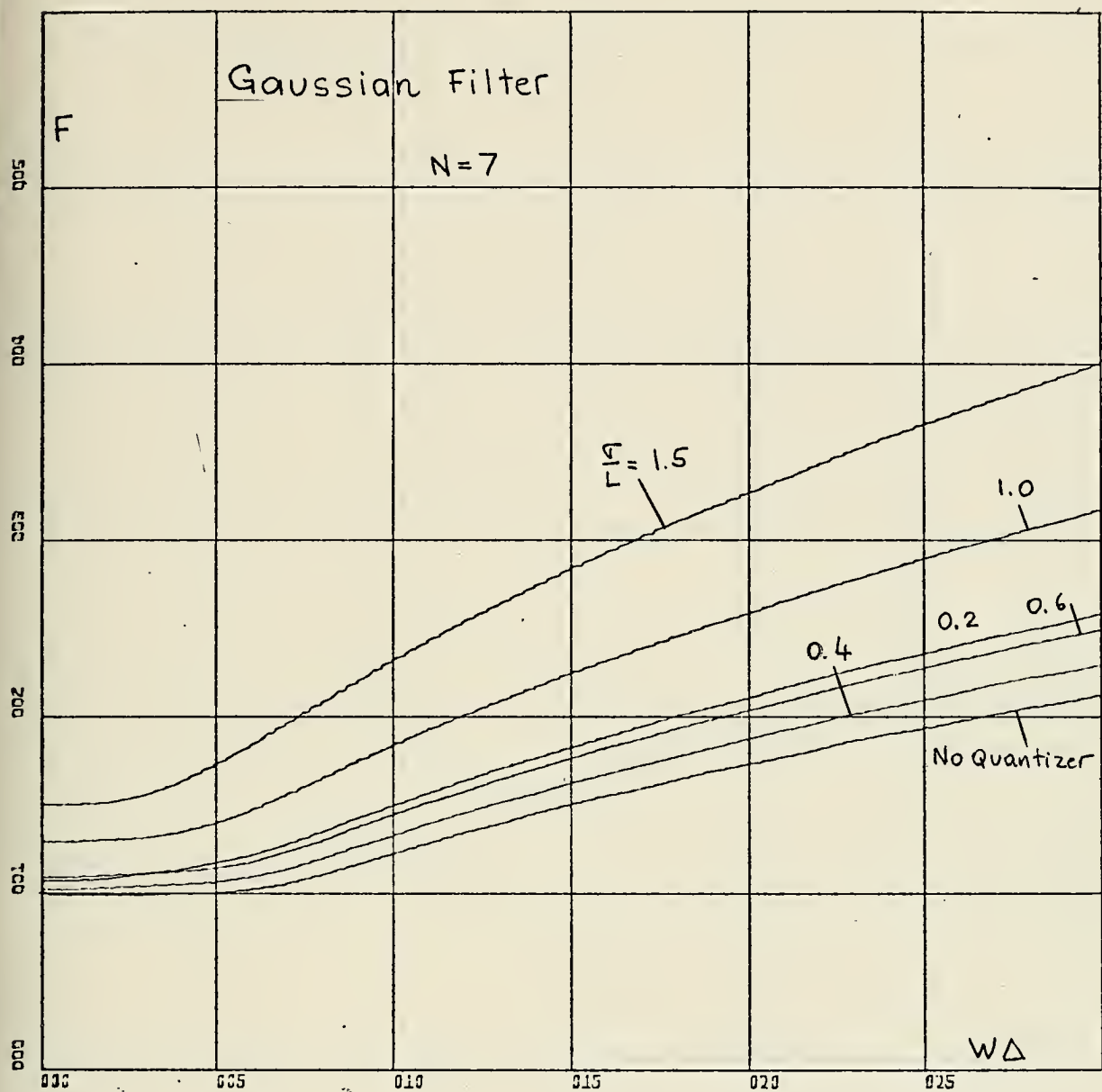


X-SCALE=5.00E-01 UNITS INCH.

Y-SCALE=1.00E+00 UNITS INCH.

FIGURE 32

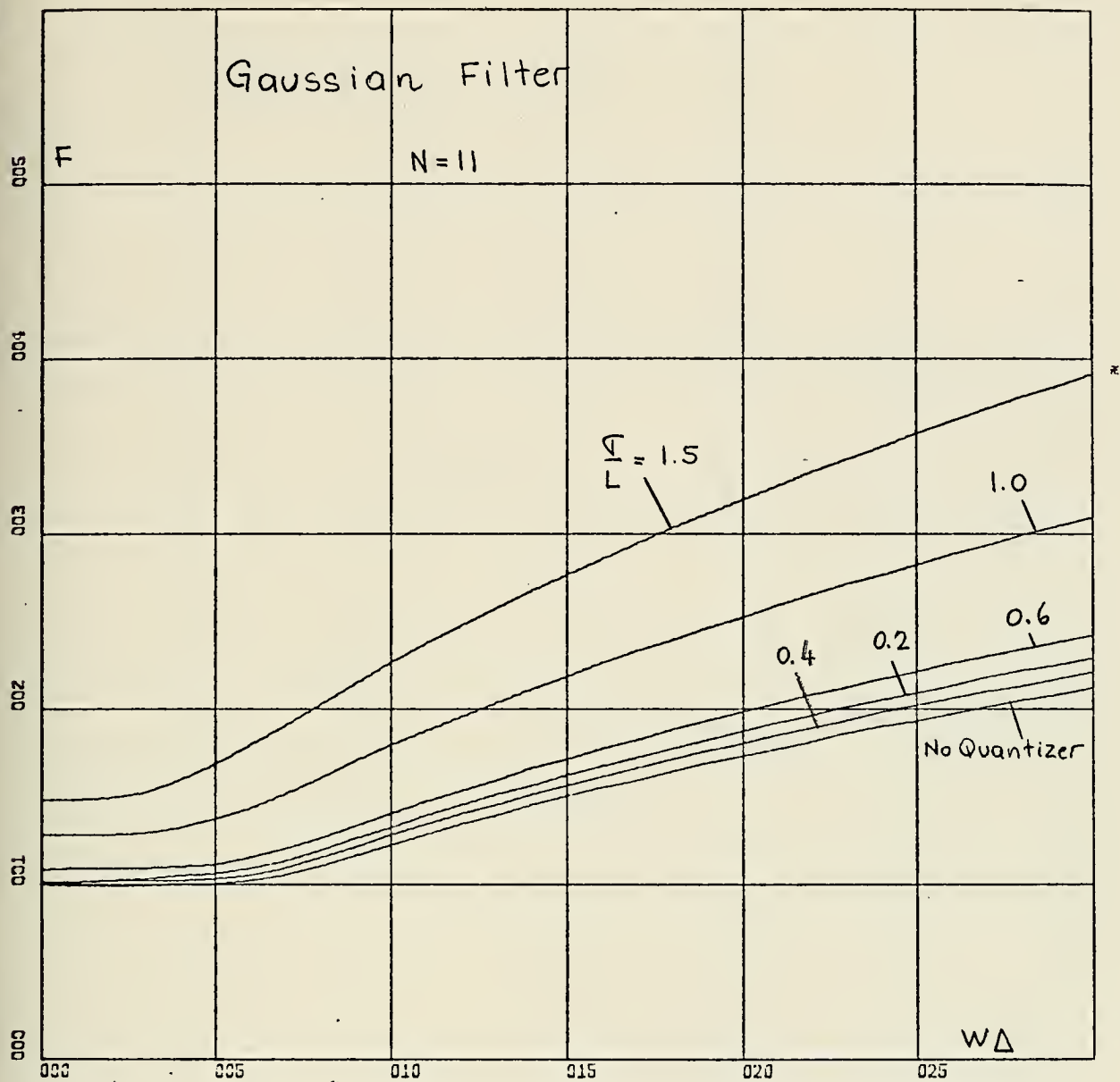




X-SCALE=5.00E-01 UNITS INCH.  
Y-SCALE=1.00E+00 UNITS INCH.

FIGURE 33



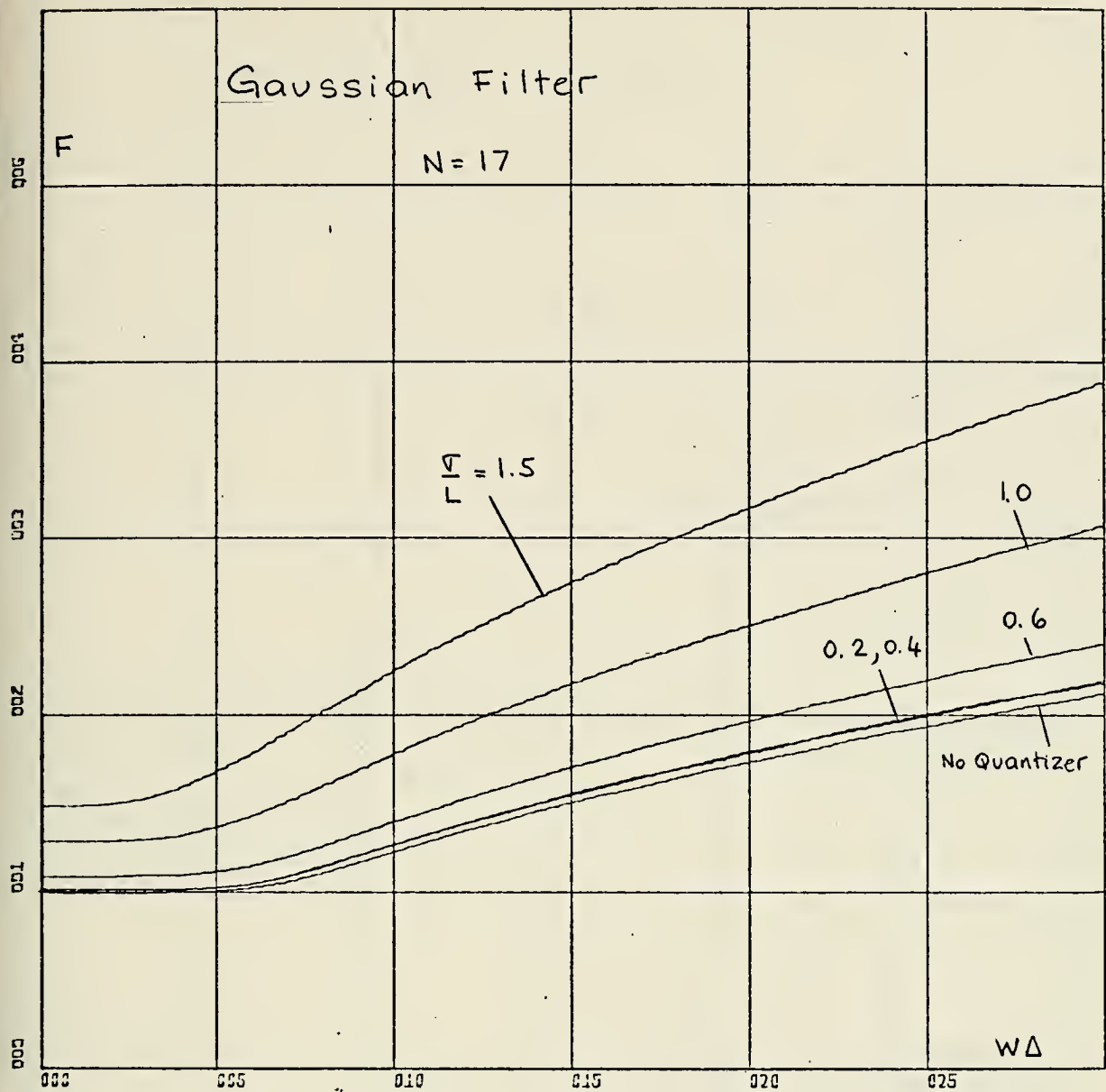


X-SCALE=5.00E-01 UNITS INCH.

Y-SCALE=1.00E+00 UNITS INCH.

FIGURE 34



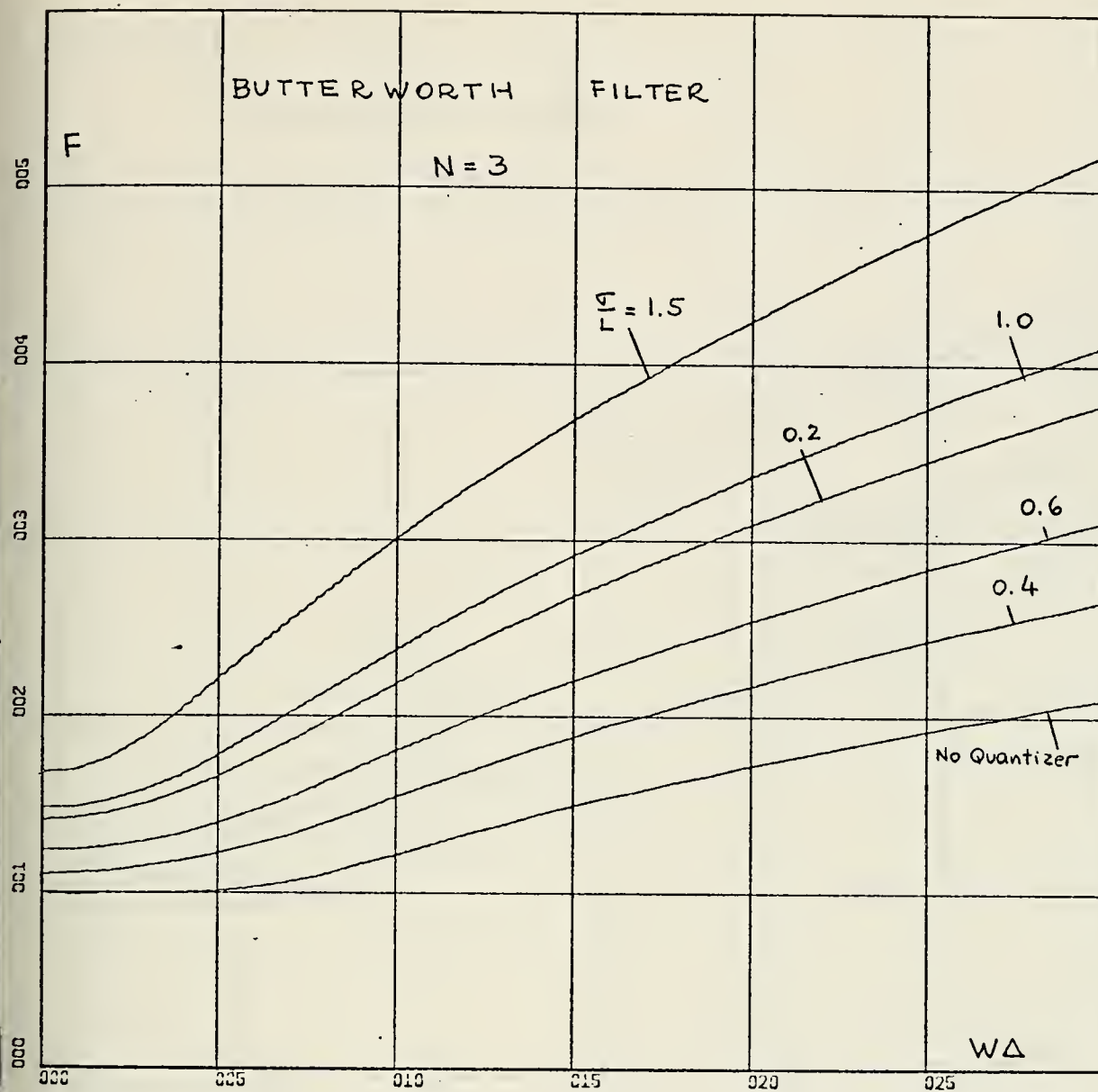


X-SCALE=5.00E-01 UNITS INCH.

Y-SCALE=1.00E+00 UNITS INCH.

FIGURE 35



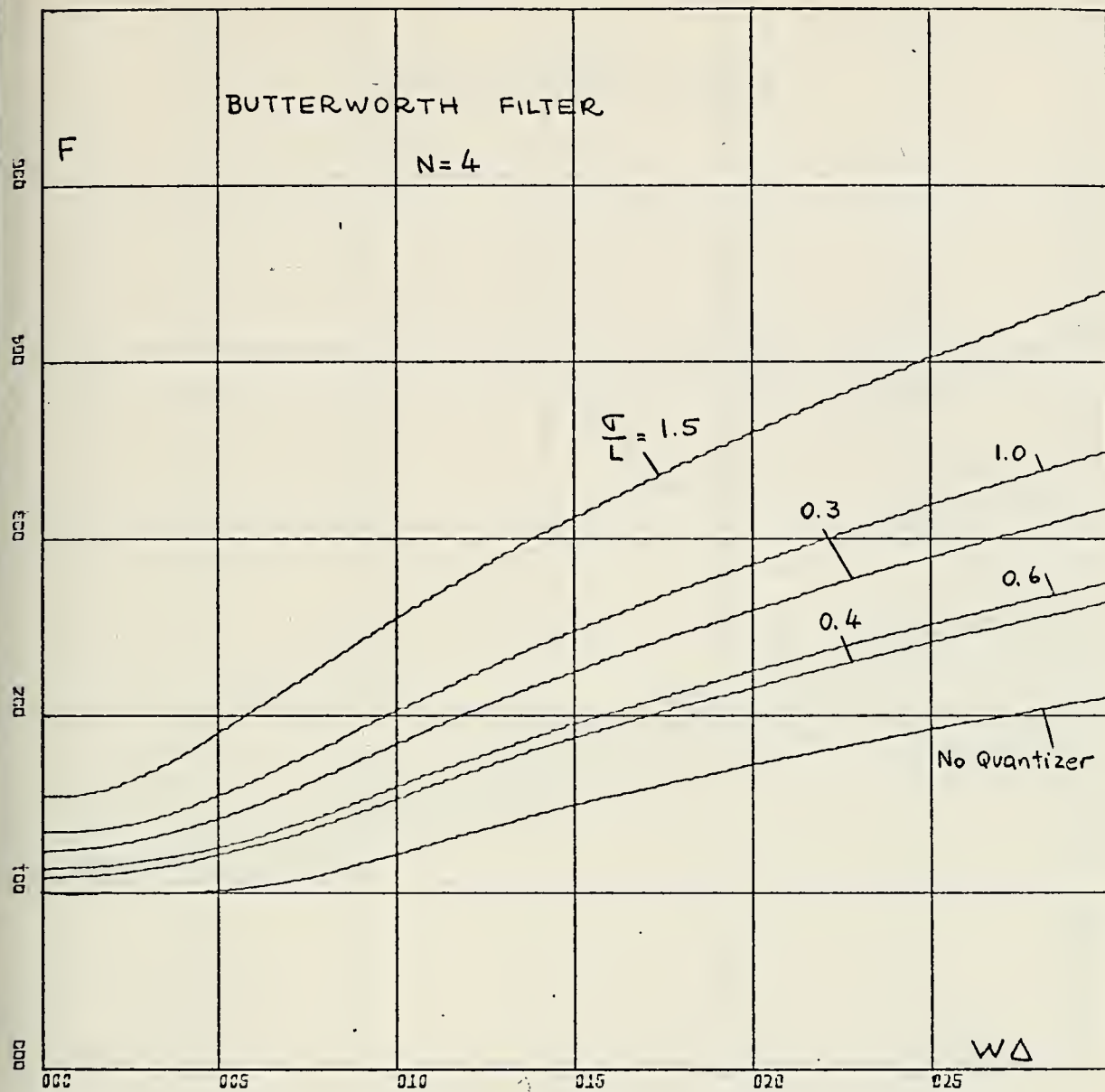


X-SCALE=5.00E-01 UNITS INCH.

Y-SCALE=1.00E+00 UNITS INCH.

FIGURE 36

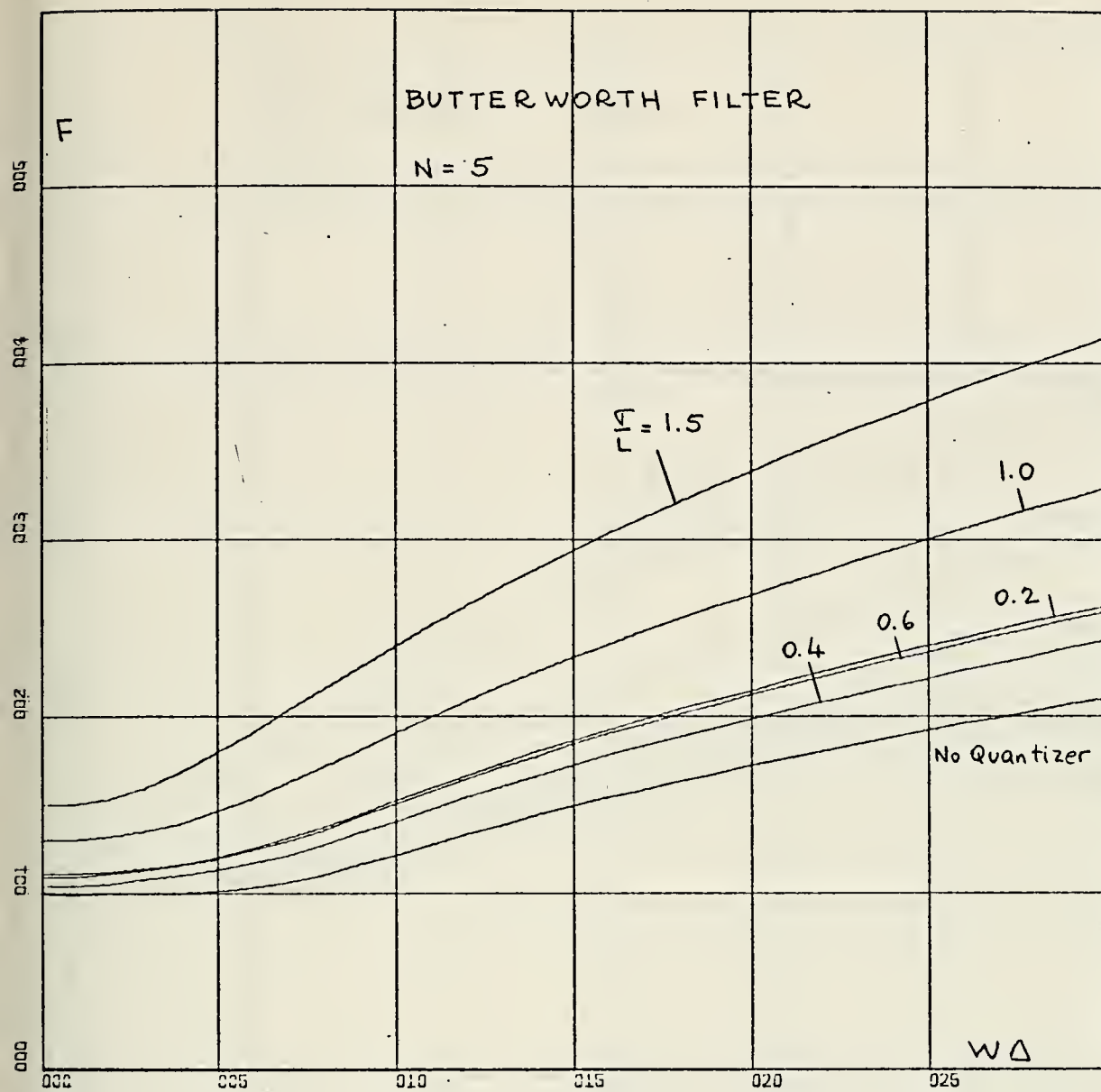




X-SCALE=5.00E-01 UNITS INCH.  
Y-SCALE=1.00E+00 UNITS INCH.

FIGURE 37



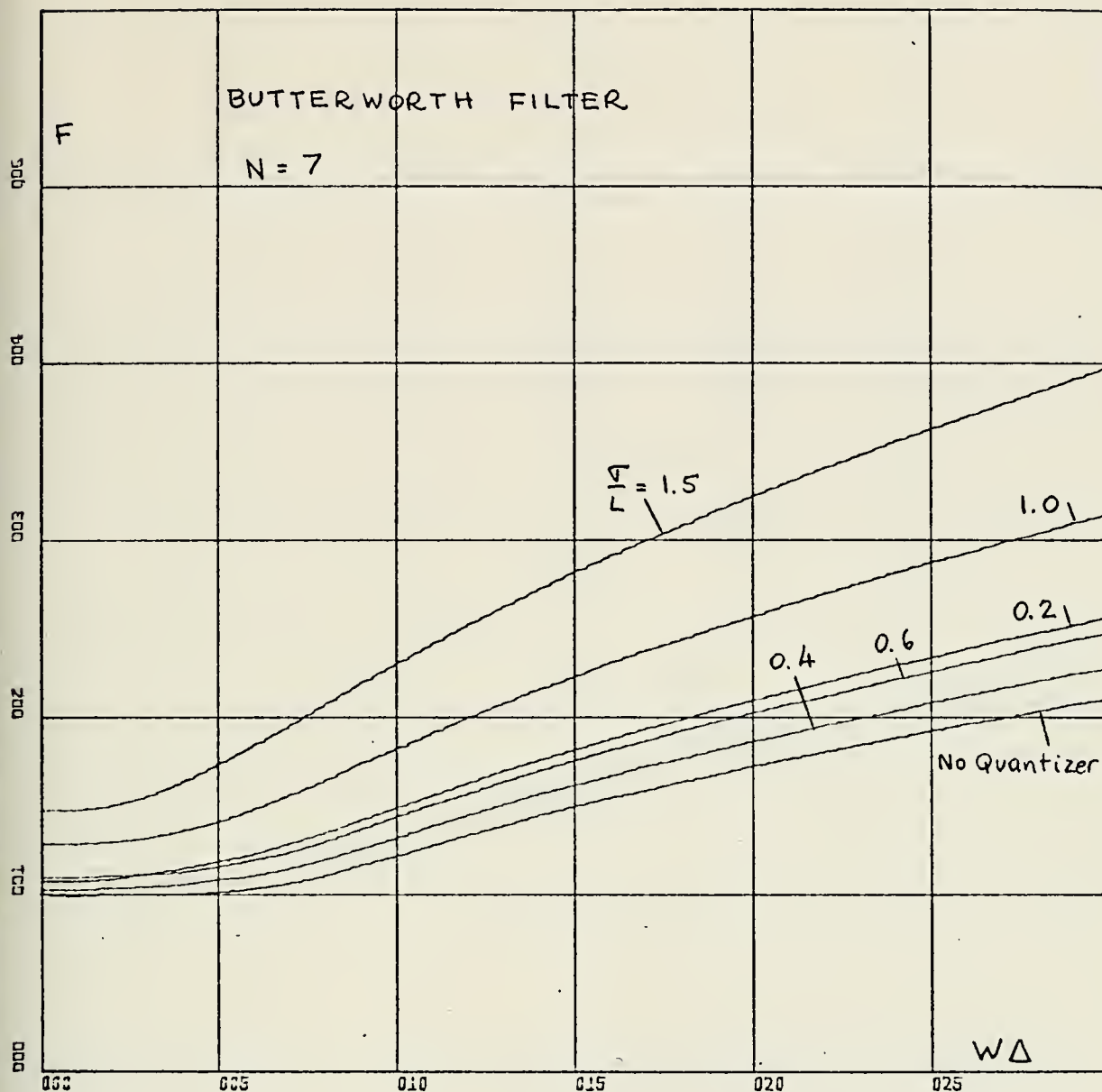


X-SCALE=5.00E-01 UNITS INCH.

Y-SCALE=1.00E+00 UNITS INCH.

FIGURE 38



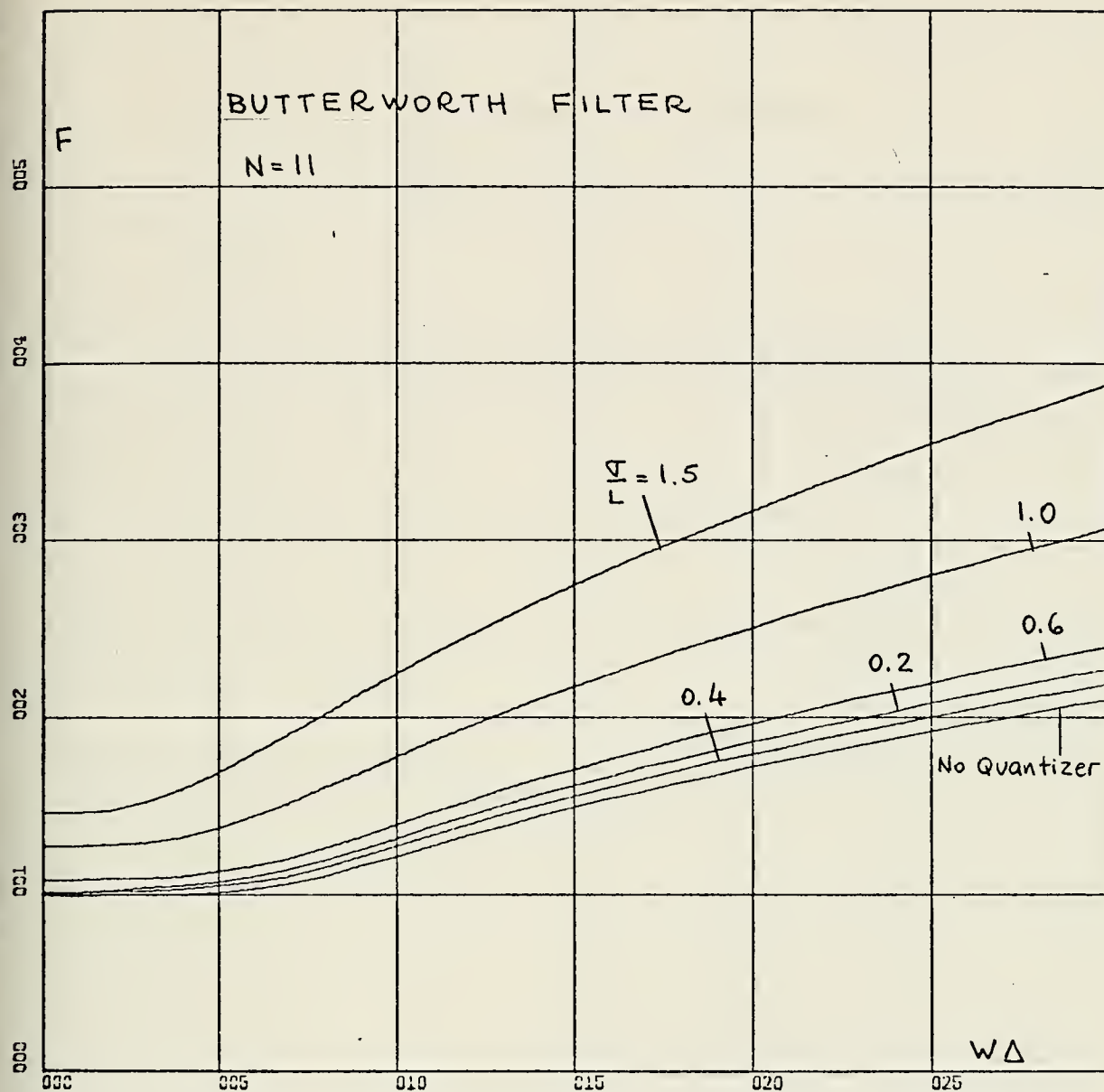


X-SCALE=5.00E-01 UNITS INCH.

Y-SCALE=1.00E+00 UNITS INCH.

FIGURE 39

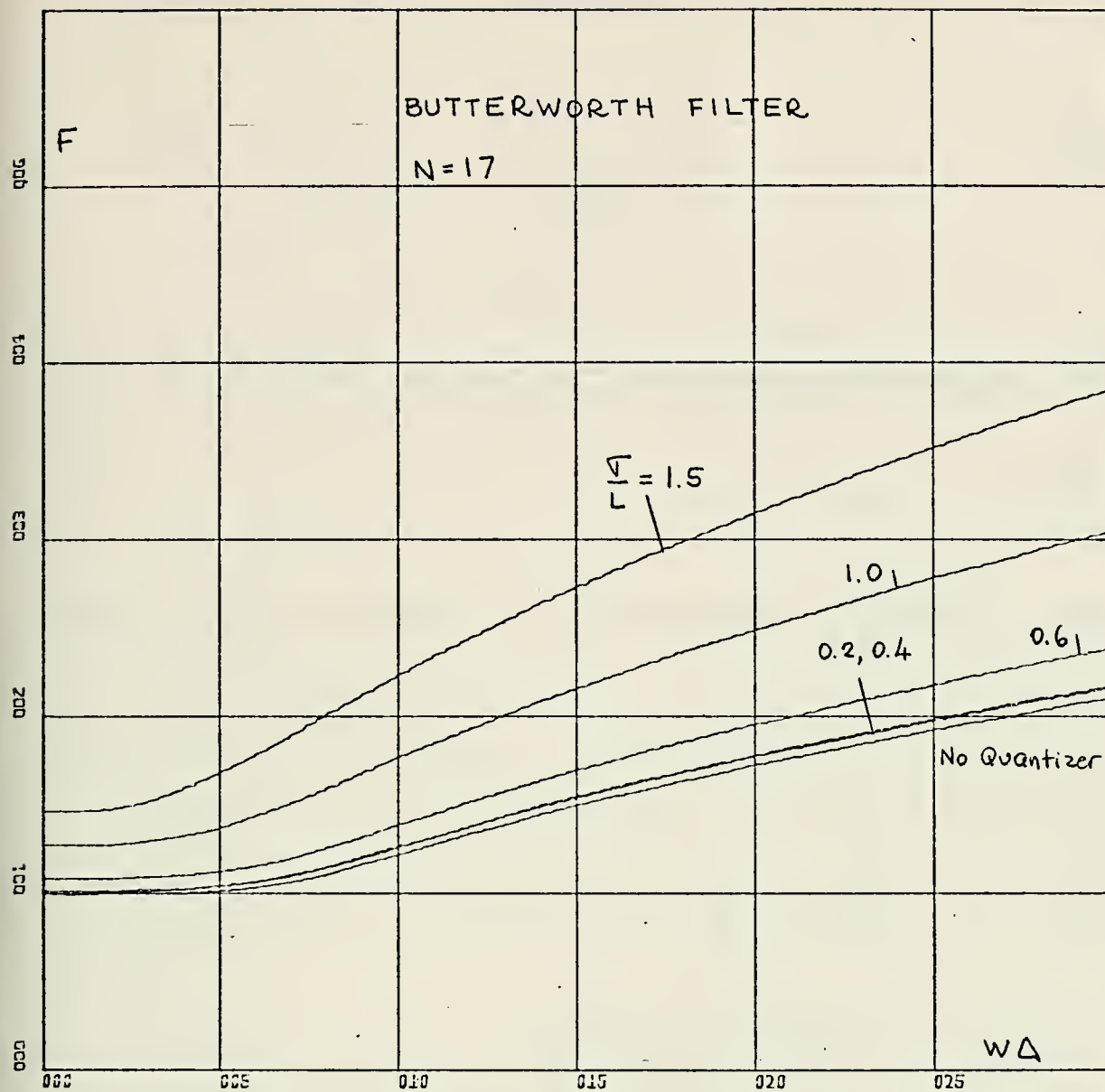




X-SCALE=5.00E-01 UNITS INCH.  
Y-SCALE=1.00E+00 UNITS INCH.

FIGURE 40





X-SCALE=5.00E-01 UNITS INCH.

Y-SCALE=1.00E+00 UNITS INCH.

FIGURE 41



function of  $e_k$  is the following [Ref. 13]

$$f(e_k) = \begin{cases} \frac{1}{a} & -\frac{a}{2} < e_k < \frac{a}{2} \\ 0 & |e_k| \geq \frac{a}{2} \end{cases} \quad (113)$$

Then

$$I_1 = \frac{1}{n} \sum_{k=1}^n q_c^2(k\Delta) = \frac{1}{n} \sum_{k=1}^n [X_c^2(k\Delta) + 2e_k X_c(k\Delta) + e_k^2] \quad (114)$$

and

$$E[I_1] = \frac{1}{n} \sum_{k=1}^n E[X_c^2(k\Delta)] + \frac{1}{n} \sum_{k=1}^n E[2e_k X_c(k\Delta)] + \frac{1}{n} \sum_{k=1}^n E[e_k^2] \quad (115)$$

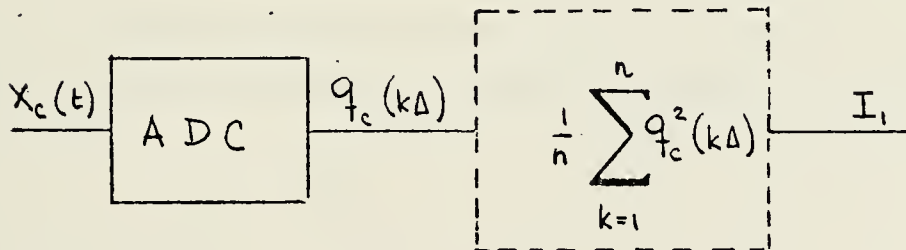


FIGURE 42



Assuming  $e_k$  and  $X_c(k\Delta)$  are uncorrelated, which is a good assumption if the step size is small compared with  $\sigma_{X_c}$ .

$$E[I_1] = \sigma_{X_c}^2 + \frac{a^2}{12} \quad (116)$$

Now

$$E[I_1^2] = \frac{1}{n^2} E \left[ \sum_{j=1}^n X_c^2(j\Delta) + 2 \sum_{j=1}^n e_j X_c(j\Delta) + \sum_{j=1}^n e_j^2 \right] \cdot \quad (117)$$

$$\left[ \sum_{k=1}^n X_c^2(k\Delta) + 2 \sum_{k=1}^n e_k X_c(k\Delta) + \sum_{k=1}^n e_k^2 \right]$$

Expanding (117) and using (23) and the assumption that  $e_k$  and  $e_j$  are independent for  $k \neq j$ , which is good if the sampling rate is slow, it follows that

$$\sigma_{I_1}^2 = \frac{2\sigma_{X_c}^4}{n} + \frac{4}{n^2} \sum_{k=1}^n (n-k) R_{X_c}^2(k\Delta) + \frac{1}{n} \frac{a^2}{3} \sigma_{X_c}^2 + \frac{1}{n} \frac{a^4}{720} \quad (118)$$

It was shown previously that for the case of Figure 2, if  $H_o(f)$  was symmetrical about  $f_o$ , then

$$\sigma_I^2 = 2\sigma_{I_1}^2 \quad (119)$$

and

$$E[I] = 2 E[I_1] \quad (120)$$



Using (119) and (120) it follows that

$$F^2 = B_E \Delta + \frac{2B_E \Delta}{\sigma_{X_c}^4} \sum_{k=1}^{n-1} \left(1 - \frac{k}{n}\right) R_{X_c}^2(k\Delta) + \frac{1}{6} \frac{a^2}{\sigma_{X_c}^2} B_E \Delta + \frac{a^4}{\sigma_{X_c}^4} \frac{1}{360} B_E \Delta \quad (121)$$

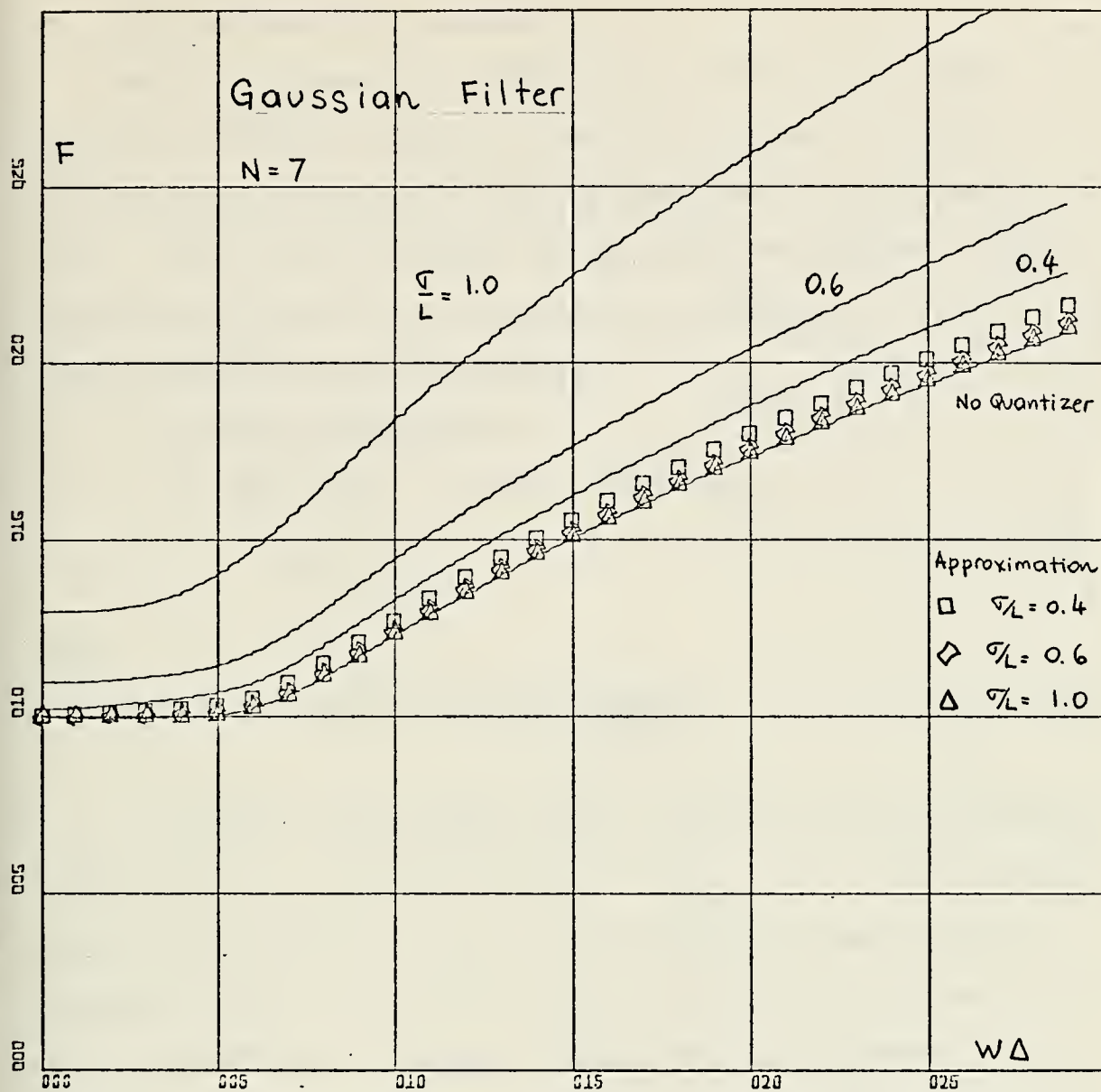
But the first two terms are just the degradation factor for the case of no quantizer, therefore (121) can be written as

$$F^2 = F_{NQ}^2 + \frac{1}{6} \frac{a^2}{\sigma_{X_c}^2} B_E \Delta + \frac{1}{360} \frac{a^4}{\sigma_{X_c}^4} B_E \Delta \quad (122)$$

where  $F_{NQ}$  is the degradation factor with no quantizer. The last two terms of (122) represent a correction, due to quantization, for the degradation factor with no quantizer.

The approximate solution is very good if the assumptions under which it was derived hold. For  $N=17$ ,  $\sigma_{X_c}/L = 0.3$  ( $a/\sigma_{X_c} = 0.42$ ) and  $W\Delta = 1.0$  the error is less than one percent. For values of  $\sigma_{X_c}/L$  greater than 0.3 the approximation is not good due to saturation. For values much smaller, it again fails due to the large value of  $a/\sigma_{X_c}$ . Figure 43 shows how the two results compare for  $N=7$  and different values of  $\sigma_{X_c}/L$ . In it, the behavior of the two solutions as  $\sigma_{X_c}/L$  is increased can be observed. For  $N$  much greater than 7, the approximation is very good when  $\sigma_{X_c}/L$  is near 0.3.





X-SCALE=5.00E-01 UNITS INCH.

Y-SCALE=5.00E-01 UNITS INCH.

FIGURE 43



## B. RC FILTERING THEN SAMPLING

Refer to Figure 3. Unfortunately there is no exact solution for this case since there is no way to get the second order probability density function of the process  $z(t)$ . This would be needed to approach the problem in the same way as done for the radiometer of Figure 2. Two approximations will be discussed.

### 1. First Approximation

It was shown in Chapter III that

$$E[Z] = g(N_o/2) \quad (123)$$

and

$$\sigma_Z^2 = g^2(N_o/2)^2 \frac{1}{2B_E t_{RC}} \quad (124)$$

Owing to the Central Limit Theorem it can be assumed that  $z(t)$  is a Gaussian process if  $B_E t_{RC} \gg 1$ . Due to the square law detector, it is obvious that  $z(t)$  can never be negative, hence the assumption is good only if the mean of  $z(t)$  is sufficiently large compared to its standard deviation so that the assumed Gaussian probability density function is negligible for negative arguments.

It is also assumed that the quantizer has a bias 'b' as shown on Figure 44. When  $b=0$  this quantizer reduces to the one shown in Figure 7. It is argued that the order in which  $z(t)$  is sampled and quantized is immaterial as far as the output  $I$  is concerned. Hence Figure 45 is a valid model of the processing done by the ADC and computer.



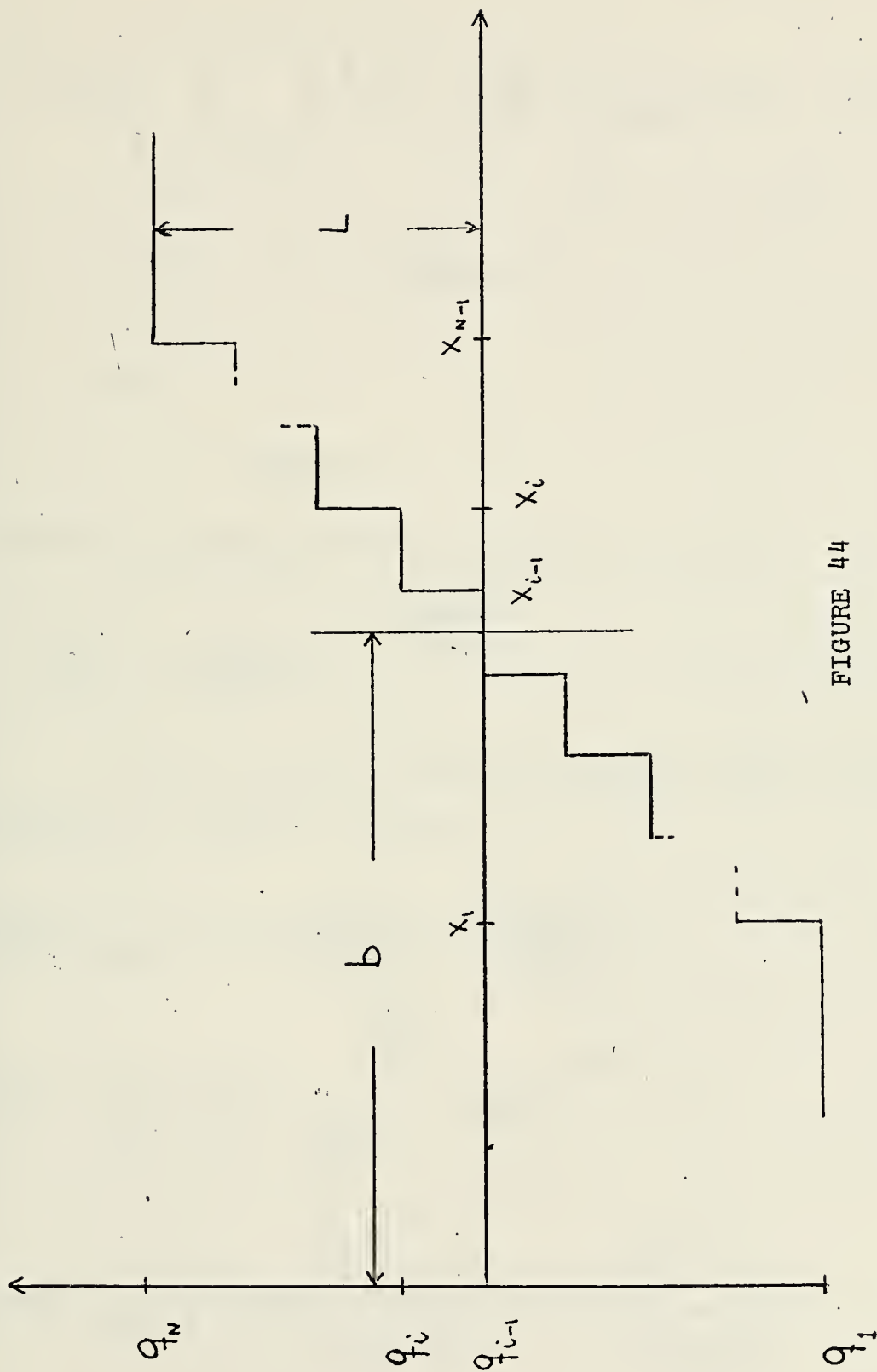


FIGURE 44



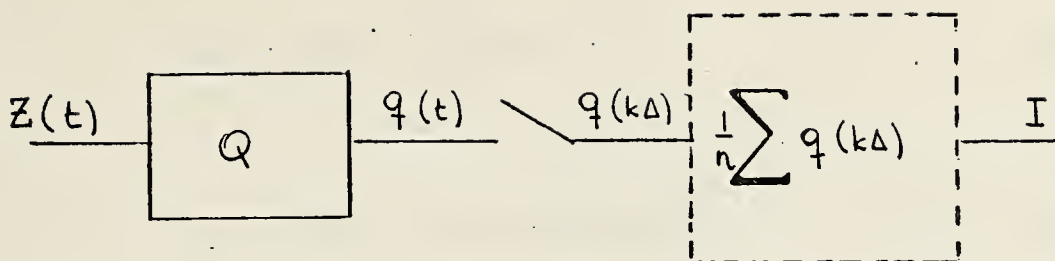


FIGURE 45

Let

$$E[Z] = m \quad (125)$$

then the probability density function of  $z(t)$  is

$$f_Z(z) = \frac{1}{(2\pi\sigma_Z^2)^{1/2}} e^{-\frac{(z-m)^2}{2\sigma_Z^2}} \quad (126)$$

It can be shown, using a procedure similar to that introduced in Chapter IV that

$$E[q(t)] = \sum_{i=1}^N \frac{q_i}{2} \left[ \operatorname{erf}\left(\frac{X_{i-1}-m}{(2)^{1/2}\sigma_Z}\right) - \operatorname{erf}\left(\frac{X_{i-1}-m}{(2)^{1/2}\sigma_Z}\right) \right] \quad (127)$$

$$R_q(\rho_Z) = \frac{1}{(2\pi)^{1/2}} \sum_{i=1}^N q_i \int_{\frac{X_{i-1}-m}{\sigma_Z}}^{\frac{X_i-m}{\sigma_Z}} \psi(\rho_Z, \beta) e^{-\beta^2/2} d\beta \quad (128)$$

$$\psi(\rho_Z, \beta) = \sum_{j=1}^N \frac{q_j}{2} \left\{ \operatorname{erf}\left[ \frac{\frac{X_j-m}{\sigma_Z} - \rho_Z\beta}{[2(1-\rho_Z^2)]^{1/2}} \right] - \operatorname{erf}\left[ \frac{\frac{X_{j-1}-m}{\sigma_Z} - \rho_Z\beta}{[2(1-\rho_Z^2)]^{1/2}} \right] \right\} \quad (129)$$



But from Figure 44

$$X_1 = 2L(1 - \frac{N}{2})/(N-1) + b \quad (130)$$

and

$$q_1 = 2L[1 - (N+1)/2]/(N-1) \quad (131)$$

Equation (130) can be written as

$$X_1 = X_{o_1} + b \quad (132)$$

where  $X_{o_1}$  is the value of  $X_1$  when the quantizer is zero centered.

Substituting (131) and (132) into Equations (127) through (129), the parameter  $b-m$  appears. Physically, this is the offset of the mean of the process  $z(t)$  with respect to the center of the quantizer. When no source is present the value of this offset will be determined by the quiescent conditions of the radiometer. When looking at a source, however, the value of the offset will change since the mean of  $z(t)$  changes linearly with temperature.

Let

$$f = m_o - b \quad (133)$$

where  $m_o$  is the expected value of  $z(t)$  at  $T_{op}$ . Then (127) through (129) can be written as



$$\frac{E[q(t)]}{L} = \sigma'_Z \sum_{i=1}^N \frac{q'_i}{\sigma'_Z} \left\{ \operatorname{erf} \left[ \frac{X'_{O1} - f' + (2Bt_{RC})^{1/2} (\sigma'_{ZO} - \sigma'_Z)}{(2)^{1/2} \sigma'_Z} \right] \right. \quad (134)$$

$$\left. - \operatorname{erf} \left[ \frac{X'_{O1-1} - f' + (2Bt_{RC})^{1/2} (\sigma'_{ZO} - \sigma'_Z)}{(2)^{1/2} \sigma'_Z} \right] \right\}$$

$$\frac{R_q(\rho_Z)}{\sigma_Z^2} = \frac{1}{(2\pi)^{1/2}} \sum_{i=1}^N \frac{q'_i}{\sigma'_Z} \frac{X'_{O1} - f'}{\sigma'_Z} \int \psi'(\rho_Z, \beta) e^{-\beta^2/2} d\beta \quad (135)$$

$$\psi'(\rho_Z, \beta) = \sum_{j=1}^N \frac{q'_j}{2\sigma'_Z} \left\{ \operatorname{erf} \left[ \frac{\frac{X'_{O1} - f'}{\sigma'_Z} - \rho_Z \beta}{[2(1-\sigma_Z^2)]^{1/2}} \right] - \operatorname{erf} \left[ \frac{\frac{X'_{O1-1} - f'}{\sigma'_Z} - \rho_Z \beta}{[2(1-\sigma_Z^2)]^{1/2}} \right] \right\} \quad (136)$$

where  $\sigma_{Z_O}$  is the value of the standard deviation of  $z(t)$  at  $T_{op}$ , and all primed variables imply that they have been normalized by  $L$ .

For the case of  $\rho_Z = 1$  (135) becomes

$$\frac{E[q^2]}{\sigma_Z^2} = \sum_{i=1}^N \frac{q_i'^2}{2\sigma_Z'^2} \left[ \operatorname{erf} \left( \frac{X'_{O1} - f'}{\sigma'_Z (2)^{1/2}} \right) - \operatorname{erf} \left( \frac{X'_{O1-1} - f'}{\sigma'_Z (2)^{1/2}} \right) \right] \quad (137)$$

Equations (134) through (137) can be solved in the same form as done in Chapter III. However, the addition of



two new parameters,  $(f'$  and  $(2Bt_{RC})^{\frac{1}{2}})$ , makes the problem difficult to solve in a general way due to the number of variables involved.

One way to get around this problem is to assume that  $(2B_E t_{RC})^{\frac{1}{2}}$  is large. Then

$$E[q] = \sum_{i=1}^N q_i \int_{X_{i-1}}^{X_i} f_Z(z, m, \sigma) dz \quad (138)$$

where

$$f_Z(z, m, \sigma) = \frac{1}{(2\pi\sigma^2)^{\frac{1}{2}}} e^{-\frac{(z-m)^2}{2\sigma^2}} \quad (139)$$

From (123) and (124)

$$m = \sigma_Z (2B_E t_{RC})^{\frac{1}{2}} \quad (140)$$

Therefore

$$\frac{dE}{dm} = \sum_{i=1}^N q_i \int_{X_{i-1}}^{X_i} \frac{df_Z(z, m, \sigma) dz}{dm} \quad (141)$$

but

$$\frac{df_Z}{dm} = \frac{\partial f}{\partial m} + \frac{\partial f}{\partial \sigma} \frac{d\sigma}{dm} \quad (142)$$

Substituting into (141) and using the fact that

$$\frac{\partial f_Z}{\partial m} = - \frac{\partial f}{\partial z} \quad (143)$$



it follows that

$$\frac{dE}{d\sigma} = (2B_E t_{RC})^{\frac{1}{2}} \sum_{i=1}^N q_i [f_Z(X_{i-1}, m, \sigma) - f_Z(X_i, m, \sigma)] + \sum_{i=1}^N q_i \frac{X_i}{X_{i-1}} \frac{\partial f_Z}{\partial \sigma} d\sigma \quad (144)$$

If  $(2B_E t_{RC})^{\frac{1}{2}}$  is large, it means that the expected value of  $z(t)$  is much greater in value than its standard deviation. Therefore it can be assumed that a change in temperature affects the expected value of  $z(t)$  but the effects on  $\sigma_Z$  are negligible. In that case the second term of (144) can be disregarded.

Using (66) it follows that

$$\frac{\sigma_I^2}{\sigma_Z^2} = \frac{\sigma_q^2}{n\sigma_Z^2} + \frac{2\Delta}{\tau} \sum_{k=1}^{n-1} \left(1 - \frac{k\Delta}{\tau}\right) \left[ \frac{R_q(k\Delta) - E^2[q]}{\sigma_Z^2} \right] \quad (145)$$

Substituting (144) and (145) into (13), it is easily shown that

$$F^2 = \frac{\frac{\sigma_q^2}{\sigma_Z^2} \frac{2B_E t_{RC}}{2} \frac{\Delta}{t_{RC}} + 2B_E t_{RC} \frac{\Delta}{t_{RC}} \sum_{k=1}^{n-1} \left[ \frac{R_q(k\Delta) - E^2[q]}{\sigma_Z^2} \right]}{\left( \frac{dE[q]}{d\sigma_Z} \right)^2} -$$

$$\frac{\frac{2B_E (\Delta/t_{RC})^2}{\tau/t_{RC}} \sum_{k=1}^{n-1} k \left[ \frac{R_q(k\Delta) - E^2[q]}{\sigma_Z^2} \right]}{\left( \frac{dE[q]}{d\sigma_Z} \right)^2} \quad (146)$$



The parameter  $2B_E t_{RC}$  on the numerator of (146) will cancel out. The third term of (146) can be neglected only if  $\tau \gg t_{RC}$  (see comments in Chapter III. The addition of a quantizer does not invalidate them).

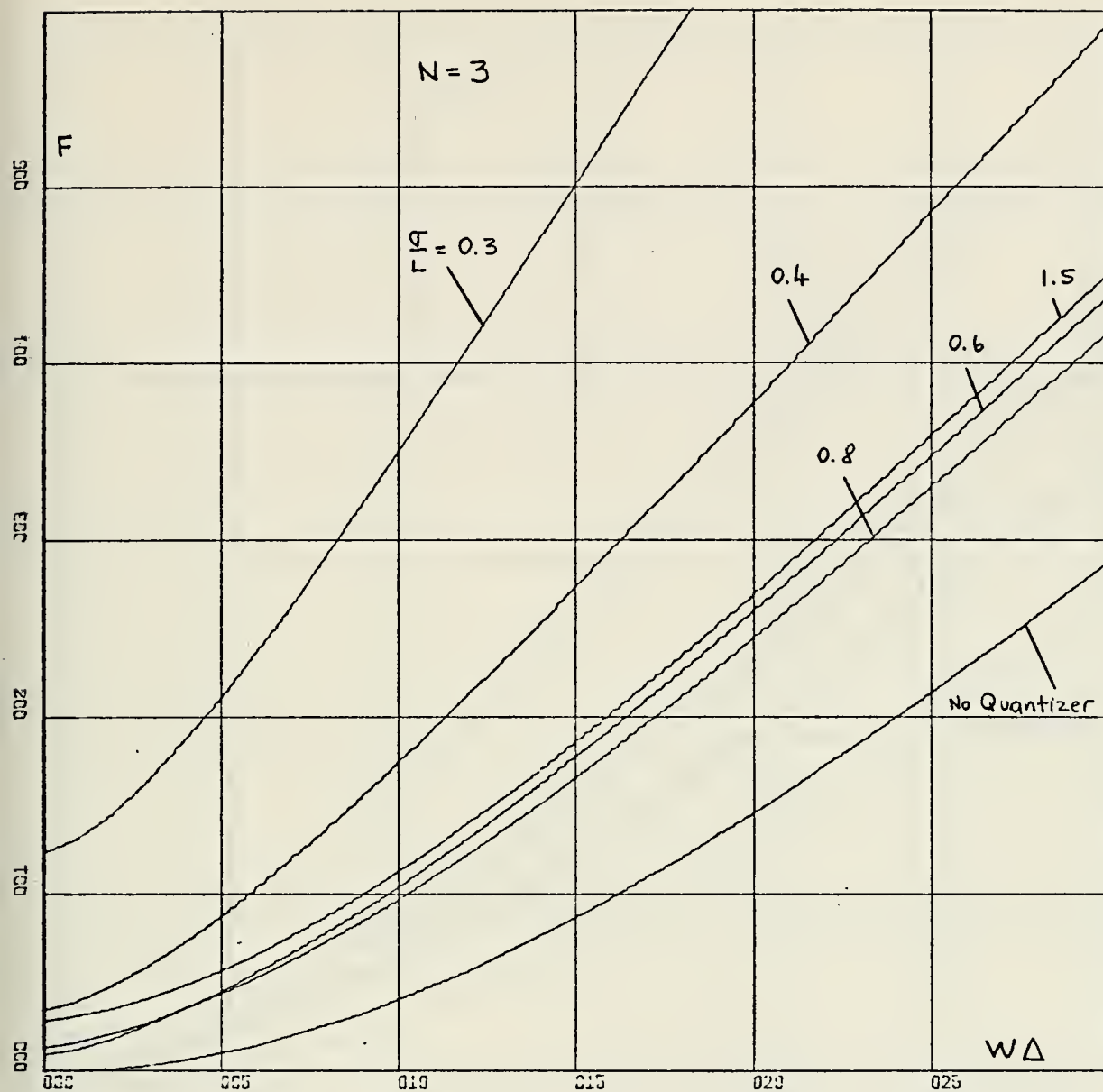
It must be pointed out that the parameter  $(2B_E t_{RC})^{\frac{1}{2}}$ , even though it does not appear in (146), is an important one. It is a measure of how much smoothing the RC filter does. A large value makes quantization difficult. On the other hand, a small value invalidates the assumption that  $z(t)$  is a Gaussian process. Other consequences of this parameter will be discussed in Chapter VI.

Equation (146) can be evaluated using (134) through (137) and (144). Basically it is done in the same form as for the case discussed in Section A of this chapter. Using (135) and (136) a set of transfer characteristics has to be computed similar to Figures 8 through 14 (that set of curves is the solution when  $f'=0$ ). The major difficulty lies in the additional parameter  $f'$  which increases the dimensionality of the problem.

The case when  $f'=0$  (no offset) was analyzed using Figures 8 through 14 and (144). The results are shown in Figures 46 through 51. For any other value of  $f'$  (134) through (137) have to be evaluated.

As an example the case of  $N=13$ ,  $\sigma_z/L=0.2$  and  $f'=0.5$  was solved. The results are shown in Figures 52 and 53. Note that they are very close to the zero offset case for a seven level quantizer with  $\sigma_z/L=0.4$ . The reason is that





X-SCALE=5.00E-01 UNITS INCH.

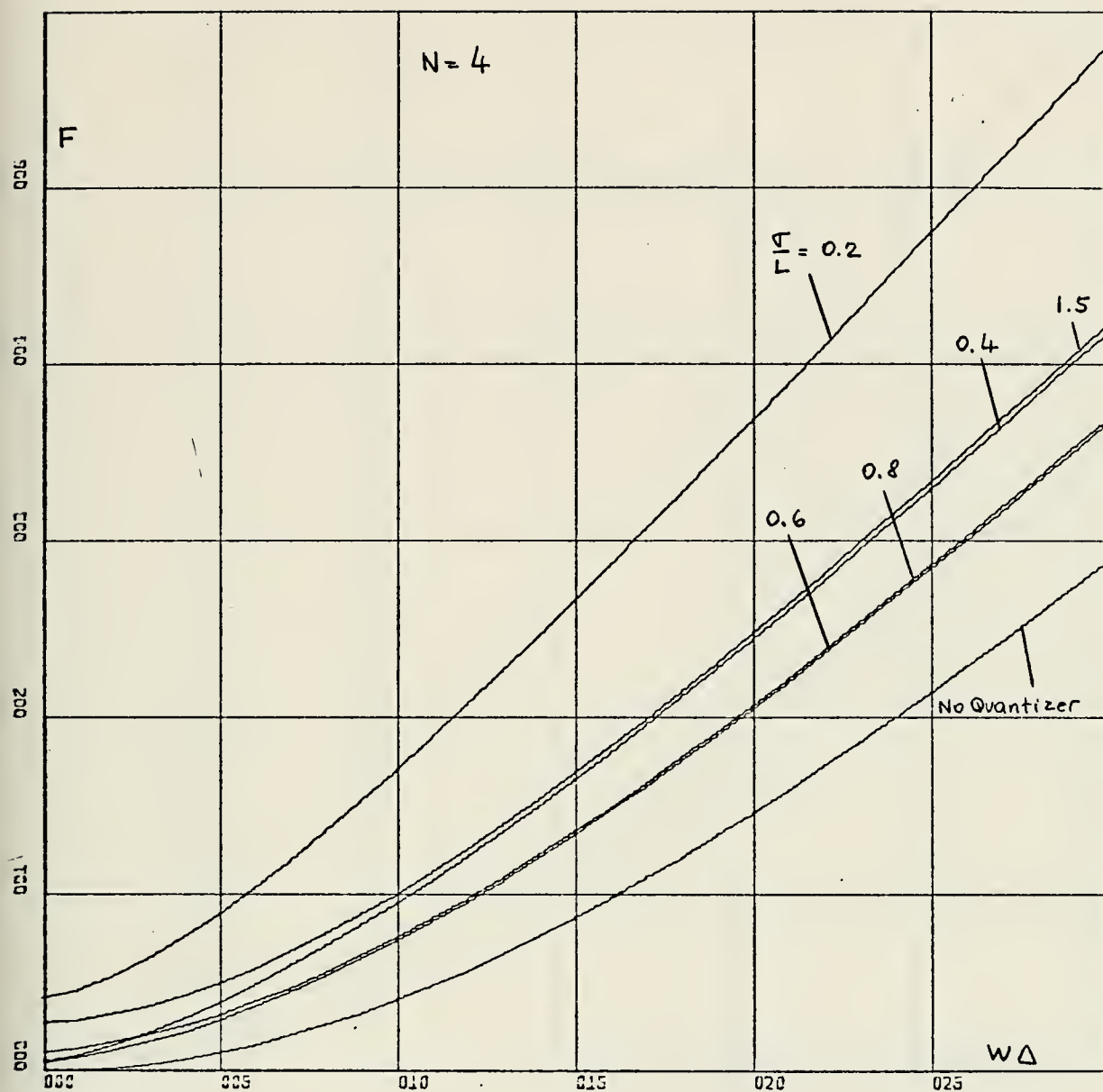
Y-SCALE=1.00E-01 UNITS INCH.

ADD +1.00E+00

UNITS TO ALL Y VALUES.

FIGURE 46





X-SCALE=5.00E-01 UNITS INCH.

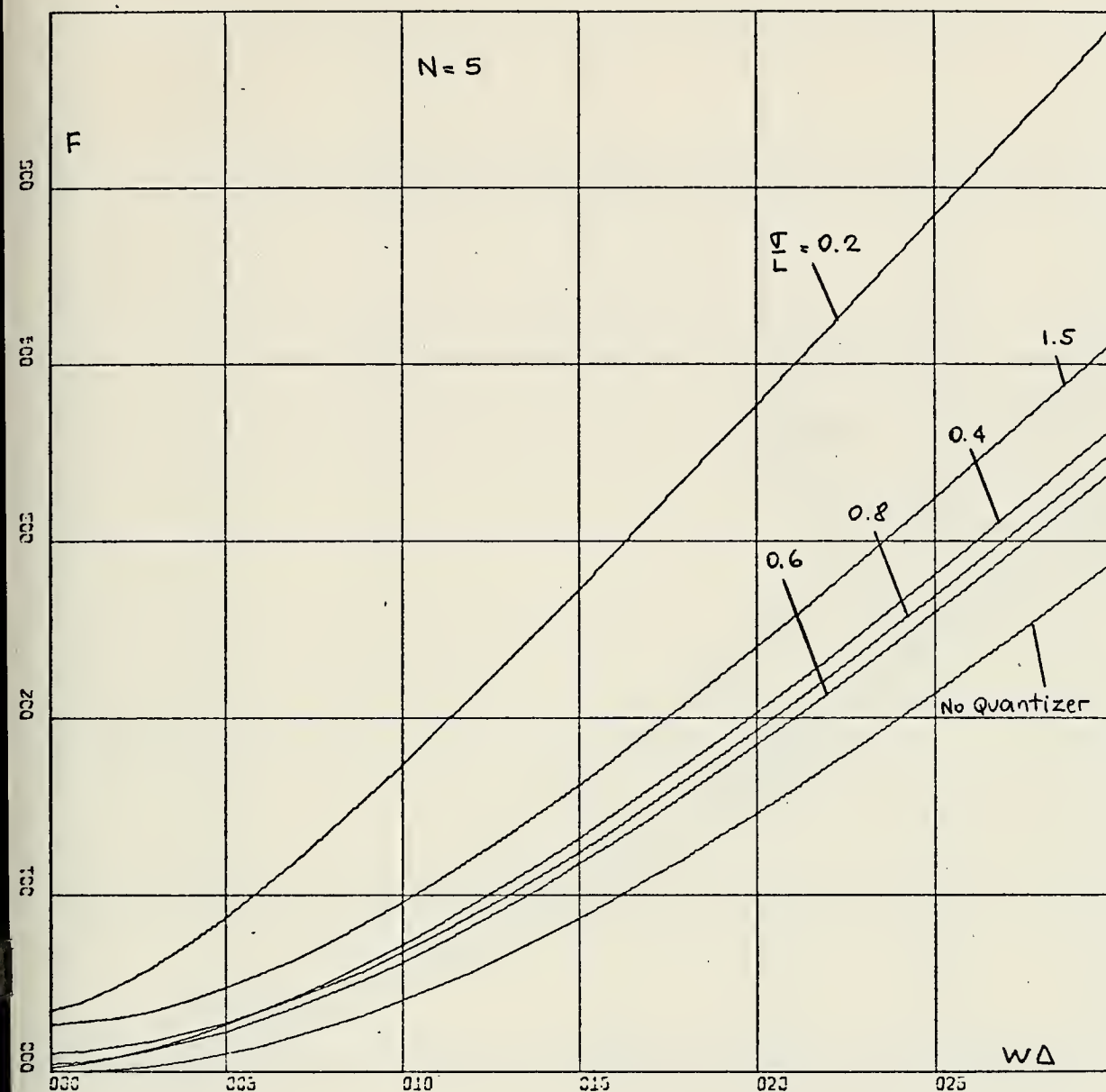
Y-SCALE=1.00E-01 UNITS INCH.

ADD +1.00E+00

UNITS TO ALL Y VALUES.

FIGURE 47





X-SCALE=5.00E-01 UNITS INCH.

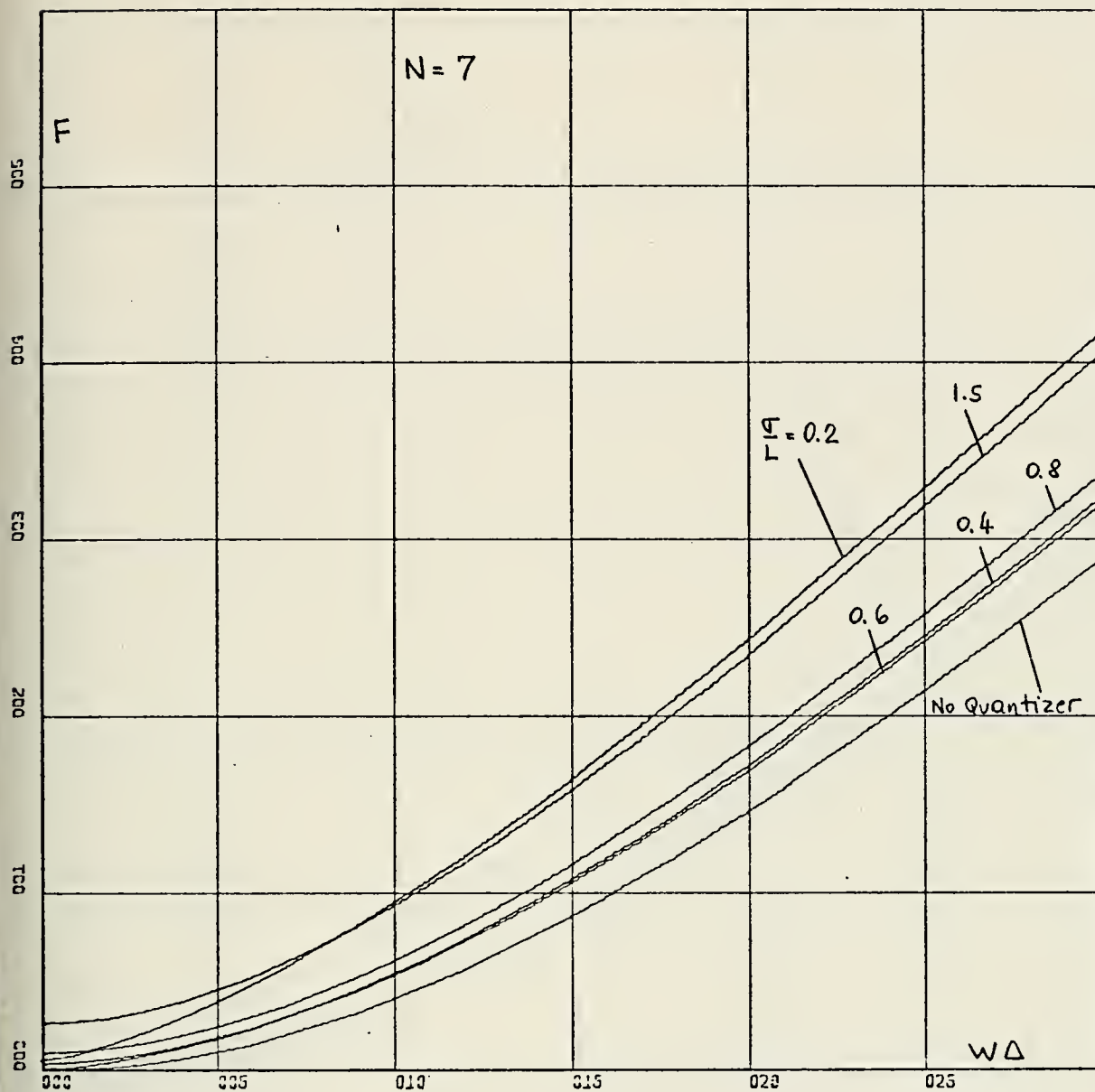
Y-SCALE=1.00E-01 UNITS INCH.

ADD +1.00E+00

UNITS TO ALL Y VALUES.

FIGURE 48



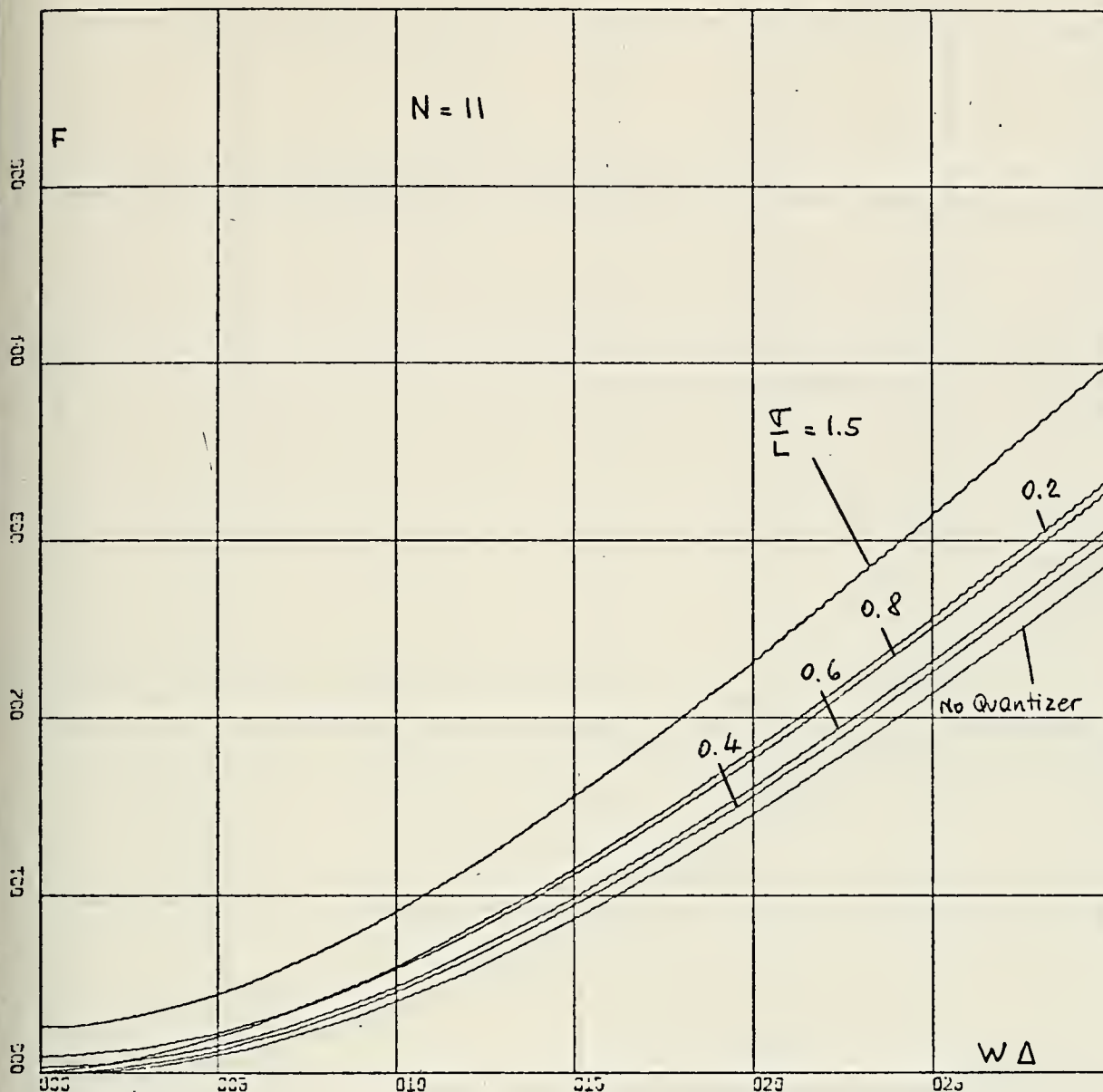


X-SCALE=5.00E-01 UNITS INCH.  
Y-SCALE=1.00E-01 UNITS INCH.  
UNITS TO ALL Y VALUES.

ADD +1.00E+00

FIGURE 49



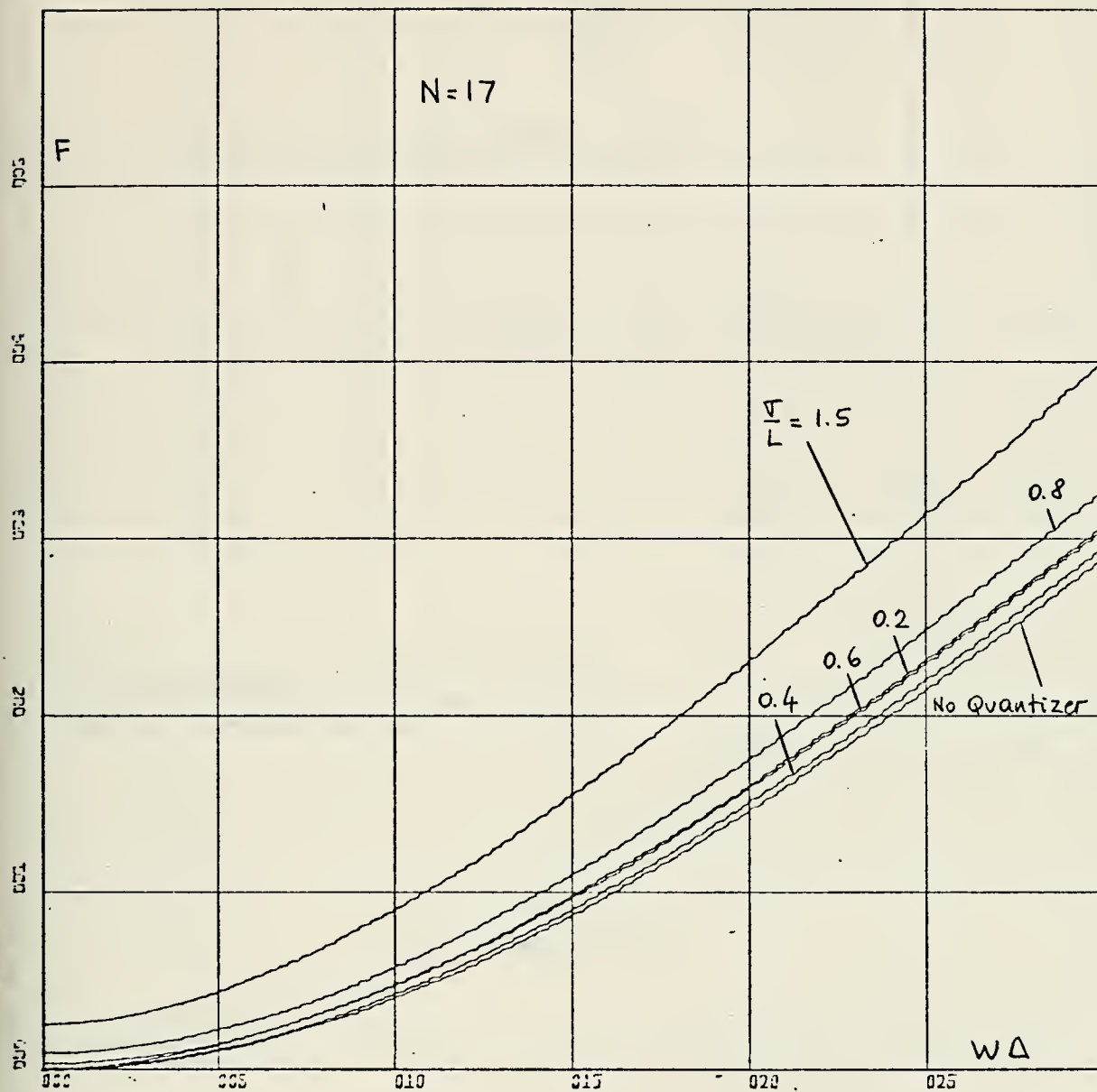


X-SCALE=5.00E-01 UNITS INCH.  
Y-SCALE=1.00E-01 UNITS INCH.  
UNITS TO ALL Y VALUES.

ADD +1.00E+00

FIGURE 50



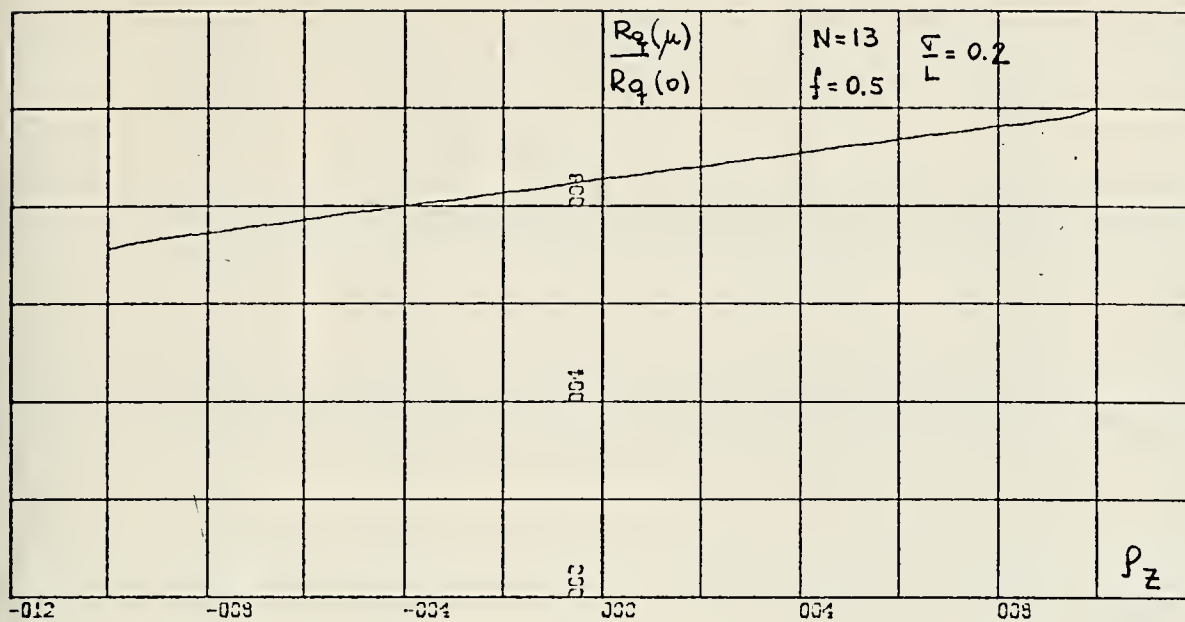


K-SCALE=5.00E-01 UNITS INCH.  
 Y-SCALE=1.00E-01 UNITS INCH.  
 UNITS TO ALL Y VALUES.

ADD +1.00E+00

FIGURE 51



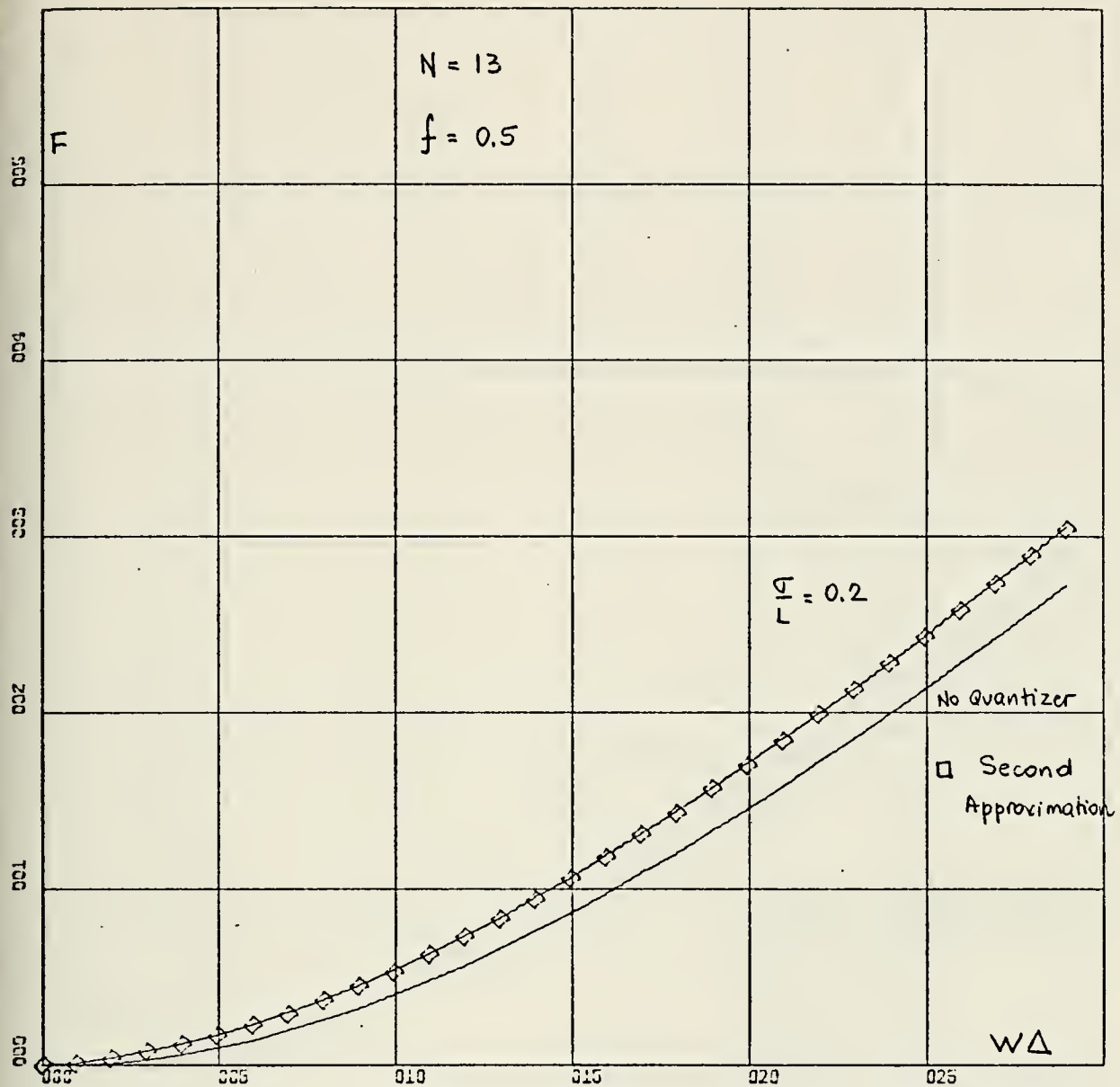


X-SCALE=4.00E-01 UNITS INCH.

Y-SCALE=4.00E-01 UNITS INCH.

FIGURE 52



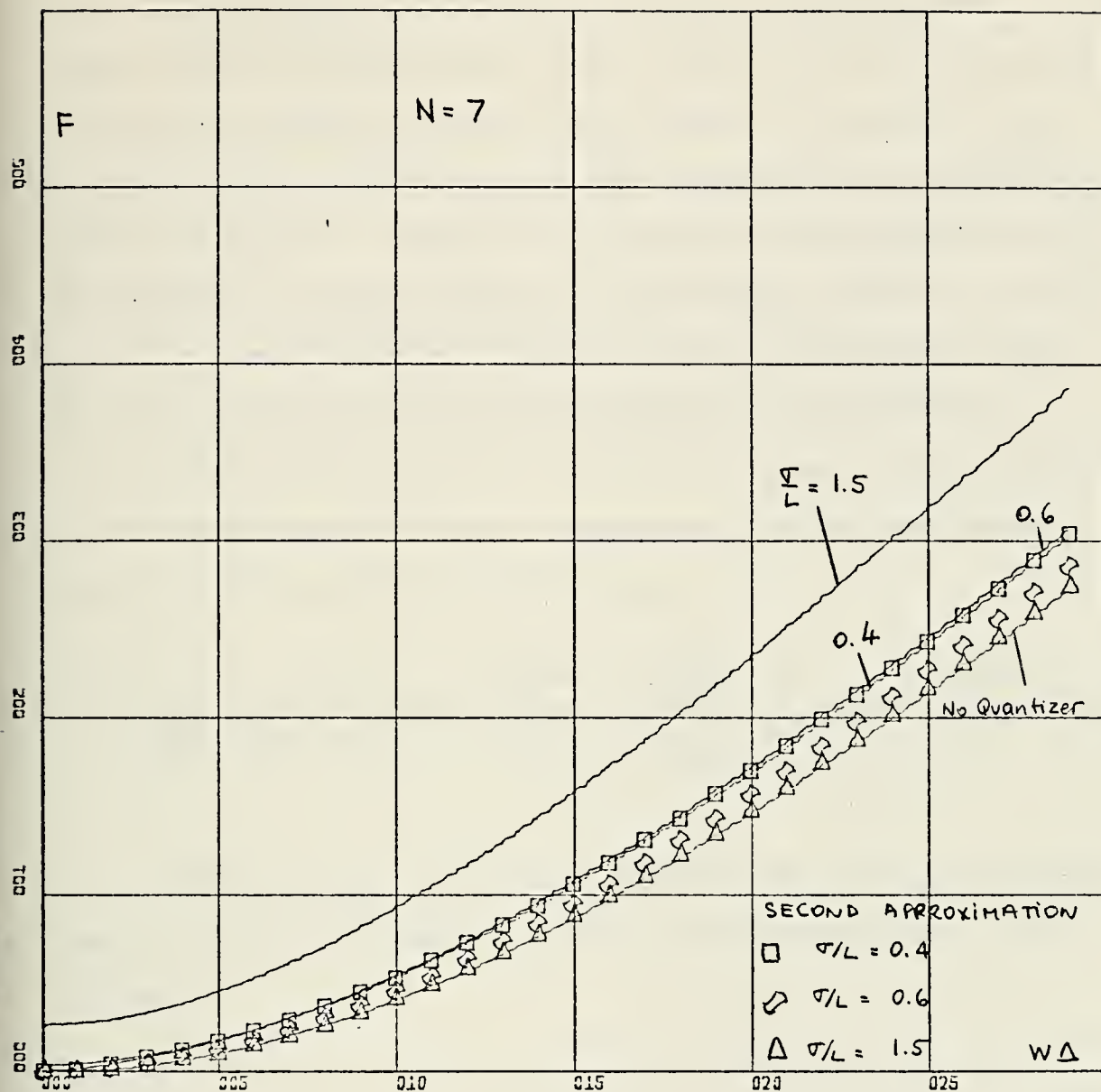


X-SCALE=5.00E-01 UNITS INCH.  
 Y-SCALE=1.00E-01 UNITS INCH.  
 UNITS TO ALL Y VALUES.

ADD +1.00E+00

FIGURE 53





X-SCALE=5.00E-01 UNITS INCH.  
 Y-SCALE=1.00E-01 UNITS INCH.  
 UNITS TO ALL Y VALUES.

ADD +1.00E+00

FIGURE 54



$a/\sigma_Z$  is the same for both cases. They are not exactly equal however, since in one case clipping occurs essentially for positive values of the signal, while in the other case clipping occurs symmetrically for both positive and negative values of signal. Figure 52 is a plot of the transfer characteristics for this example. The programs used are in the appendix (See "Transfer Characteristics of Quantizer With Offset," and "RC Filtering Then Sampling, Offset Case").

The case when  $N=2$ ,  $f'=0$  is of interest since results are obtained easily without extensive computer programming. Using (146) and (96) it can be shown that

$$F^2 = \frac{\pi}{4} \frac{\Delta}{t_{RC}} + \frac{\Delta}{t_{RC}} \sum_{k=1}^{n-1} \arcsin \frac{R_Z(k\Delta)}{R_Z(0)} - \frac{\left(\frac{\Delta}{t_{RC}}\right)^2}{\frac{\tau}{t_{RC}}} \sum_{k=1}^{n-1} k \arcsin \frac{R_Z(k\Delta)}{R_Z(0)} \quad (147)$$

The last term can be neglected when  $\tau \gg t_{RC}$ . As the sampling rate increases,  $\Delta$  goes to zero and Equation (147) becomes

$$F^2 = \int_0^{\tau} \arcsin e^{-u} du \quad (148)$$

For large  $\tau$ , the upper limit can be replaced by infinity and (148) integrates to

$$F^2 = \frac{\pi}{2} \ln 2 \quad (149)$$

therefore

$$F = 1.04 \quad (150)$$



The results are surprising since it means that a hard limiter degrades the system only by four percent. However, the dynamic range of a radiometer using a hard limiter would be very small hence this result is of little practical use. More on the problem of dynamic range will be discussed in Chapter VI.

## 2. Second Approximation

Using the same arguments as in part A of this chapter, it can be shown that [Ref. 9]

$$F^2 = F_{NQ} + \frac{\Delta}{t_{RC}} \frac{a^2}{\sigma_Z^2 24} \quad (151)$$

The results obtained from (151) are in close agreement with those obtained using the first approximation even for low values of  $N$ . It must be kept in mind that the second approximation does not take into account saturation effects of the quantizer. For the case when  $f'=0$  it was found that if  $\sigma_Z/L < .6$   $W\Delta > 1$ ,  $a/\sigma_Z < 2$  and  $N > 5$ , the second approximation was within 1.5 percent of the first (For  $N=17$  and the above conditions, the difference was less than 0.6 percent). These results indicate that a sizable amount of saturation can occur before (151) no longer holds. Figure 53 shows how the two approximation compare for the example done on page 91. Figure 54 shows a comparison for  $N=7$ ,  $f'=0$  and different values of  $\sigma_Z/L$ . The different behavior of the two approximations as  $\sigma_Z/L$  is increased can be observed.



To summarize, in this chapter an exact solution has been found for degradation factor of the radiometer of Figure 2. For the radiometer of Figure 3 no such solution exists, but an approximation can be made under the reasonably good assumption that  $z(t)$  is a Gaussian random process. For both cases the major difficulty in global analysis lies in the number of parameters involved.

An approximate solution was developed which is in close agreement with the first solution. Its major advantage is that it is easy to compute and as the number of steps increases, it gets better. For practical ADC it should be adequate.



## VI. DYNAMIC RANGE AND LINEARITY OF A DIGITAL RADIOMETER

In this chapter the effects of the addition of an ADC on the linearity of the output of a radiometer is investigated. The main problem here is the saturation effect of the quantizer.

### A. IF SAMPLING

Refer to Figure 2. The output voltage versus temperature characteristics for this case was investigated previously, and is shown in Figure 17. If the ADC was ideal (no saturation and  $a/\sigma = 0$ ) there would be one straight-line curve with slope equal to two. It can be seen that for small  $\sigma_{X_c}^2/L^2$  (proportional to temperature) the curves tend to have a slope of two.

Figure 17 provides all the information needed for the problem under investigation in this chapter. However, the way the curves were normalized makes them awkward to use. They can be changed starting with (108) and (95).

$$\frac{E[I]}{L^2} = \frac{\sigma_{X_c}^2}{L^2} \sum_{i=1}^N \left( \frac{q_i'}{\sigma_{X_c}} \right)^2 \left[ \operatorname{erf} \left( \frac{X_i'}{\sigma_X(2)^{1/2}} \right) - \operatorname{erf} \left( \frac{X_{i-1}'}{\sigma_X(2)^{1/2}} \right) \right] \quad (152)$$

but

$$\frac{\sigma_{X_c}}{L} = \frac{2}{(N-1)a/\sigma_{X_c}} \quad (153)$$



Therefore (152) becomes

$$\frac{E[I]}{a^2} = \frac{\sigma_{X_c}^2}{a^2} \sum_{i=1}^N \left[ \frac{q_i'(N-1)}{2\sigma_{X_c}/a} \right]^2 \left\{ \operatorname{erf} \left[ \frac{X_i'(N-1)}{2(2)^{1/2}\sigma_{X_c}/a} \right] - \operatorname{erf} \left[ \frac{X_{i-1}'(N-1)}{2(2)^{1/2}\sigma_{X_c}/a} \right] \right\} \quad (154)$$

Equation (154) is plotted in Figure 55. The curves asymptote to

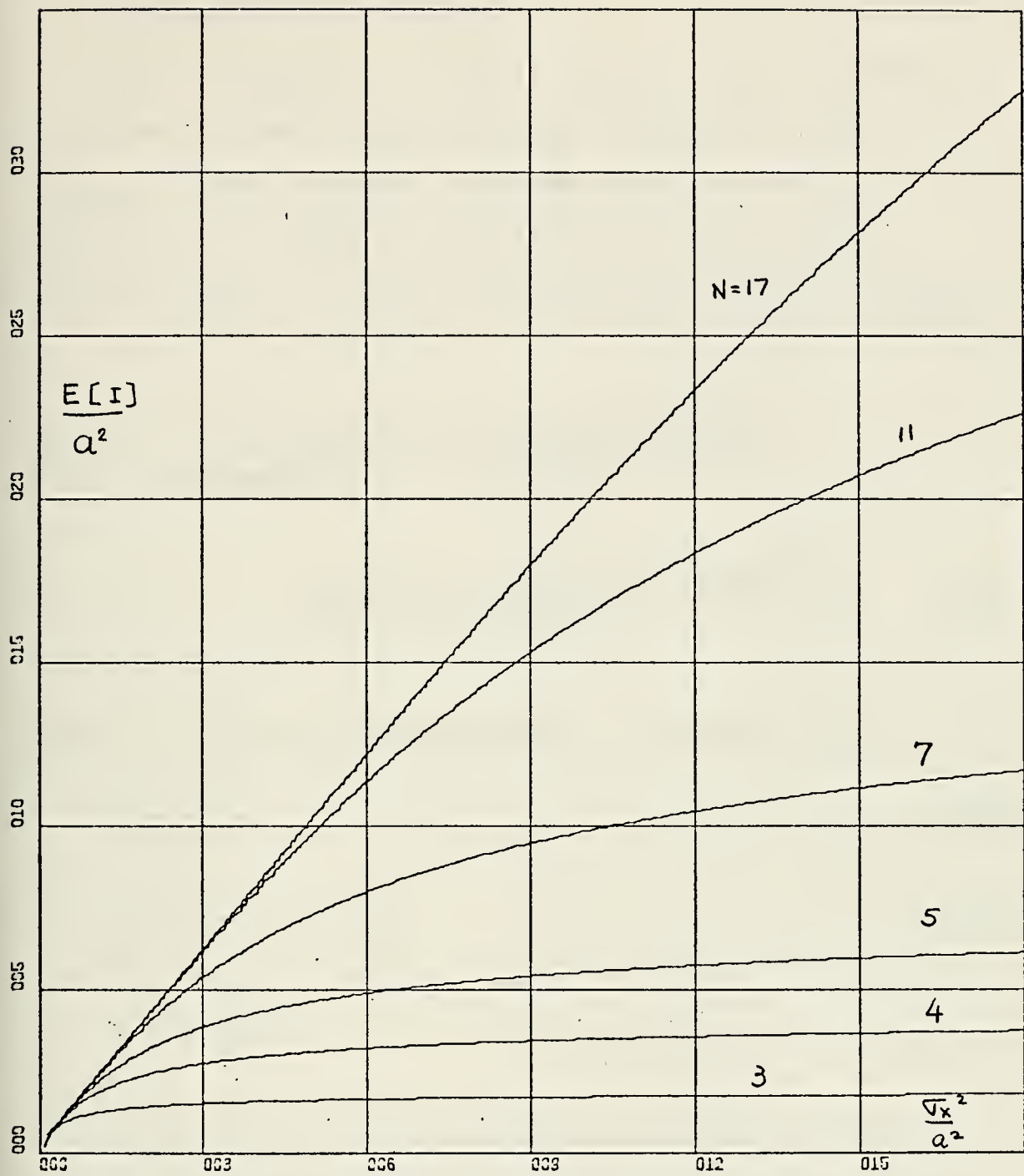
$$\frac{E[I]}{a^2} = \frac{(N-1)^2}{2} \quad (155)$$

This can be shown by using the fact that as  $\sigma_X/a$  gets large the quantizer appears as a hard limiter.

Figure 55 shows that a substantial range of linear output can be obtained with this scheme before saturation dominates.

In order to use Figure 55 a criterion must be defined for how much departure from linearity is allowed for the temperature range expected (one percent, for example). Once that is defined, Figure 55 can be entered to determine the number of steps of the quantizer required. The value of the abscissa at  $T_{op}$  will be determined mainly by how much degradation of performance is allowed (Chapter V). We thus have a trade-off of linear dynamic range versus minimum detectable temperature  $\Delta T$ .





X-SCALE=3.00E+00 UNITS INCH.  
Y-SCALE=5.00E+00 UNITS INCH.

FIGURE 55



## B. RC FILTERING THEN SAMPLING

Refer to Figure 3. A similar analysis can be made for this case. However the additional parameters ( $f'$  and  $(2B_E t_{RC})^{1/2}$ ) make a general representation difficult. Basically, (127) has to be rewritten in terms of  $\sigma_Z/a$  instead of  $\sigma_Z/L$ . It can be shown easily that (127) becomes

$$\frac{E[I]}{a} = \sigma_Z'' \sum_{i=1}^N \frac{q_i'}{2s\sigma_Z''} \left\{ \operatorname{erf} \left[ \frac{X_{O_i}' - f' + (\sigma_{Z_O}'' - \sigma_Z'')s(2B_E t_{RC})^{1/2}}{(2)^{1/2} s \sigma_Z''} \right] - \operatorname{erf} \left[ \frac{X_{O_{i-1}}' - f' + (\sigma_{Z_O}'' - \sigma_Z'')s(2B_E t_{RC})^{1/2}}{(2)^{1/2} s \sigma_Z''} \right] \right\} \quad (156)$$

where  $f'$ ,  $q_i'$  and  $X_i'$  are as previously defined, and

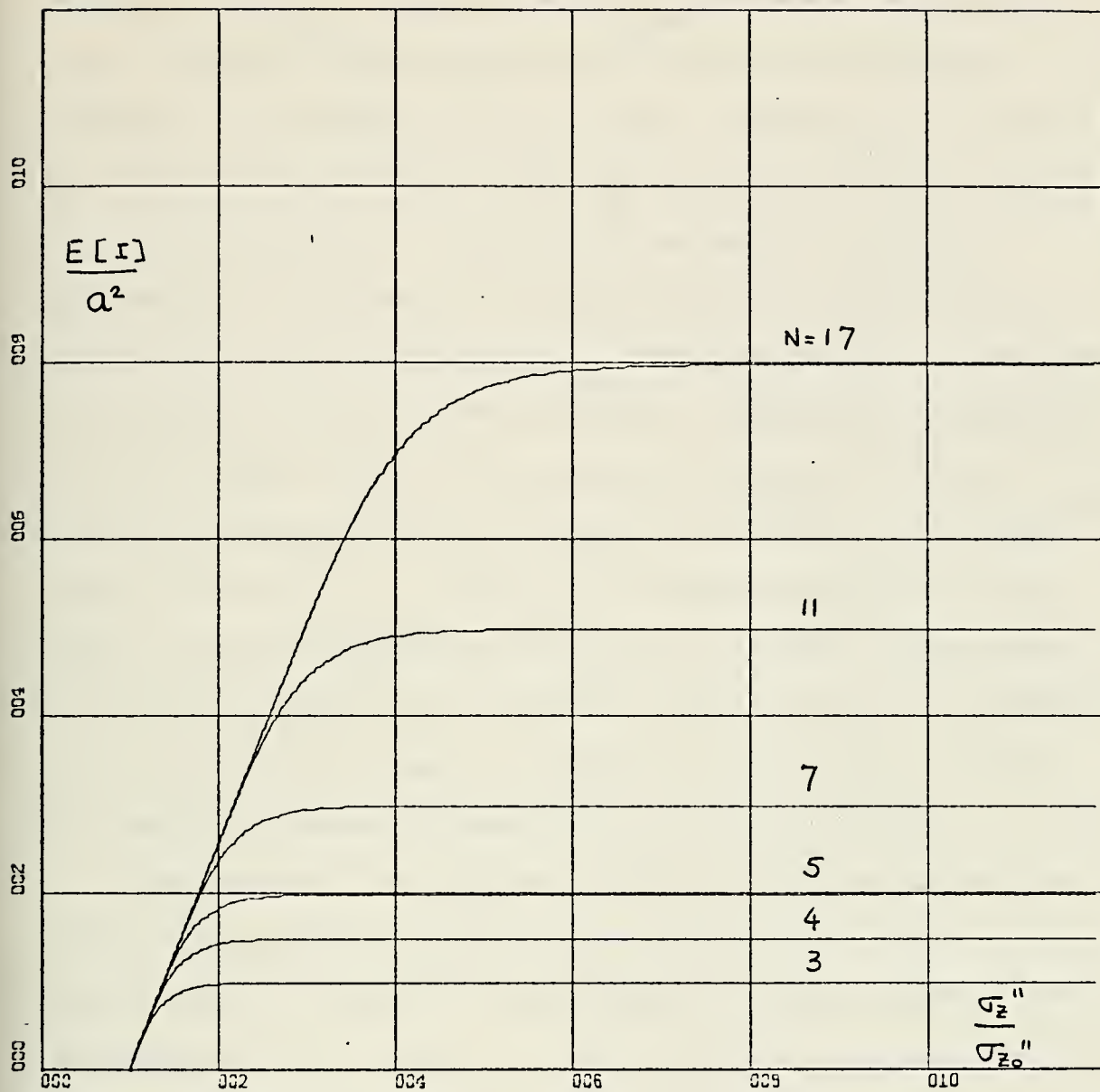
$$\sigma_Z'' = \sigma_Z/a \quad (157)$$

$$\sigma_{Z_O}'' = \sigma_Z/a \quad \text{at} \quad T_{op} \quad (158)$$

$$s = 2/(N-1)$$

Figure 56 is a plot of (156) for the case of  $f'=0$ ,  $\sigma_{Z_O}'' = 0.5$  and  $(2B_E t_{RC})^{1/2} = 1.0$ . The abscissa axis is shown as a function of  $\sigma_Z''/\sigma_{Z_O}''$  (or  $T/T_{op}$ ). The curves asymptote to  $(N-1)/2$ . Some observations are of interest. First, the slope near the origin is equal to  $(2B_E t_{RC})^{1/2} \sigma_{Z_O}''$ . Since for a given quantizer  $E[I]/a$  reaches a fixed value for large





X-SCALE=2.00E+00 UNITS INCH.  
Y-SCALE=2.00E+00 UNITS INCH.

FIGURE 56



values of  $\sigma_Z''/\sigma_{Z_0}''$ , increasing  $(2B_E t_{RC})^{1/2}$  (which physically means that more smoothing will be done by the RC filter) decreases the range of linear output. Therefore  $t_{RC}$  should be chosen as the minimum value which will enable the sampler to operate properly. Second, the parameter  $\sigma_{Z_0}''$  will be determined by the amount of degradation tolerated at  $T_{op}$ . And third, the desired range of linear output will determine the number of steps of the quantizer. Therefore a procedure to use a Figure such as 56 would be as follows: First, determine  $(2B_E t_{RC})^{1/2}$  and  $\sigma_{Z_0}''$  using the criteria given above. Second, draw a set of curves of the expected value of the output versus temperature using (156). Third, decide upon a criterion of how much departure from linearity is allowed in the temperature range of operation, and finally obtain the required number of steps from the curves drawn.

To summarize, the effects of the addition of an ADC on the linearity of the output of the radiometers under consideration, have been investigated in this chapter. The knowledge of the behavior of the output is important for calibration purposes.



values of  $\sigma_Z''/\sigma_{Z_0}''$ , increasing  $(2B_E t_{RC})^{1/2}$  (which physically means that more smoothing will be done by the RC filter) decreases the range of linear output. Therefore  $t_{RC}$  should be chosen as the minimum value which will enable the sampler to operate properly. Second, the parameter  $\sigma_{Z_0}''$  will be determined by the amount of degradation tolerated at  $T_{op}$ . And third, the desired range of linear output will determine the number of steps of the quantizer. Therefore a procedure to use a Figure such as 56 would be as follows: First, determine  $(2B_E t_{RC})^{1/2}$  and  $\sigma_{Z_0}''$  using the criteria given above. Second, draw a set of curves of the expected value of the output versus temperature using (156). Third, decide upon a criterion of how much departure from linearity is allowed in the temperature range of operation, and finally obtain the required number of steps from the curves drawn.

To summarize, the effects of the addition of an ADC on the linearity of the output of the radiometers under consideration, have been investigated in this chapter. The knowledge of the behavior of the output is important for calibration purposes.



where  $F$  is the degradation factor for the equivalent total power radiometer. The factor multiplying  $F$  is the performance figure of a balanced Dicke radiometer.

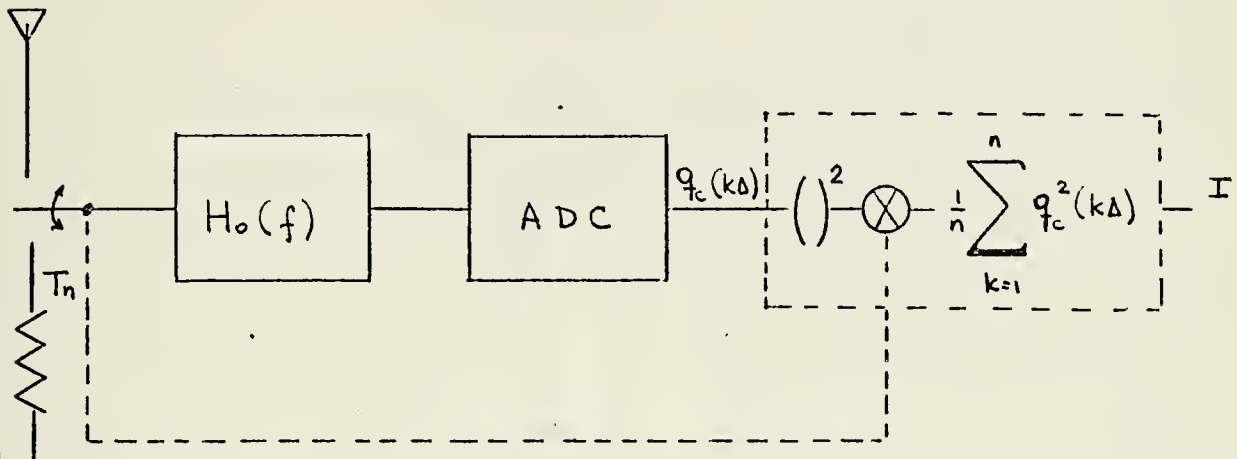


FIGURE 57

Equation (160) follows from the fact that for the half of the switching cycle that the radiometer is connected to the source, it behaves as a total power radiometer.

Care must be taken however on the selection of  $\tau$ . If commencement of sampling is delayed after switching, it must be corrected for the loss in integration time. Also, for the case of RC filtering followed by sampling, the introduction of the RC filter must be reflected in an increase of  $\tau$  since  $F$  takes only into account the effects of the inclusion of the ADC.

The problem of dynamic range and linearity of the output can be handled with the curves developed in Chapter VI.



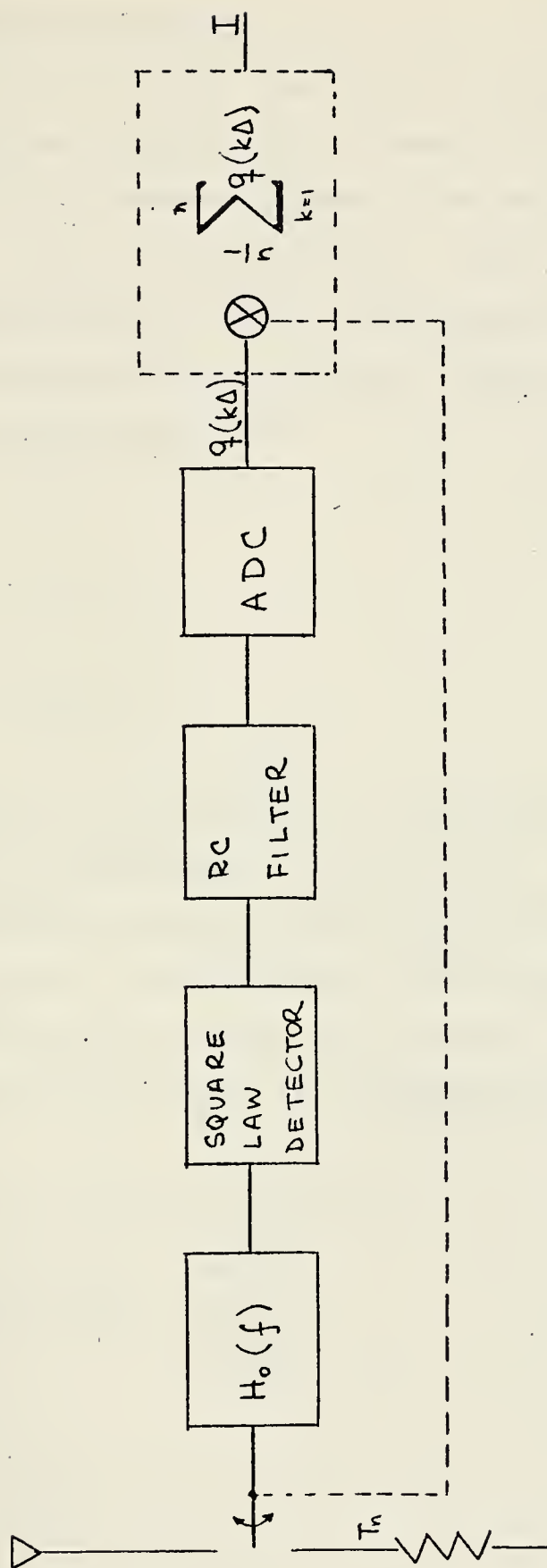


FIGURE 58



## B. NOISE ADDING RADIOMETER

Figures 59 and 60 show two digital noise adding radiometers. The one in Figure 59 corresponds to the IF sampling case and only one channel is shown. The one in Figure 60 corresponds to the RC filtering case. The extension of results already found to NAR is considerably more difficult than for a balanced Dicke radiometer. This is due to the processing involved [Ref. 13].

Let

$$I_n = E_n + \epsilon_n \quad (161)$$

and

$$I_o = E_o + \epsilon_o \quad (162)$$

where  $I_n$  and  $I_o$  are the outputs of the radiometer with  $T_{op}+T_n$  and  $T_{op}$  respectively.  $E_n$  and  $E_o$  are the expected value of the output for the case of  $T_{op}+T_n$  and  $T_{op}$  respectively.  $\epsilon_n$  and  $\epsilon_o$  are independent, zero mean random variables with standard deviation equal to  $\sigma_{I_n}$  and  $\sigma_{I_o}$ , and represent the deviation from the mean for a particular measurement (one cycle).

Then the Y-factor is [Ref. 14]

$$Y = \frac{I_n}{I_o} = \frac{E_n}{E_o} \left[ \frac{1 + \frac{\epsilon_n}{E_n}}{1 + \frac{\epsilon_o}{E_o}} \right] \quad (163)$$



If  $\epsilon_n$  and  $\epsilon_o$  are small compared with  $E_n$  and  $E_o$ , then

$$Y = \frac{E_n}{E_o} \left[ 1 + \frac{\epsilon_n}{E_n} - \frac{\epsilon_o}{E_o} \right] \quad (164)$$

$$E[Y] = \frac{E_n}{E_o} \quad (165)$$

and

$$\sigma_Y^2 = \left[ \frac{E_n}{E_o} \right]^2 \left[ \left( \frac{\sigma_{I_n}}{E_n} \right)^2 + \left( \frac{\sigma_{I_o}}{E_o} \right)^2 \right] \quad (166)$$

Using Equation (166) and the fact that for a NAR

$$\frac{\Delta T}{T_{op}} = \left( 1 + \frac{T_{op}}{T_n} \right) \left( \frac{4}{B_E t} \right)^{1/2} \quad (167)$$

where  $t$  is the switching period; for the case of Figure 2 it can be shown by straight substitution that,

$$F_{NAR}^2 = \frac{\frac{1}{2} \left[ \left( \frac{dE[I_n]}{d\sigma_X^2} \right)^2 \Big|_{T_{op}+T_n} \left( 1 + \frac{\sigma_{X_n}^2}{\sigma_{X_o}^2} \right) F_n^2 + \left( \frac{dE[I_o]}{d\sigma_X^2} \right)^2 \Big|_{T_{op}} F_o^2 \right]}{\left( 1 + \frac{\sigma_{X_o}^2}{\sigma_{X_n}^2} \right)^2 \left[ \frac{d[I_n]}{d\sigma_X^2} \Big|_{T_n+T_{op}} - \frac{dE[I_o]}{d\sigma_X^2} \Big|_{T_{op}} \right]} \quad (168)$$

where  $\sigma_{X_o}$  is  $\sigma_X$  at  $T_{op}$ ,  $\sigma_{X_n}$  is  $\sigma_X$  at  $T_n$ .



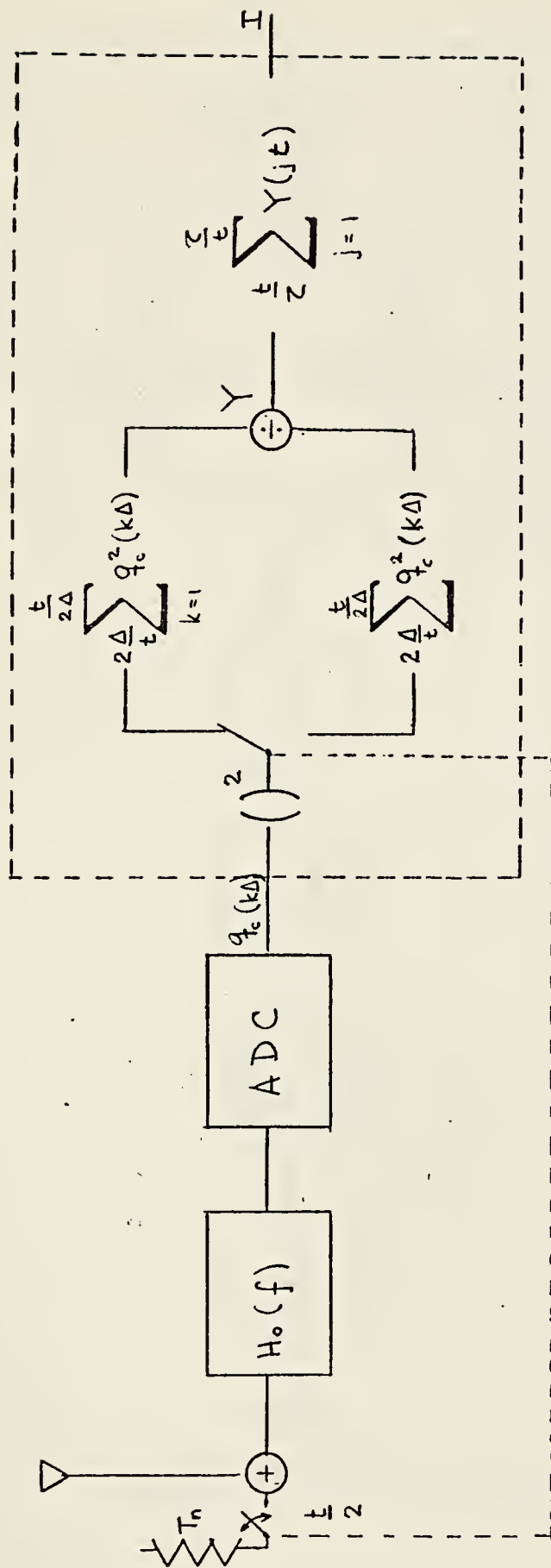


FIGURE 59



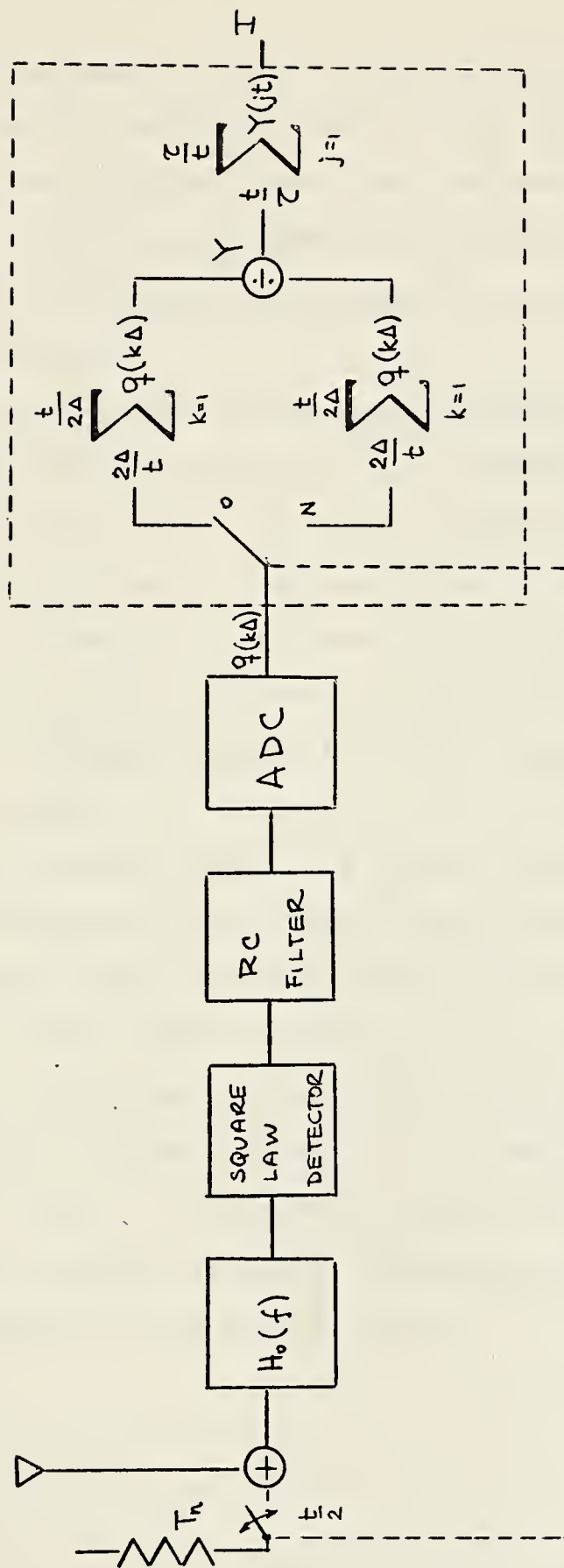


FIGURE 60



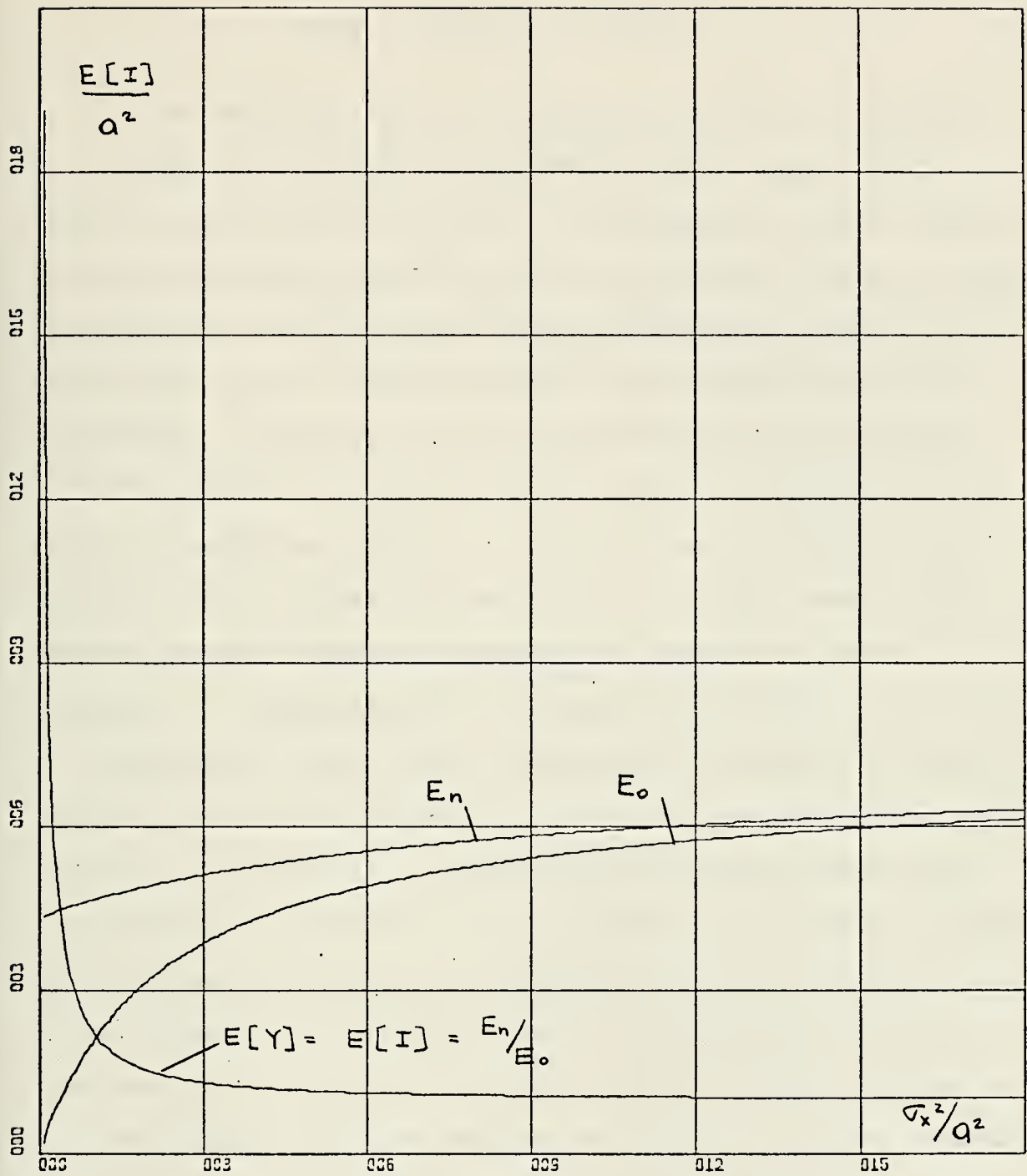
$F_n$  is the degradation factor of the corresponding total power radiometer at  $T=T_n+T_{op}$ , and  $F_o$  is the degradation factor of the corresponding total power radiometer at  $T=T_{op}$ . For the case of Figure 3,  $\sigma_X^2$  must be replaced by  $\sigma_Z$  in (168). All the terms of (168) can be calculated from equations previously developed.

It must be noted that for the case when the signal is filtered before sampling (Figure 60),  $f'$  (offset) cannot be zero at  $T_{op}$  or  $T_{op}+T_n$  since the ADC would give zero output.

The problem of dynamic range and linearity is easy to handle. From Figures 55 or 56, depending on the system under consideration, and (165) a plot can be made relating  $E[I]$  to temperature. Figure 61 shows how this is done for the system of Figure 59.

In summary, in this chapter the results obtained in the six previous chapters for the digital total power radiometers shown in Figures 2 and 3, have been used to determine performance of other digital radiometers. The balanced Dicke and noise adding radiometers were investigated. For the balanced Dicke radiometer, there is a simple and straightforward relationship. For the NAR, however, a relationship was found but it is more involved. The problem of dynamic range and linearity can be handled easily.





X-SCALE=3.00E+00 UNITS INCH.  
Y-SCALE=3.00E+00 UNITS INCH.

FIGURE 61



## VIII. DIGITAL FILTERING

In the analysis of the classical total power radiometer an integrator is used to smooth the output signal. This scheme works well but it has the disadvantage that it gives output information only at discrete intervals of time, corresponding to blocks of data. Such performance might not be acceptable in some cases because a smooth output might be desirable. Therefore, a pure integrator is not generally used but rather a low pass filter (such as a RC) that provides a continuous output. The theory and equations of a classical total power radiometer do not change when using these low pass filters instead of an integrator if an equivalent integration time is defined [Ref. 1].

The digital total power radiometers of Figures 2 and 3 suffer the same disadvantage as the classical TPR. That is, output information is obtained only after the summers have completed the summation of the  $n$  samples. Therefore a scheme where output information is obtained more often must be investigated. This chapter deals with the substitution of the summers of Figures 2 and 3 by digital filters. There is an additional reason for wanting to do this analysis. Since a computer is already being used in the radiometers of Figures 2 and 3, the use of a digital filter often does not require any more hardware.

Figure 62 shows a digital filter operating on a digital signal  $X_k$ . The filter is characterized by its impulse



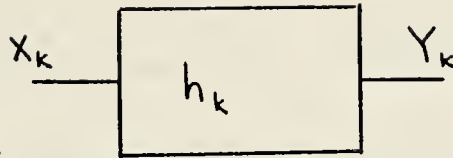


FIGURE 62

response  $h_k$ , and the output is  $Y_k$ . The filter is assumed to be causal (i.e.  $h_k=0$  for  $k<0$ ) and time invariant. This filter can replace the summers of the radiometers defined in the previous chapters.

Referring then to Figure 62

$$Y_k = \sum_{i=-\infty}^{\infty} X_i h_{k-i} \quad (169)$$

By straightforward algebra it can be shown that

$$E[Y_k] = E[Y] = E[X] \sum_{i=0}^{\infty} h_i \quad (170)$$

and

$$\sigma_Y^2 = \sum_{i=0}^{\infty} h_i \sum_{m=0}^{\infty} [R_{X_{m-i}} - E^2[X]] h_m \quad (171)$$

where  $R_{X_n} = E[X_k X_{k+n}]$  is the discrete autocorrelation of  $X_k$ .

Let

$$j = i - m \quad (172)$$



then

$$\sigma_Y^2 = \sum_{i=0}^{\infty} h_i \sum_{j=-\infty}^1 [R_{X_j} - E^2[X]] h_{i-j} \quad (173)$$

Assume that  $h_j$  decays much slower than  $R_{X_j}$ . This can be seen by observing the location where this filter would go in Figures 2 and 3. For the case of Figure 2, the power spectral density at the input of the digital filters is shaped by the RF, Mixer, IF filter which is broad-band. For the case of Figure 3, it can be assumed only when  $t_{RC}$  is small (this is the case for which Figures 46 through 51 apply).

Then (173) becomes

$$\sigma_Y^2 = \sum_{i=0}^{\infty} h_i \sum_{j=-\infty}^1 [R_{X_j} - E^2[X]] h_i \quad (174)$$

Let  $j_0$  be the value where  $R(j_0)$  is negligible. Then (174) can be rewritten as

$$\sigma_Y^2 = \sum_{i=0}^{j_0} h_i^2 \sum_{j=-\infty}^1 [R_{X_j} - E^2[X]] + \sum_{i=j_0}^{\infty} h_i^2 \sum_{j=-\infty}^1 [R_{X_j} - E^2[X]] \quad (175)$$

It can be shown that the first summation is much smaller than the second, and hence it can be ignored. Furthermore the limits of the second summation can be changed as follows without altering the value of  $\sigma_Y^2$  significantly



$$\sigma_Y^2 = \sum_{i=0}^{\infty} h_i^2 \sum_{j=-\infty}^{\infty} [R_{X_j} - E^2[X]] \quad (176)$$

For the summer used in previous chapters, it can be shown (using the same notation of Figure 62) that

$$\sigma_Y^2 = \sigma_X^2 + 2n \sum_{k=1}^{n-1} [R_{X_k} - E^2[X]] - 2n \sum_{k=1}^{n-1} \frac{k}{n} [R_{X_k} - E^2[X]] \quad (177)$$

and

$$E[Y] = E[X] \quad (178)$$

The upper limit of the summation of (177) can be replaced by infinity (due to the narrowness of  $R_X(u)$ ) and the third term can be ignored (see Chapters III and V).

Substituting (170) and (176) into (4) for the general digital filter, it follows that

$$\left( \frac{\Delta T}{T_{op}} \right)^2 = \frac{\frac{\sigma_X^2}{T_{op}^2} \sum_{i=0}^{\infty} h_i^2 + \frac{2}{T_{op}^2} \sum_{i=0}^{\infty} h_i^2 \sum_{j=1}^{\infty} [R_{X_j} - E^2[X]]}{\left( \sum_{i=0}^{\infty} h_i \right)^2 \left( \frac{dE[X]}{dT} \right)^2} \bigg|_{T_{op}} \quad (179)$$

Doing the same with (177) and (178) it follows that

$$\left( \frac{\Delta T}{T_{op}} \right)^2 = \frac{\frac{\sigma_X^2}{n T_{op}^2} + \frac{2}{n T_{op}^2} \sum_{k=1}^{\infty} [R_{X_k} - E^2[X]]}{\left[ \frac{dE[X]}{dT} \right]^2} \bigg|_{T_{op}} \quad (180)$$



Now if a comparison is made of (179) and (180) it is clear that they are equal if  $n_E$  is defined as follows

$$n_E = \frac{\left( \sum_{i=0}^{\infty} h_i \right)^2}{\sum_{i=0}^{\infty} h_i^2} \quad (181)$$

and  $n_E$  can be interpreted as an equivalent summation number. Physically it is a measure of the performance of a general digital filter in terms of the performance of a pure summer. In other words, it provides a way to replace the digital filter by a summer of  $n_E$  samples without changing the performance of the radiometer. Then for a given sampling rate and known  $n_E$  an equivalent integration time can be determined and a performance figure can be calculated using the curves of Chapter V.

For a digital total power radiometer such as those of Figures 2 or 3 using a digital filter,  $\frac{\Delta T}{T_{op}}$  would be given by

$$\frac{\Delta T}{T_{op}} = \frac{1}{(B_E n_E \Delta)^{1/2}} F \quad (182)$$

where  $F$  is the degradation factor for the equivalent radiometer using summers and  $(B_E n_E \Delta)^{-1/2}$  is the performance figure of a total power radiometer with integration time equal to  $n_E \Delta$ .



It is often convenient to express (181) in its equivalent z-transform since the transfer function of a digital filter is usually given in terms of its z-transform. It can be shown that [Ref. 15]

$$n_E = \frac{(H(z)|_{z=1})^2}{\frac{1}{2\pi j} \oint_{\Gamma} H(z)H(z^{-1})z^{-1}dz} \quad (183)$$

where the contour integration denoted by  $\Gamma$  is around a unit circle and  $H(z)$  is the transfer function of the filter.

As an example of the use of (183) a first and second order digital filter will be considered.

For a first order filter, the transfer function is given by [Ref. 13]

$$H(z) = \frac{1}{1 - rz^{-1}} \quad (184)$$

It can be easily shown that (183) becomes

$$n_E = \frac{1 + r}{1 - r} \quad (185)$$

The transfer function of a second order filter is given by

$$H(z) = \frac{1}{1 - z^{-1}\alpha - z^{-2}\lambda} \quad (186)$$

Substituting (186) into (183) and after considerable algebra, it can be shown that



$$n_E = \frac{\lambda^4 - \lambda^2(\alpha^2 + 2) - 2\lambda\alpha^2 - \alpha^2 + 1}{(1 - \alpha - \lambda)^2 (1 - \lambda^2)} \quad (187)$$

Equation (182) and (183) are very similar to the ones defining the equivalent integration time of a low pass filter of an analog total power radiometer. This is not surprising since many similarities exist between digital and analog networks even though they are not equivalent.



## IX. CONCLUSION

This work investigates the performance of radiometers using digital processing. It is assumed that the changing of the signal from an analog to digital form is performed before the final output is obtained. Two digital total power radiometers were considered in detail.

In Chapter II a figure of merit is defined in order to evaluate performance. The effects of the addition of an analog to digital converter are discussed.

In Chapter III the effects of an ideal ADC are investigated. It serves as an introduction to the problem of sampling and quantization. The results are useful since they provide a lower bound for the degradation factor as defined in Chapter II.

Chapter IV deals exclusively with the effects of a quantizer on the autocorrelation function of a zero mean Gaussian input process. The problem of a quantizer followed by a square law detector is investigated.

Chapter V combines the information of Chapters II, III and IV and treats the effects of a real ADC. Both quantization and sampling effects are investigated. For one of the radiometers under investigation, exact results are obtained. For the other a reasonably good assumption is made and an approximate solution is obtained. Other approximations are discussed and compared.



Chapter VI discusses the problem of dynamic range and linearity involved in a digital radiometer.

In Chapter VII the results obtained in the previous chapters are used to investigate other types of digital radiometers. Balanced Dicke and noise adding radiometers are considered.

Chapter VIII investigates the problem of using a general digital filter for processing of signals in a radiometer.

The major difficulty encountered throughout the work was the number of variables that enter into the problem. Therefore it was impossible to do a global analysis. However, the factors and considerations that enter into the design of digital radiometers were treated in sufficient depth so that a good understanding of the advantages, problems and limitations of digital radiometers is presented.



## APPENDIX

The following is a list of the programs used to evaluate the equations and draw the figures throughout the thesis. They are listed in the order they were used.

```
C      TRANSFER CHARACTERISTICS OF ODD LEVEL QUANTIZER
C      N=NUMBER OF STEPS
C      VAR=NORMALIZED STANDARD DEVIATION OF X
C      RHC=CORRELATION COEFFICIENT OF X
C      DEL=INTEGRATION STEP
C      XF=X(N)
C      XC=X(0)
C      IMPLICIT REAL*8(A-H,C-Z)
C      DIMENSION SYS(5001),Q(34),X(34),FUN(5001),W(18,2)
C      1,M(18,2)
C      PROBLEM PARAMETERS
C      207 READ(5,207)N
C      666 FORMAT(I2)
C      666 WRITE(6,666)N
C      200 DO 205 NN=1,8
C      200 READ(5,200)VAR
C      200 FORMAT(F4.1)
C      ALGORITHM PARAMETERS
C      DEL=.001
C      RHC=0.0
C      RQQ=0.0
C      XF=1000.
C      XO=-1000.
C      SY=-5.0
C      SS=0.0
C      S=0.0
C      B=0.0
C      STP=(2./((N-1.)))/VAR
C      PP=.3989423
C      N1=(N-1)/2
C      L=DABS(SY)/DEL
C      QUANTIZER CHARACTERISTICS
C      DO 81 I=1,N
C      Q(I)=(I-(N+1.)/2.0)*STP
C      X(I)=(I-N/2.0)*STP
C      81 CONTINUE
C      LIMITS OF INTEGRATION
C      DO 97 J=1,L
C      SYS(J)=SY
C      SY=SY+DEL
C      97 CONTINUE
C      DO 91 IR=1,N1
C      IF(IR.NE.1) GO TO 92
C      M(1,1)=1
C      K3=(X(1)+5.0)/DEL+1.
C      WQ=X(1)-SYS(K3)
C      M(1,2)=K3
```



```

      W(1,2)=WO
      GO TO 91
92  M(IR,1)=M(IR-1,2)+1
      W(IR,1)=DEL-WO
      K4=(X(IR)+5.0)/DEL+1.
      WO=X(IR)-SYS(K4)
      M(IR,2)=K4
      W(IR,2)=WO
91  CCNTINUE
C   FINAL POINT
      DO 98 I=1,N
      IF(I.NE.1) GO TO 99
      E2=XO/1.414
      E1=X(I)/1.414
      GO TO 100
99  IF(I.NE.N) GO TO 101
      E2=E1
      E1=XF/1.414
      GO TO 100
101 E2=E1
      E1=X(I)/1.414
100 R2=DERF(E1)-DERF(E2)
      RR=Q(I)**2*R2
      SS=SS+RR
98  CCNTINUE
      RATT=SS/2.0
      RAT=DSQRT(RATT)
      WRITE(6,102)RATT,RAT
102 FORMAT(2F15.9)
      SY=-5.0
      DO 30 MM=1,21
C   FORM FUNCTION PHI
      A=2.0*(1.0-RHO**2)
      AA=DSQRT(A)
      DO 2 J=1,L
      DO 1 I=1,N
      IF(I.NE.1) GO TO 5
      E2=(XO-RHO*SY)/AA
      E1=(X(I)-RHO*SY)/AA
      GO TO 25
5   IF(I.NE.N) GO TO 3
      E2=E1
      E1=(XF-RHO*SY)/AA
      GO TO 25
3   E2=E1
      E1=(X(I)-RHO*SY)/AA
25  R1=DERF(E1)-DERF(E2)
      R=Q(I)*R1
      S=S+R
1   CCNTINUE
      FUN(J)=(S/2.0)*DEXP((SY**2)/(-2.0))
      S=.0
      SY=SY+DEL
2   CCNTINUE
C   MAIN INTEGRATION
      DO 7 I1=1,N1
44  IF(I1.NE.1) GO TO 11
      M1=M(1,1)
      M2=M(1,2)
      CORR=W(1,2)*FUN(M2)
      GO TO 15
11  M1=M(I1,1)
      M2=M(I1,2)
      CORR=W(I1,1)*FUN(M1)+W(I1,2)*FUN(M2)
15  M3=M2-1
      DO 21 KO=M1,M3
      Q11=FUN(KO)+FUN(KO+1)
      B=B+Q11
21  CCNTINUE
      RQ=Q(I1)*(DEL*B+CORR)
      RQO=RQO+RQ
      B=.0

```



```

7  CONTINUE
  RQQQ=RQC*PP
  RQQQ=(1.0/RATT)*RQQQ
  WRITE(6,40)RHO,RQQQ,RQQQ
40  FORMAT(3D25.9)
  WRITE(7,204)RQQQ,RQCQ
204  FORMAT(2F8.5)
  RQC=0.0
  S=.0
  SY=-5.0
  IF(MM.EQ.20) GO TO 67
  RHO=RHO+.05
  GO TO 30
67  RHO=RHO+.03
30  CONTINUE
205  CONTINUE
  STOP
  END

```

```

C  TRANSFER CHARACTERISTICS OF EVEN LEVEL QUANTIZER
C  N=NUMBER OF STEPS
C  VAR=NORMALIZED STANDARD DEVIATION OF X
C  RHC=CORRELATION COEFFICIENT OF X
C  DEL=INTEGRATION STEP
C  XF=X(N)
C  XC=X(0)
C  IMPLICIT REAL*8(A-H,O-Z)
  DIMENSION SYS(5001),Q(34),X(34),FUN(5001),W(18,2)
1  ,M(18,2)
C  PROBLEM PARAMETERS
  N=4
  WRITE(6,666)N
666  FORMAT(' ',I2, '//')
  DO 205 NN=1,8
  READ(5,200)VAR
200  FORMAT(F4.1)
C  ALGORITHM PARAMETERS
  RHO=0.0
  DEL=0.001
  RQC=0.0
  XF=1000.
  XC=-1000.
  SY=-5.0
  SS=0.0
  S=0.0
  B=0.0
  STP=(2./(N-1.))/VAR
  PP=.3989423
  N1=N/2
  L=CABS(SY)/DEL+1
C  QUANTIZER CHARACTERISTICS
  DO 81 I=1,N
  Q(I)=(I-(N+1.)/2.0)*STP
  X(I)=(I-N/2.0)*STP
81  CONTINUE
C  LIMITS OF INTEGRATION
  DO 97 J=1,L
  SYS(J)=SY
  SY=SY+DEL
97  CONTINUE
  DO 91 IR=1,N1
  IF(IR.NE.1) GO TO 92
  M(1,1)=1
  K3=(X(1)+5.0)/DEL+1.
  WD=X(1)-SYS(K3)
  M(1,2)=K3
  W(1,2)=WC
  GO TO 91
92  M(IR,1)=M(IR-1,2)+1

```



```

W(IR,1)=DEL-WO
K4=(X(IR)+5.0)/DEL+1.
WO=X(IR)-SYS(K4)
M(IR,2)=K4
W(IR,2)=WO
C 91 CONTINUE
    FINAL POINT
    DO 98 I=1,N
    IF(I.NE.1) GO TO 99
    E2=XO/1.414
    E1=X(I)/1.414
    GO TO 100
99 IF(I.NE.N) GO TO 101
    E2=E1
    E1=XF/1.414
    GO TO 100
101 E2=E1
    E1=X(I)/1.414
100 R2=DERF(E1)-DERF(E2)
    RR=Q(I)**2*R2
    SS=SS+PR
98 CONTINUE
    RATT=SS/2.0
    RAT=DSQRT(RATT)
    WRITE(6,102) RATT,RAT
102 FORMAT(2F15.9)
    SY=-5.0
    DO 30 MM=1,21
    FORM FUNCTION PHI
    A=2.0*(1.0-RHO**2)
    AA=DSQRT(A)
    DO 2 J=1,L
    DO 1 I=1,N
    IF(I.NE.1) GO TO 5
    E2=(XO-RHO*SY)/AA
    E1=(X(I)-RHO*SY)/AA
    GO TO 25
5 IF(I.NE.N) GO TO 3
    E2=E1
    E1=(XF-RHO*SY)/AA
    GO TO 25
3 E2=E1
    E1=(X(I)-RHO*SY)/AA
25 R1=DERF(E1)-DERF(E2)
    R=Q(I)*R1
    S=S+R
1 CONTINUE
    FUN(J)=(S/2.0)*DEXP((SY**2)/(-2.0))
    S=.0
    SY=SY+DEL
2 CONTINUE
C MAIN INTEGRATION
    DO 7 I1=1,N1
44 IF(I1.NE.1) GO TO 11
    M1=M(1,1)
    M2=M(1,2)
    CORR=W(1,2)*FUN(M2)
    GO TO 15
11 M1=M(I1,1)
    M2=M(I1,2)
    CORR=W(I1,1)*FUN(M1)+W(I1,2)*FUN(M2)
15 M3=M2-1
    DO 21 KO=M1,M3
    Q11=FUN(KO)+FUN(KO+1)
    B=B+Q11
21 CONTINUE
    RQ=Q(I1)*(DEL*B+CORR)
    RQQ=RQQ+RQ
    B=.0
7 CONTINUE
    RQQQ=RQQ*PP
    RQQQ=(1.0/RATT)*RQQQ

```



```

WRITE(6,40) RHO,RQCC,RQQO
40  FORMAT(3D25.9)
WRITE(7,204) RQQO,RQQO
204  FORMAT(2F8.5)
RQQ=0.0
S=.0
SY=-5.0
IF(MM.EQ.20) GO TO 67
RHC=RHC+.05
GO TO 30
67  RHO=RHC+.03
30  CONTINUE
205 CONTINUE
STOP
END

```

```

C      TRANSFER CHARACTERISTICS OF ODD LEVEL QUANTIZER
C      FOLLOWED BY A SQUARE LAW DETECTOR
C      N=NUMBER OF STEPS
C      VAR=NORMALIZED STANDARD DEVIATION OF X
C      RHC=CORRELATION COEFFICIENT OF X
C      DEL=INTEGRATION STEP
C      XF=X(N)
C      XC=X(0)
C      IMPLICIT REAL*8(A-H,O-Z)
C      DIMENSION SYS(5001),Q(34),X(34),FUN(5001),W(18,2)
1,M(18,2)
C      PROBLEM PARAMETERS
N=17
CC 205 NN=1,2
READ(5,200)VAR
200  FORMAT(F4.1)
WRITE(6,888)VAR
888  FORMAT(' ',F4.1)
C      ALGORITHM PARAMETERS
RHC=0.0
DEL=.001
RQQ=0.0
XF=1000.
XO=-1000.
SY=-5.0
SS=0.0
S=0.0
B=0.0
STP=(2./(N-1.))/VAR
PP=.3989423
N1=(N-1)/2
L=DABS(SY)/DEL
C      QUANTIZER CHARACTERISTICS
DO 81 I=1,N
Q(I)=(I-(N+1.)/2.0)*STP
X(I)=(I-N/2.0)*STP
81  CONTINUE
C      LIMITS OF INTEGRATION
DO 97 J=1,L
SYS(J)=SY
SY=SY+DEL
97  CCNTINUE
DO 91 IR=1,N1
IF(IR.NE.1) GO TO 92
M(1,1)=1
K3=(X(1)+5.0)/DEL+1.
WO=X(1)-SYS(K3)
M(1,2)=K3
W(1,2)=WO
GO TO 91
92  M(IR,1)=M(IR-1,2)+1
W(IR,1)=DEL-WO
K4=(X(IR)+5.0)/DEL+1.

```



```

      WO=X(IR)-SYS(K4)
      M(IR,2)=K4
      W(IR,2)=WO
C 91 CONTINUE
      FINAL POINT
      DO 98 I=1,N
      IF(I.NE.1) GO TO 99
      E2=XO/1.414
      E1=X(I)/1.414
      GO TO 100
99 IF(I.NE.N) GO TO 101
      E2=E1
      E1=XF/1.414
      GO TO 100
101 E2=E1
      E1=X(I)/1.414
100 R2=DERF(E1)-DERF(E2)
      RR=Q(I)**4*R2
      SS=SS+RR
98 CCNTINUE
      RATT=SS/2.0
      RAT=DSQRT(RATT)
      WRITE(6,102)RATT,RAT
102 FORMAT(2F15.9)
      SY=-5.0
      DO 30 MM=1,21
C FORM FUNCTION LAMNA
      A=2.0*(1.0-RHO**2)
      AA=DSQRT(A)
      DO 2 J=1,L
      DO 1 I=1,N
      IF(I.NE.1) GO TO 5
      E2=(XO-RHO*SY)/AA
      E1=(X(I)-RHO*SY)/AA
      GO TO 25
5 IF(I.NE.N) GO TO 3
      E2=E1
      E1=(XF-RHO*SY)/AA
      GO TO 25
3 E2=E1
      E1=(X(I)-RHO*SY)/AA
25 R1=DERF(E1)-DERF(E2)
      R=Q(I)**2*R1
      S=S+R
1 CCNTINUE
      FUN(J)=(S/2.0)*DEXP((SY**2)/(-2.0))
      S=.0
      SY=SY+DEL
2 CCNTINUE
C MAIN INTEGRATION
      DO 7 I1=1,N1
44 IF(I1.NE.1) GO TO 11
      M1=M(1,1)
      M2=M(1,2)
      CORR=W(1,2)*FUN(M2)
      GO TO 15
11 M1=M(I1,1)
      M2=M(I1,2)
      CORR=W(I1,1)*FUN(M1)+W(I1,2)*FUN(M2)
15 M3=M2-1
      DO 21 KO=M1,M3
      Q11=FUN(KO)+FUN(KO+1)
      B=B+Q11
21 CONTINUE
      RQ=Q(I1)**2*(DEL*B+CORR)
      RQQ=RQQ+RQ
      B=.0
7 CONTINUE
      RQQQ=RQQ*PP
      RQQQ=(1.0/RATT)*RQQQ
      WRITE(6,40)RHO,RQQQ,RQQQ
40 FORMAT(3D25.9)

```



```

WRITE(7,230)RQQQ
230 FORMAT(F8.5)
RQQ=0.0
S=.0
SY=-5.0
IF(MM.EQ.20) GO TO 67
RHC=RHO+.05
GO TO 30
67 RHO=RHO+.03
30 CCNTINUE
205 CONTINUE
STOP
END

```

```

C      TRANSFER CHARACTERISTICS OF EVEN LEVEL QUANTIZER
C      FOLLOWED BY A SQUARE LAW DETECTOR
C      N=NUMBER OF STEPS
C      VAR=NORMALIZED STANDARD DEVIATION OF X
C      RHO=CORRELATION COEFFICIENT OF X
C      DEL=INTEGRATION STEP
C      XF=X(N)
C      XO=X(0)
C      IMPLICIT REAL*8(A-H,O-Z)
C      DIMENSION SYS(5001),O(34),X(34),FUN(5001),W(18,2)
C      1,M(18,2)
C      PROBLEM PARAMETERS
C      N=4
C      DO 205 NN=1,3
C      READ(5,200)VAR
200  FORMAT(F4.1)
C      WRITE(6,888)VAR
888  FORMAT(' ',F4.1)
C      ALGORITHM PARAMETERS
C      RHO=0.0
C      DEL=.001
C      RQQ=0.0
C      XF=1000.
C      XO=-1000.
C      SY=-5.0
C      SS=0.0
C      S=0.0
C      B=0.0
C      STP=(2./((N-1.)))/VAR
C      PP=.3989423
C      N1=N/2
C      L=CABS(SY)/DEL+1
C      QUANTIZER CHARACTERISTICS
C      DO 81 I=1,N
C      Q(I)=(I-(N+1.)/2.0)*STP
C      X(I)=(I-N/2.0)*STP
81  CCNTINUE
C      LIMITS OF INTEGRATION
C      DO 97 J=1,L
C      SYS(J)=SY
C      SY=SY+DEL
97  CONTINUE
C      DO 91 IR=1,N1
C      IF(IR.NE.1) GO TO 92
C      M(1,1)=1
C      K3=(X(1)+5.0)/DEL+1.
C      WO=X(1)-SYS(K3)
C      M(1,2)=K3
C      W(1,2)=WO
C      GO TO 91
92  M(IR,1)=M(IR-1,2)+1
C      W(IR,1)=DEL-WO
C      K4=(X(IR)+5.0)/DEL+1.
C      WO=X(IR)-SYS(K4)
C      M(IR,2)=K4

```



```

W(IR,2)=WO
91 CONTINUE
DO 91 IR=1,N1
IF(IR.NE.1) GO TO 92
M(1,1)=1
DO 93 K3=1,L
WO=SYS(K3)-X(1)
IF(WO.GT.0.0) GO TO 94
93 CONTINUE
94 M(1,2)=K3-1
W(1,2)=DEL-WO
GO TO 91
92 M(IR,1)=M(IR-1,2)+1
W(IR,1)=WO
DO 95 K4=1,L
WO=SYS(K4)-X(IR)
IF(WO.GT.0.0) GO TO 96
95 CONTINUE
96 M(IR,2)=K4-1
W(IR,2)=DEL-WO
91 CONTINUE
C FINAL POINT
DO 98 I=1,N
IF(I.NE.1) GO TO 99
E2=XO/1.414
E1=X(1)/1.414
GO TO 100
99 IF(I.NE.N) GO TO 101
E2=E1
E1=XF/1.414
GO TO 100
101 E2=E1
E1=X(1)/1.414
100 R2=DERF(E1)-DERF(E2)
RR=Q(1)**4*R2
SS=SS+RR
98 CONTINUE
RATT=SS/2.0
RAT=DSORT(RATT)
WRITE(6,102)RATT,RAT
102 FORMAT(2F15.9)
SY=-5.0
DO 30 MM=1,21
C FORM FUNCTION LAMNA
A=2.0*(1.0-RHO**2)
AA=DSORT(A)
DO 2 J=1,L
DO 1 I=1,N
IF(I.NE.1) GO TO 5
E2=(XO-RHO*SY)/AA
E1=(X(1)-RHO*SY)/AA
GO TO 25
5 IF(I.NE.N) GO TO 3
E2=E1
E1=(XF-RHO*SY)/AA
GO TO 25
3 E2=E1
E1=(X(1)-RHO*SY)/AA
25 R1=DERF(E1)-DERF(E2)
R=Q(1)**2*R1
S=S+R
1 CCNTINUE
FUN(J)=(S/2.0)*DEXP((SY**2)/(-2.0))
S=.0
SY=SY+DEL
2 CONTINUE
C MAIN INTEGRATION
DO 7 I1=1,N1
44 IF(I1.NE.1) GO TO 11
M1=M(1,1)
M2=M(1,2)
CORR=W(1,2)*FUN(M2)

```



```

GO TO 15
11 M1=M(I1,1)
M2=M(I1,2)
CORR=W(I1,1)*FUN(M1)+W(I1,2)*FUN(M2)
15 M3=M2-1
DO 21 KO=M1,M3
Q11=FUN(KO)+FUN(KO+1)
B=B+Q11
21 CONTINUE
RQ=Q(I1)**2*(DEL*B+CORR)
RQQ=RQQ+RQ
B=.0
7 CONTINUE
RQQQ=RQQ*PP
RQQC=(1.0/RATT)*RQQQ
WRITE(6,40)RHO,RQQC,RQQQ
40 FORMAT(3D25.9)
WRITE(7,230)RQQC
230 FORMAT(F8.5)
RQQ=0.0
S=.0
SY=-5.0
IF(MM.EQ.20) GO TO 67
RHO=RHO+.05
GO TO 30
67 RHO=RHO+.03
30 CONTINUE
205 CONTINUE
STOP
END

```

```

C      EXPECTED VALUE OF OUTPUT AND DERIVATIVE I.F. SAMPLING
C      N=NUMBER OF STEPS
C      XF=X(N)
C      XO=X(0)
IMPLICIT REAL*8(A-H,O-Z)
DIMENSION Q(34),X(34),Y(440),SIG(440),V(440),Z(440)
XF=100.0
XC=-100.
71 READ(5,71)N
FORMAT(I2)
S=.0
VARR=.02
DO 8 L=1,440
VAR=DSQRT(VARR)
STP=(2./(N-1.))/VAR
DO 1 I=1,N
X(I)=(I-N/2.)*STP
Q(I)=(I-(N+1.)/2.)*STP
IF(I.NE.1) GO TO 5
E2=XO/1.414
E1=X(I)/1.414
GO TO 6
5 IF(I.NE.N) GO TO 3
E2=E1
E1=XF/1.414
GO TO 6
3 E2=E1
E1=X(I)/1.414
6 R1=DERF(E1)-DERF(E2)
R=Q(I)**2*R1
S=S+R
1 CONTINUE
QARR=VARR*S
Y(L)=QARR
V(L)=VARR
SIG(L)=S/2.0
VARR=VARR+.01
S=0.0

```



```

8 CONTINUE
CALL DDET5(.01,Y,Z,440,IER)
WRITE(6,82)(V(L),Y(L),Z(L),SIG(L),L=1,440)
82 FORMAT(' ',4F15.9)
STOP
END

```

```

C   DEGRADATION FACTOR OF IDEAL FILTER
IMPLICIT REAL*8(A-H,O-Z)
REAL*8 ITITLE(12)/' SWETT',11*' '
REAL*4 X3,F5,F6,F7,F8,F9,F10
REAL*8 TITLE(10)/10*' '/
REAL*4 LABEL/4H /
DIMENSION Z(43),F2(43),WI(43),Y(43),DELY(43),B(21),
1 F(9,31),F5(31),F6(31),F7(31),F8(31),F9(31),F10(31),
2 AP1(31),AP2(31),AP3(31),AP4(31),AP5(31),AP6(31),
3 F12(31),F13(31),SB(21),X3(31)
DO 98 I=1,22
98 READ(5,99)WI(I)
99 FORMAT(F7.1)
DO 55 MM=1,6
READ(5,999)VAR1,VAR2,VAR3,VAR4,VAR5
999 FORMAT(5F4.1)
DO 5 M=2,6
DO 1 I=1,22
READ(5,2)F2(I)
2 FORMAT(F8.5)
1 CONTINUE
READ(5,47)AA,E,C,D
47 FORMAT(4F15.7)
A=AA-C**2
WRITE(6,48)A,E,C,D
48 FORMAT(' ',4F15.7)
Z(21)=.98
Z(22)=1.0
S=0.0
DO 3 I=1,20
Z(I)=S
S=S+.05
3 CONTINUE
FIT POLYNOMIAL
CALL LSQPL2(22,-16,Z,F2,WI,Y,DELY,B,SB,TITLE)
B(1)=0.0
WT=100.0
XX=.01
DO 35 I=1,31
N=WT/XX-1.0
RUN=0.0
DO 4 J=1,N
IF(J.GT.650) GO TO 49
T=3.1416*J*XX
X7=DSIN(T)/T
X=DABS(X7)
IF(X.LT.0.1) GO TO 3332
PUN=B(1)+B(2)*X+B(3)*X**2+B(4)*X**3+B(5)*X**4
1+B(6)*X**5+B(7)*X(6)+B(8)*X**7+B(9)*X(8)+B(10)*X**9
2+B(11)*X**10+B(12)*X**11+B(13)*X**12+B(14)*X**13
3+B(15)*X**14+B(16)*X**15+B(17)*X**16
GO TO 3333
3332 PUN=(F2(3)-F2(1))*X*10.0
3333 RUN=RUN+PUN
4 CONTINUE
49 A1=A*XX
A2=2.0*XX*E*RUN
F4=2.0*(A1+A2)/D**2
F(M,I)=DSQRT(F4)
IF(I.NE.1) GO TO 66
XX=XX+.09
GO TO 35

```



```

66 XX=XX+.1
35 CCNTINUE
5 CONTINUE
XX=.1
F(1,1)=1.0
X3(1)=0.0
C NO QUANTIZER CASE
DO 7 I=2,31
N=WT/XX-1.0
R=0.0
DO 8 J=1,N
T=3.1416*J*XX
S=(DSIN(T)/T)**2
R=R+S
8 CONTINUE
YY=XX+2.0*XX*R
F(1,I)=DSQRT(YY)
X3(I)=XX
XX=XX+.1
7 CONTINUE
WRITE(6,987)
987 FORMAT('1')
WRITE(6,31)(X3(I),F(1,I),F(2,I),F(3,I),F(4,I),F(5,I),
1 F(6,I),I=1,31)
31 FORMAT(' ',7F12.7)
WRITE(6,888)
888 FORMAT(' ',./////)
X=0.0
READ(5,88)N
88 FORMAT(I2)
WRITE(6,89)N
89 FORMAT(' ',I2)
C APPROXIMATION
DO 297 J=1,31
RR=F(1,J)**2
SS=X*(2.0/(N-1))**2/6.0
SSS=X*(1.0/360.0)*(2.0/(N-1))**4
APP=RR+SS/VAR1**2+SSS/VAR1**4
AP1(J)=DSQRT(APP)
APP=RR+SS/VAR2**2+SSS/VAR2**4
AP2(J)=DSQRT(APP)
APP=RR+SS/VAR3**2+SSS/VAR3**4
AP3(J)=DSQRT(APP)
APP=RR+SS/VAR4**2+SSS/VAR4**4
AP4(J)=DSQRT(APP)
APP=RR+SS/VAR5**2+SSS/VAR5**4
AP5(J)=DSQRT(APP)
X=X+.1
297 CONTINUE
WRITE(6,1100)(X3(J),F(1,J),AP1(J),AP2(J),AP3(J),AP4(J),
1 AP5(J),J=1,31)
1100 FORMAT(' ',7F12.7)
DO 18 K=1,31
F5(K)=F(1,K)
F6(K)=F(2,K)
F7(K)=F(3,K)
F8(K)=F(4,K)
F9(K)=F(5,K)
18 F10(K)=F(6,K)
CALL DRAW(31,X3,F5,1,0,LABEL,ITITLE,0.5,1.0,0,0,2,2,6,
16.1, LAST)
CALL DRAW(31,X3,F6,2,0,LABEL,ITITLE,0.5,1.0,0,0,2,2,6,
16.1, LAST)
CALL DRAW(31,X3,F7,2,0,LABEL,ITITLE,0.5,1.0,0,0,2,2,6,
16.1, LAST)
CALL DRAW(31,X3,F8,2,0,LABEL,ITITLE,0.5,1.0,0,0,2,2,6,
16.1, LAST)
CALL DRAW(31,X3,F9,2,0,LABEL,ITITLE,0.5,1.0,0,0,2,2,6,
16.1, LAST)
CALL DRAW(31,X3,F10,3,0,LABEL,ITITLE,0.5,1.0,0,0,2,2,6,
16.1, LAST)
55 CONTINUE

```



STOP  
END

```

C      DEGRADATION FACTOR OF SINGLE TUNED FILTER
      IMPLICIT REAL*8(A-H,O-Z)
      REAL*4 X3,F5,F6,F7,F8,F9,F10
      REAL*8 ITITLE(12)/' ' SWETT',11*' ' /
      REAL*8 TITILE(11)/10*' ' /
      REAL*4 LABEL/4H /
      DIMENSION Z(43),F2(43),WI(43),Y(43),DELY(43),B(21),
1F(9,31),F5(31),F6(31),F7(31),F8(31),F9(31),F10(31),
2AP1(31),AP2(31),AP3(31),AP4(31),AP5(31),AP6(31),
3F12(31),F13(31),SB(21),X3(31)
      DO 98 I=1,22
98 READ(5,99)WI(I)
99 FCRMAT(F7.1)
      DO 55 MM=1,6
      READ(5,999)VAR1,VAR2,VAR3,VAR4,VAR5
999 FORMAT(5F4.1)
      DO 5 M=2,6
      DO 1 I=1,22
      READ(5,2)F2(I)
      2 FORMAT(F8.5)
      1 CONTINUE
      READ(5,47)AA,E,C,D
47 FORMAT(4F15.7)
      A=AA-C**2
      WRITE(6,48)A,E,C,D
48 FORMAT(' ',4F15.7)
      Z(21)=.98
      Z(22)=1.0
      S=0.0
      DO 3 I=1,20
      Z(I)=S
      S=S+.05
      3 CONTINUE
C      FIT POLYNOMIAL
      CALL LSQPL2(22,-16,Z,F2,WI,Y,DELY,B,SB,TITLE)
      B(1)=0.0
      WT=10.0
      XX=.01
      DO 35 I=1,31
      N=WT/XX-1.0
      RUN=0.0
      DO 4 J=1,N
      IF(J.GE.200) GO TO 4
      T=3.1416*XX*J
      X=DEXP(-T)
      IF(X.LT.0.1) GO TO 3332
      PUN=B(1)+B(2)*X+B(3)*X**2+B(4)*X**3+B(5)*X**4
      1+B(6)*X**5+B(7)*X**6+B(8)*X**7+B(9)*X**8+B(10)*X**9
      2+B(11)*X**10+B(12)*X**11+B(13)*X**12+B(14)*X**13
      3+B(15)*X**14+B(16)*X**15+B(17)*X**16
      GO TO 3333
3332 PUN=(F2(3)-F2(1))*X*10.0
3333 RUN=RUN+PUN
      4 CONTINUE
      A1=A*XX*3.1416
      A2=2.0*3.1416*XX*E*RUN
      F4=2.0*(A1+A2)/D**2
      F(M,I)=DSQRT(F4)
      IF(I.NE.1) GO TO 66
      XX=XX+.09
      GO TO 35
66 XX=XX+.1
35 CONTINUE
      5 CONTINUE
      XX=.1
      F(1,1)=1.0

```



```

C      X3(1)=0.0
      NO QUANTIZER CASE
      DO 7 I=2,31
      R=3.1416*XX
      YY=R/DTANH(R)
      F(1,I)=DSQRT(YY)
      X3(I)=XX
      XX=XX+.1
7      CCNTINUE
      WRITE(6,987)
987     FORMAT('1')
      WRITE(6,31)(X3(I),F(1,I),F(2,I),F(3,I),F(4,I),F(5,I),
1      F(6,I),I=1,31)
31     FORMAT(' ',7F12.7)
      WRITE(6,888)
888     FORMAT(' ',7F12.7)
      X=0.0
      READ(5,88)N
88     FORMAT(I2)
      WRITE(6,89)N
89     FORMAT(' ',I2)
C      APPROXIMATION
      DO 297 J=1,31
      RR=F(1,J)**2
      SS=X*(2.0/(N-1))**2/6.0
      SSS=X*(1.0/360.0)*(2.0/(N-1))**4
      APP=RR+SS/VAR1**2+SSS/VAR1**4
      AP1(J)=DSQRT(APP)
      APP=RR+SS/VAR2**2+SSS/VAR2**4
      AP2(J)=DSQRT(APP)
      APP=RR+SS/VAR3**2+SSS/VAR3**4
      AP3(J)=DSQRT(APP)
      APP=RR+SS/VAR4**2+SSS/VAR4**4
      AP4(J)=DSQRT(APP)
      APP=RR+SS/VAR5**2+SSS/VAR5**4
      AP5(J)=DSQRT(APP)
      X=X+.1
297     CONTINUE
      WRITE(6,1100)(X3(J),F(1,J),AP1(J),AP2(J),AP3(J),AP4(J),
1      AP5(J),J=1,31)
1100    FORMAT(' ',7F12.7)
      DO 18 K=1,31
      F5(K)=F(1,K)
      F6(K)=F(2,K)
      F7(K)=F(3,K)
      F8(K)=F(4,K)
      F9(K)=F(5,K)
18     F10(K)=F(6,K)
      CALL DRAW(31,X3,F5,1,0,LABEL,ITITLE,0.5,1.0,0,0,2,2,8,
16.1, LAST)
      CALL DRAW(31,X3,F6,2,0,LABEL,ITITLE,0.5,1.0,0,0,2,2,6,
16.1, LAST)
      CALL DRAW(31,X3,F7,2,0,LABEL,ITITLE,0.5,1.0,0,0,2,2,6,
16.1, LAST)
      CALL DRAW(31,X3,F8,2,0,LABEL,ITITLE,0.5,1.0,0,0,2,2,6,
16.1, LAST)
      CALL DRAW(31,X3,F9,2,0,LABEL,ITITLE,0.5,1.0,0,0,2,2,6,
16.1, LAST)
      CALL DRAW(31,X3,F10,3,0,LABEL,ITITLE,0.5,1.0,0,0,2,2,6,
16.1, LAST)
55     CCNTINUE
      STOP
      END

C      DEGRADATION FACTOR OF GAUSSIAN FILTER
      IMPLICIT REAL*8(A-H,C-Z)
      REAL*4 X3,F5,F6,F7,F8,F9,F10,F11
      REAL*8 TITLE(10)/10*'/
      REAL*4 LABEL/4H /

```



```

    DIMENSION Z(43),F2(43),WI(43),Y(43),DELY(43),B(21),
1F(9,31),F5(31),F6(31),F7(31),F8(31),F9(31),F10(31),
2AP1(31),AP2(31),AP3(31),AP4(31),AP5(31),AP6(31),
3F12(31),F13(31),SB(21),X3(31),F11(31)
    DO 98 I=1,22
98 READ(5,99)WI(I)
99 FORMAT(F7.1)
    DO 55 MM=1,2
    READ(5,999)VAR1,VAR2,VAR3
999 FORMAT(3F4.1)
    DO 5 M=2,4
    DO 1 I=1,22
    READ(5,2)F2(I)
    2 FORMAT(F8.5)
    1 CONTINUE
    READ(5,47)AA,E,C,D
47 FORMAT(4F15.7)
    A=AA-C**2
    WRITE(6,48)A,E,C,D
48 FORMAT(' ',4F15.7)
    Z(21)=.98
    Z(22)=1.0
    S=0.0
    DO 3 I=1,20
    Z(I)=S
    S=S+.05
    3 CCNTINUE
C FIT POLYNOMIAL
    CALL LSQPL2(22,-16,Z,F2,WI,Y,DELY,B,SB,TITLE)
    U=2.773
    B(1)=0.0
    WT=10.0
    XX=.01
    DO 35 I=1,30
    N=WT/XX-1.0
    RUN=0.0
    DO 4 J=1,N
    IF(J.GE.100) GO TO 4
    T=((3.1416*XX*J)**2)/U
    X=DEXP(-T)
    IF(X.LT.0.1) GO TO 3332
    PUN=B(1)+B(2)*X+B(3)*X**2+B(4)*X**3+B(5)*X**4
1+B(6)*X**5+B(7)*X**6+B(8)*X**7+B(9)*X**8+B(10)*X**9
2+B(11)*X**10+B(12)*X**11+B(13)*X**12+B(14)*X**13
3+B(15)*X**14+B(16)*X**15+B(17)*X**16
    GO TO 3333
3332 PUN=(F2(3)-F2(1))*X*10.0
3333 RUN=RUN+PUN
    4 CONTINUE
    A1=A*XX*1.505
    A2=2.0*1.505*XX*E*RUN
    F4=2.0*(A1+A2)/D**2
    F(M,I)=DSQRT(F4)
    IF(I.NE.1) GO TO 66
    XX=XX+.09
    GO TO 35
66 XX=XX+.1
35 CCNTINUE
    5 CONTINUE
    XX=.1
    F(1,1)=1.0
C NO QUANTIRZER CASE
    DO 7 I=2,30
    N=WT/XX-1.0
    R=0.0
    X3(1)=0.0
    S=0.0
    DO 8 J=1,N
    T=(2.0*(3.1416*XX*J)**2)/U
    S=DEXP(-T)
    R=R+S
    8 CCNTINUE

```



```

V=1.505*XX+3.01*XX#R
F(1,1)=DSQRT(V)
X3(1)=XX
XX=XX+.1
7 CONTINUE
WRITE(6,987)
987 FORMAT('1')
WRITE(6,31)(X3(I),F(1,I),F(2,I),F(3,I),F(4,I),I=1,30)
31 FORMAT(' ',5F12.7)
WRITE(6,888)
888 FORMAT(' ',7F12.7)
X=0.0
READ(5,88)N
88 FORMAT(I2)
WRITE(6,89)N
89 FORMAT(' ',I2)
C APPROXIMATION
DO 297 J=1,30
RR=F(1,J)**2
SS=X*(2.0/(N-1))**2/6.0
SSS=X*(1.0/360.0)*(2.0/(N-1))**4
APP=RR+SS/VAR1**2+SSS/VAR1**4
AP1(J)=DSQRT(APP)
APP=RR+SS/VAR2**2+SSS/VAR2**4
AP2(J)=DSQRT(APP)
APP=RR+SS/VAR3**2+SSS/VAR3**4
AP3(J)=DSQRT(APP)
X=X+.1
297 CONTINUE
WRITE(6,31)(X3(J),F(1,J),AP1(J),AP2(J),AP3(J),J=1,30)
DO 18 K=1,30
F5(K)=F(1,K)
19 F6(K)=F(2,K)
20 F7(K)=F(3,K)
21 F8(K)=F(4,K)
F9(K)=AP1(K)
F10(K)=AP2(K)
18 F11(K)=AP3(K)
CALL DRAW(30,X3,F5,1,0,LABEL,ITITLE,0.5,0.5,0,0,2,2,6,
16.1, LAST)
CALL DRAW(30,X3,F6,2,0,LABEL,ITITLE,0.5,1.0,0,0,2,2,6,
16.1, LAST)
CALL DRAW(30,X3,F7,2,0,LABEL,ITITLE,0.5,1.0,0,0,2,2,6,
16.1, LAST)
CALL DRAW(30,X3,F8,2,0,LABEL,ITITLE,0.5,1.0,0,0,2,2,6,
16.1, LAST)
CALL DRAW(30,X3,F9,2,3,LABEL,ITITLE,0.5,1.0,0,0,2,2,6,
16.1, LAST)
CALL DRAW(30,X3,F10,2,4,LABEL,ITITLE,0.5,1.0,0,0,2,2,6,
16.1, LAST)
CALL DRAW(30,X3,F11,3,5,LABEL,ITITLE,0.5,1.0,0,0,2,2,6,
16.1, LAST)
55 CCNTINUE
STOP
END

```

```

C DEGRADATION FACTOR OF BUTTERWORTH FILTER
IMPLICIT REAL*8(A-H,O-Z)
REAL*4 X3,F5,F6,F7,F8,F9,F10
REAL*8 ITITLE(12)/' SWETT',11*' '/'
REAL*8 TITLE(10)/10*' '/'
REAL*4 LABEL/4H '/'
DIMENSION Z(43),F2(43),W1(43),Y(43),DELY(43),B(21),
1F(9,31),F5(31),F6(31),F7(31),F8(31),F9(31),F10(31),
2AP1(31),AP2(31),AP3(31),AP4(31),AP5(31),AP6(31),
3F12(31),F13(31),SB(21),X3(31)
DO 98 I=1,22
98 READ(5,99)W1(I)
99 FORMAT(F7.1)

```



```

DO 55 MM=1,6
READ(5,999)VAR1,VAR2,VAR3,VAR4,VAR5
999 FORMAT(5F4.1)
DO 5 M=2,6
DO 1 I=1,22
READ(5,2)F2(I)
2 FORMAT(F8.5)
1 CONTINUE
READ(5,47)AA,E,C,D
47 FORMAT(4F15.7)
A=AA-C**2
WRITE(6,48)A,E,C,D
48 FORMAT(' ',4F15.7)
Z(21)=.98
Z(22)=1.0
S=0.0
DO 3 I=1,20
Z(I)=S
S=S+.05
3 CONTINUE
C FIT POLYNOMIAL
CALL LSQPL2(22,-16,Z,F2,WI,Y,DELY,B,SB,TITLE)
B(1)=0.0
WT=10.0
XX=.01
DO 35 I=1,31
N=WT/XX-1.0
RUN=0.0
DO 4 J=1,N
IF(J.GT.30) GO TO 49
T=1.414*DEXP(-J*3.1416*XX/1.414)
X7=T*DCOS(J*3.1416*XX/1.414-3.1416/4.0)
X=DABS(X7)
IF(X.LT.0.1) GO TO 3332
PUN=B(1)+B(2)*X+B(3)*X**2+B(4)*X**3+B(5)*X**4
1+B(6)*X**5+B(7)*X**6+B(8)*X**7+B(9)*X**8+B(10)*X**9
2+B(11)*X**10+B(12)*X**11+B(13)*X**12+B(14)*X**13
3+B(15)*X**14+B(16)*X**15+B(17)*X**16
GO TO 3333
3332 PUN=(F2(3)-F2(1))*X*10.0
3333 RUN=RUN+PUN
4 CONTINUE
49 A1=A*XX*1.48
A2=2.0*1.48*XX*E*RUN
F4=2.0*(A1+A2)/D**2
F(M,I)=DSQRT(F4)
IF(I.NE.1) GO TO 66
XX=XX+.09
GO TO 35
66 XX=XX+.1
35 CONTINUE
5 CONTINUE
XX=.1
F(1,1)=1.0
X3(1)=0.0
U=1.414
C NO QUANTIZER CASE
DO 7 I=2,31
N=WT/XX-1.0
R=0.0
DO 8 K=1,N
O=3.1416*K*XX*U
S=DEXP(-O)*(1.0+DSIN(O))
R=R+S
8 CONTINUE
YY=1.48*XX+2.96*XX*R
F(1,I)=DSQRT(YY)
X3(I)=XX
XX=XX+.1
7 CONTINUE
WRITE(6,987)
987 FORMAT('1')

```



```

        WRITE(6,31)(X3(I),F(1,I),F(2,I),F(3,I),F(4,I),F(5,I),
1F(6,I),I=1,31)
31  FORMAT(' ',7F12.7)
        WRITE(6,888)
888  FORMAT(' ',7F12.7)
        X=0.0
        READ(5,88)N
        FORMAT(I2)
        WRITE(6,89)N
89  FORMAT(' ',I2)
C  APPROXIMATION
        DO 297 J=1,31
        RR=F(1,J)**2
        SS=X*(2.0/(N-1))**2/6.0
        SSS=X*(1.0/360.0)*(2.0/(N-1))**4
        APP=RR+SS/VAR1**2+SSS/VAR1**4
        AP1(J)=DSQRT(APP)
        APP=RR+SS/VAR2**2+SSS/VAR2**4
        AP2(J)=DSQRT(APP)
        APP=RR+SS/VAR3**2+SSS/VAR3**4
        AP3(J)=DSQRT(APP)
        APP=RR+SS/VAR4**2+SSS/VAR4**4
        AP4(J)=DSQRT(APP)
        APP=RR+SS/VAR5**2+SSS/VAR5**4
        AP5(J)=DSQRT(APP)
        X=X+.1
297  CONTINUE
        WRITE(6,1100)(X3(J),F(1,J),AP1(J),AP2(J),AP3(J),AP4(J),
1,AP5(J),J=1,31)
1100  FORMAT(' ',7F12.7)
        DO 18 K=1,31
        F5(K)=F(1,K)
        F6(K)=F(2,K)
        F7(K)=F(3,K)
        F8(K)=F(4,K)
        F9(K)=F(5,K)
        F10(K)=F(6,K)
18  CALL DRAW(31,X3,F5,1,0,LABEL,ITITLE,0.5,1.0,0,0,2,2,6,
16,1,LAST)
        CALL DRAW(31,X3,F6,2,0,LABEL,ITITLE,0.5,1.0,0,0,2,2,6,
16,1,LAST)
        CALL DRAW(31,X3,F7,2,0,LABEL,ITITLE,0.5,1.0,0,0,2,2,6,
16,1,LAST)
        CALL DRAW(31,X3,F8,2,0,LABEL,ITITLE,0.5,1.0,0,0,2,2,6,
16,1,LAST)
        CALL DRAW(31,X3,F9,2,0,LABEL,ITITLE,0.5,1.0,0,0,2,2,6,
16,1,LAST)
        CALL DRAW(31,X3,F10,3,0,LABEL,ITITLE,0.5,1.0,0,0,2,2,6,
16,1,LAST)
55  CONTINUE
        STOP
        END

```

```

C  DEGRADATION FACTOR. RC FILTERING AND SAMPLING
        IMPLICIT REAL*8(A-H,O-Z)
        REAL*8 ITITLE(12)/' SWETT',11*' '
        REAL*4 X3,F5,F6,F7,F8,F9,F10
        REAL*4 LABEL/4H /
        REAL*8 TITLE(10)/10*' '
        DIMENSION Z(43),F2(43),WI(43),Y(43),DELY(43),B(21),
1F(9,31),F5(31),F6(31),F7(31),F8(31),F9(31),F10(31),
2AP1(31),AP2(31),AP3(31),AP4(31),AP5(31),AP6(31),
3F12(31),F13(31),SB(21),X3(31)
4,FC(9,31),E(20),Q(20)
        GAUSS(E,VAR)=0.3989423*(DEXP(-(E/VAR)**2/2.))/VAR
        DO 98 I=1,22
98  READ(5,99)WI(I)
99  FORMAT(F7.1)
        DO 55 MM=1,6

```



```

      READ(5,88)N
88  FORMAT(I2)
      WRITE(6,89)N
89  FORMAT(' ',I2)
      READ(5,999)VAR1,VAR2,VAR3,VAR4,VAR5
999  FORMAT(5F4.1)
      DO 5 M=2,6
      DO 1 I=1,22
      READ(5,2)F2(I)
2  FORMAT(F8.5)
1  CONTINUE
      READ(5,47)A,VAR
47  FORMAT(2F15.7)
      STP=(2/(N-1.0))
      FF=0.0
      DER=0.0
C    CALCULATION OF DERIVATIVE OF EXPECTED VALUE
      DO 79 I=1,N
      Q(I)=(1-(N+1.0)/2.0)*STP
      E(I)=(I-N/2.0)*STP+FF
      IF(I.NE.1) GO TO 2000
      E3=E(I)
      E1=0.0
      E2=GAUSS(E3,VAR)
      GO TO 2500
2000 IF(I.NE.N) GO TO 2001
      E1=E2
      E2=0.0
      GO TO 2500
2001 E4=E(I)
      E1=E2
      E2=GAUSS(E4,VAR)
2500 PPEL=Q(I)*(E1-E2)
      79 DER=DER+PPEL
      WRITE(6,48)A,VAR,DER
48  FORMAT(' ',3F15.7)
      Z(21)=.98
      Z(22)=1.0
      S=0.0
      DO 3 I=1,20
      Z(I)=S
      S=S+.05
3  CONTINUE
C  FIT POLYNOMIAL
      CALL LSQPL2(22,-16,Z,F2,WI,Y,DELY,B,SB,TITLE)
      TRC=20.0
      XX=.01
      DO 35 I=1,31
      NN=TRC/XX-1.0
      RUN=0.0
      RRUN=0.0
      DO 4 J=1,NN
      T=XX*J
      X=DEXP(-T)
      IF(X.LT.0.1) GO TO 3332
      PUN=B(1)+B(2)*X+B(3)*X**2+B(4)*X**3+B(5)*X**4
      1+B(6)*X**5+B(7)*X**6+B(8)*X**7+B(9)*X**8+B(10)*X**9
      2+B(11)*X**10+B(12)*X**11+B(13)*X**12+B(14)*X**13
      3+B(15)*X**14+B(16)*X**15+B(17)*X**16
      GO TO 3333
3332 PUN=F2(3)*10.0*X
3333 RUN=RUN+PUN
      RRUN=RRUN+J*PUN
4  CCNTINUE
      A1=A*XX/2.0
      A2=XX*A*RUN
      A3=XX**2*A*RRUN/TRC
      F41=A1+A2-A3
      F42=A1+A2
      F(M,I)=DSQRT(F42)/DER
      FC(M,I)=DSQRT(F41)/DER
      IF(I.NE.1) GO TO 66

```



```

        XX=XX+.09
        GO TO 35
66      XX=XX+.1
35      CCNTINUE
5       CONTINUE
        XX=.1
        F(1,1)=1.0
        YYY=1.0-(1.0-DEXP(-TRC))/TRC
        FC(1,1)=DSQRT(YYY)
        X3(1)=0.0
C       NO QUANTIZER CASE
        DO 7 I=2,31
        YY=(XX/2.0)/DTANH(XX/2.0)
        Y4=(XX/2.0)/DSINH(XX/2.0)
        Y3=YY-(1.0-DEXP(-TRC))*Y4**2/TRC
        F(1,I)=DSQRT(YY)
        FC(1,I)=DSQRT(Y3)
        X3(I)=XX
        XX=XX+.1
7       CCNTINUE
987     WRITE(6,987)
        FORMAT('1')
        WRITE(6,31)(X3(I),F(1,I),F(2,I),F(3,I),F(4,I),F(5,I),
1       F(6,I),I=1,31)
        X=0.0
C       APPROXIMATION
        DO 297 J=1,31
        RR=F(1,J)**2
        SS=X*(2.0/(N-1.0))**2/24.0
        APP=RR+SS/VAR1**2
        AP1(J)=DSQRT(APP)
        APP=RR+SS/VAR2**2
        AP2(J)=DSQRT(APP)
        APP=RR+SS/VAR3**2
        AP3(J)=DSQRT(APP)
        APP=RR+SS/VAR4**2
        AP4(J)=DSQRT(APP)
        APP=RR+SS/VAR5**2
        AP5(J)=DSQRT(APP)
        X=X+.1
297     CONTINUE
        WRITE(6,888)
888     FORMAT('1,//////')
        WRITE(6,1100)(X3(J),F(1,J),AP1(J),AP2(J),AP3(J),AP4(J),
1       AP5(J),J=1,31)
1100    FORMAT('1,7F12.7')
        WRITE(6,13)
13      FORMAT('1,//////')
31      FORMAT('1,7F12.7')
        DO 18 K=1,31
        F5(K)=F(1,K)
        F6(K)=F(2,K)
        F7(K)=F(3,K)
        F8(K)=F(4,K)
        F9(K)=F(5,K)
18      F10(K)=F(6,K)
        CALL DRAW(31,X3,F6,1,0,LABEL,ITITLE,0.5,0.0,0,0,1,2,6,
16,1,1,LAST)
        CALL DRAW(31,X3,F5,2,0,LABEL,ITITLE,0.5,0.0,0,0,1,2,6,
16,1,1,LAST)
        CALL DRAW(31,X3,F7,2,0,LABEL,ITITLE,0.5,0.5,0,0,2,2,6,
16,1,1,LAST)
        CALL DRAW(31,X3,F8,2,0,LABEL,ITITLE,0.5,0.5,0,0,2,2,6,
16,1,1,LAST)
        CALL DRAW(31,X3,F9,2,0,LABEL,ITITLE,0.5,0.5,0,0,2,2,6,
16,1,1,LAST)
        CALL DRAW(31,X3,F10,3,0,LABEL,ITITLE,0.5,0.5,0,0,2,2,6,
1,6,1,1,LAST)
55      CONTINUE
        STOP
        END

```



```

C      TRANSFER CHARACTERISTICS OF QUANTIZER WITH OFFSET
C      N=NUMBER OF STEPS
C      VAR=NORMALIZED STANDARD DEVIATION OF X
C      RHO=CORRELATION COEFFICIENT OF X
C      DEL=INTEGRATION STEP
C      XF=X(N)
C      XO=X(0)
C      F=OFFSET
C      IMPLICIT REAL*8(A-H,O-Z)
C      DIMENSION Q(34),X(34),FUN(10001),W(18,2),M(18,2)
C      PROBLEM PARAMETERS
C      N=13
C      WRITE(6,666)N
666   FORMAT(' ',I2, '//')
C      VAR=0.2
C      ALGORITHM PARAMETERS
C      RHO=-0.9999
C      DEL=.001
C      F=-0.5
C      RHO=0.0
C      XF=10.0D 10
C      XO=-10.0D 10
C      SY=-5.0
C      SS=0.0
C      S=0.0
C      B=0.0
C      STP=(2./(N-1.))/VAR
C      PP=.3989423
C      L=10.0/DEL+1
C      QUANTIZER CHARACTERISTICS
C      DO 81 I=1,N
C      Q(I)=(I-(N+1.)/2.0)*STP
C      X(I)=((I-N/2.0)*STP)+F/VAR
81   CONTINUE
C      LIMITS OF INTEGRATION
C      N1=1
C      N2=N
C      N3=N-1
C      DO 911 IRR=1,N3
C      IF(X(IRR).LE.-5.0) GO TO 1000
C      IF(X(IRR).GE.+5.0) GO TO 1001
C      GO TO 911
1000  N1=IRR+1
C      GO TO 911
911   CONTINUE
C      GO TO 912
1001  N2=IRR
912   DO 91 IR=N1,N2
C      IF(IR.NE.N1) GO TO 922
C      M(IR,1)=1
C      K3=(X(IR)+5.0)/DEL+1.0
C      WO=X(IR)-(K3-1)*DEL+5.0
C      M(IR,2)=K3
C      W(IR,2)=WO
C      GO TO 91
922   IF(IR.NE.N2) GO TO 92
C      M(IR,1)=M(IR-1,2)+1
C      W(IR,1)=DEL-WO
C      M(IR,2)=L
C      GO TO 91
92    M(IR,1)=M(IR-1,2)+1
C      W(IR,1)=DEL-WO
C      K4=(X(IR)+5.0)/DEL+1
C      WO=X(IR)-(K4-1)*DEL+5.0
C      M(IR,2)=K4
C      W(IR,2)=WO
91    CONTINUE
C      FINAL POINT
C      DO 98 I=1,N
C      IF(I.NE.1) GO TO 99
C      E2=XO/1.414
C      E1=X(I)/1.414

```



```

      GO TO 100
99  IF(I.NE.N) GO TO 101
      E2=E1
      E1=XF/1.414
      GO TO 100
101  E2=E1
      E1=X(I)/1.414
100  R2=DERF(E1)-DERF(E2)
      RR=Q(I)**2*R2
      SS=SS+RR
98  CCNTINUE
      RATT=SS/2.0
      RAT=DSQRT(RATT)
      WRITE(6,102) RATT,RAT
102  FORMAT(2F15.9)
      SY=-5.0
      WRITE(6,84) N1,N2
84  FORMAT(' ',2I4)
      DO 30 MM=1,21
      FORM FUNCTION PHI
      A=2.0*(1.0-RHO**2)
      AA=DSQRT(A)
      DO 2 J=1,L
      DO 1 I=1,N
      IF(I.NE.1) GO TO 5
      E2=(XO-RHO*SY)/AA
      E1=(X(I)-RHO*SY)/AA
      GO TO 25
5  IF(I.NE.N) GO TO 3
      E2=E1
      E1=(XF-RHO*SY)/AA
      GO TO 25
3  E2=E1
      E1=(X(I)-RHO*SY)/AA
25  R1=DERF(E1)-DERF(E2)
      R=Q(I)*R1
      S=S+R
1  CONTINUE
      FUN(J)=(S/2.0)*DEXP((SY**2)/(-2.0))
      S=.0
      SY=SY+DEL
2  CCNTINUE
C  MAIN INTEGRATION
      DO 7 I1=N1,N2
      IF(I1.NE.N1) GO TO 111
      M1=M(I1,1)
      M2=M(I1,2)
      CORR=W(I1,2)*FUN(M2)
      GO TO 15
111  IF(I1.NE.N2) GO TO 11
      M1=M(I1,1)
      M2=M(I1,2)
      CORR=W(I1,1)*FUN(M1)
      GO TO 15
11  M1=M(I1,1)
      M2=M(I1,2)
      CORR=W(I1,1)*FUN(M1)+W(I1,2)*FUN(M2)
15  M3=M2-1
      DO 21 KC=M1,M3
      Q11=FUN(KO)+FUN(KO+1)
      B=B+Q11
21  CCNTINUE
      RQ=Q(I1)*(DEL*B*0.5+CORR)
      RQQ=RQQ+RQ
      B=.0
7  CONTINUE
      RQQQ=RQQ*PP
      RQQQ=(1.0/RATT)*RQQQ
      WRITE(6,40) RHO,RQQQ,RQQQ
40  FORMAT(3E25.9)
      WRITE(7,204) RQQQ,RQQQ
204  FORMAT(2F8.5)

```



```

RQQ=0.0
S=.0
SY=-5.0
IF(MM.NE.1) GO TO 67
RHO=RHO+0.0499
GO TO 30
67 RFC=RHO+0.05
30 CONTINUE
STOP
END

```

```

C   DEGRADATION FACTOR. RC FILTERING AND SAMPLING
C   OFFSET CASE
IMPLICIT REAL*8(A-H,O-Z)
REAL*4 F5,F6,F7,X3
REAL LABEL/4H /
REAL*8 ITITLE(12) / 'SWETT' , '11*' , '/'
REAL*8 TITILE(1) / '10*' , '/'
DIMENSION Z(22),F2(22),WI(22),DELY(22),B(22),SB(22)
1,FC(2,31),AP1(31),E(20),Q(20),F5(31),F6(31),F7(31),
2X3(31),F(2,31)
GAUSS(E,VAR)=0.3989423*(DEXP(-(E/VAR)**2/2.))/VAR
VAR=0.2
FF=-0.5
N=13
AA=7.2906748
G=6.24225363
A=AA-G
STP=(2/(N-1.0))
DER=0.0
C   CALCULATION OF DERIVATIVE OF EXPECTED VALUE
DO 79 I=1,N
Q(I)=(I-(N+1.0)/2.0)*STP
E(I)=(I-N/2.0)*STP+FF
IF(I.NE.1) GO TO 2000
E3=E(I)
E1=0.0
E2=GAUSS(E3,VAR)
GO TO 2500
2000 IF(I.NE.N) GO TO 2001
E1=E2
E2=0.0
GO TO 2500
2001 E4=E(I)
E1=E2
E2=GAUSS(E4,VAR)
2500 PPEL=Q(I)*(E1-E2)
79 DER=DER+PPEL
WRITE(6,2501)A,DER
2501 FORMAT(' ',2F12.7)
DO 98 I=1,21
98 READ(5,99)WI(I)
99 FORMAT(F7.1)
DO 1 I=1,21
READ(5,2)F2(I)
1 CONTINUE
2 FORMAT(F8.5)
S=0.0
DO 3 I=1,21
Z(I)=S
S=S+.05
3 CONTINUE
C   FIT POLYNOMIAL
CALL LSQPL2(21,-11,Z,F2,WI,Y,DELY,B,SB,TITLE)
TRC=20.0
B(1)=0.0
XX=.01
DO 35 I=1,31
NN=TRC/XX-1.0

```



```

RUN=0.0
RRUN=0.0
DO 4 J=1,NN
T=XX*J
X=DEXP(-T)
IF(X.LT.0.1) GO TO 3332
PUN=B(1)+B(2)*X+B(3)*X**2+B(4)*X**3+B(5)*X**4
1+B(6)*X**5+B(7)*X**6+B(8)*X**7+B(9)*X**8+B(10)*X**9
2+B(11)*X**10+B(12)*X**11
GO TO 3333
3332 PUN=(F2(3)-F2(1))*10.0*X
3333 RUN=RUN+PUN
RRUN=RRUN+J*PUN
4 CONTINUE
A1=A*XX/2.0
A2=XX*AA*RUN
A3=XX**2*AA*RRUN/TRC
F41=A1+A2-A3
F42=A1+A2
FC(2,1)=DSQRT(F41)/DER
F(2,1)=DSQRT(F42)/DER
IF(I.NE.1) GO TO 66
XX=XX+.09
GO TO 35
66 XX=XX+.1
35 CONTINUE
XX=.1
F(1,1)=1.0
YYY=1.0-(1.0-DEXP(-TRC))/TRC
FC(1,1)=DSQRT(YYY)
X3(1)=0.0
DO 7 I=2,31
YY=(XX/2.0)/DTANH(XX/2.0)
Y4=(XX/2.0)/DSINH(XX/2.0)
Y3=YY-(1.0-DEXP(-TRC))*Y4**2/TRC
F(1,I)=DSQRT(YY)
FC(1,I)=DSQRT(Y3)
X3(I)=XX
XX=XX+.1
7 CONTINUE
WRITE(6,987)
987 FORMAT('1')
WRITE(6,31)(X3(I),F(1,I),F(2,I),I=1,31)
X=0.0
DO 297 J=1,31
RR=F(1,J)**2
SS=(X*STP**2)/24.0
APP=RR+SS/VAR**2
AP1(J)=DSQRT(APP)
X=X+.1
297 CONTINUE
WRITE(6,888)
888 FORMAT(' ',/////)
WRITE(6,31)(X3(J),F(1,J),AP1(J),J=1,31)
WRITE(6,13)
13 FORMAT(' ',/////)
WRITE(6,31)(X3(I),FC(1,I),FC(2,I),I=1,31)
31 FORMAT(' ',3F12.7)
DO 67 K=1,30
F5(K)=F(1,K)
F6(K)=F(2,K)
67 F7(K)=AP1(K)
CALL DRAW(30,X3,F6,1,0,LABEL,ITITLE,0.5,0.0,0,0,1,2,6,
16,1,LAST)
CALL DRAW(30,X3,F5,2,0,LABEL,ITITLE,0.5,0.0,0,0,1,2,6,
16,1,LAST)
CALL DRAW(30,X3,F7,3,4,LABEL,ITITLE,0.5,0.0,0,0,1,2,6,
16,1,LAST)
STOP
END

```



```

C      DYNAMIC RANGE OF I.F. SAMPLING
      IMPLICIT REAL*8(A-H,O-Z)
      REAL*4 X3,F5,F6,F7,F8,F9,F10
      REAL LABEL/4H /
      REAL*8 ITITLE(12) / 'SWETT',11*,' /
      DIMENSION Q(34),X(34),Y(6,250),X3(250),F5(250),
1 F8(250),F9(250),F10(250),PER(250),F6(250),F7(250)
      X0=-10.0E 10
      XF=10.0E 10
      DO 50 JJ=1,6
      READ(5,99)N
99  FORMAT(I2)
      WRITE(6,88)N
88  FORMAT(' ',I2)
      S=.0
      VVAR=.1
      DO 8 L=1,250
      VAR=DSORT(VVAR)
      DO 1 I=1,N
      X(I)=(I-N/2.)/VAR
      Q(I)=(I-(N+1.)/2.)/VAR
      IF(I.NE.1) GO TO 5
      E2=X0/1.414
      E1=X(I)/1.414
      GO TO 6
5  IF(I.NE.N) GO TO 3
      E2=E1
      E1=XF/1.414
      GO TO 6
3  E2=E1
      E1=X(I)/1.414
6  R1=DERF(E1)-DERF(E2)
      R=Q(I)**2*R1
      S=S+R
1  CCNTINUE
      QARR=VVAR*S
      Y(JJ,L)=QARR
      X3(L)=VVAR
      PER(L)=(1.0-QARR/(2.*VVAR))*100.
      VVAR=VVAR+.1
      S=.0
8  CONTINUE
      WRITE(6,82)(X3(L),Y(JJ,L),PER(L),L=1,250,3)
82  FORMAT(' ',3F15.9)
50  CONTINUE
      DO 46 K=1,250
      F5(K)=Y(1,K)
      F6(K)=Y(2,K)
      F7(K)=Y(3,K)
      F8(K)=Y(4,K)
      F9(K)=Y(5,K)
46  F10(K)=Y(6,K)
      CALL DRAW(250,X3,F5,1,0,LABEL,ITITLE,3.0,5.0,0,0,2,2,6
1,7,1, LAST)
      CALL DRAW(250,X3,F6,2,0,LABEL,ITITLE,3.0,5.0,0,0,2,2,6
1,7,1, LAST)
      CALL DRAW(250,X3,F7,2,0,LABEL,ITITLE,3.0,5.0,0,0,2,2,6
1,7,1, LAST)
      CALL DRAW(250,X3,F8,2,0,LABEL,ITITLE,3.0,5.0,0,0,2,2,6
1,7,1, LAST)
      CALL DRAW(250,X3,F9,2,0,LABEL,ITITLE,3.0,5.0,0,0,2,2,6
1,7,1, LAST)
      CALL DRAW(250,X3,F10,3,0,LABEL,ITITLE,3.0,5.0,0,0,2,2,
16,7,1, LAST)
      STOP
      END

```



```

C      DYNAMIC RANGE OF RC FILTERING AND THEN SAMPLING
      IMPLICIT REAL*8(A-H,O-Z)
      REAL*8 ITITLE(12) / 'SWETT', 11*, ''
      REAL LABEL / 4H /
      REAL*4 X3, F5, F6, F7, F8, F9, F10
      DIMENSION Q(34), X(34), Y(7, 250), X3(250), F5(250),
1 F8(250), F9(250), F10(250), PER(250), NN(8), VAN(5)
2, F6(250), F7(250)
      SQ=5.0
      XF=10.0E 10
      XC=-10.0E 10
      READ(5,73) (VAN(I), I=1,1)
73  FORMAT(F4.1)
      READ(5,71) (NN(I), I=1,7)
71  FORMAT(7I2)
      I=1
      WRITE(6,76) VAN(I)
76  FORMAT(' ', F4.1, '//')
      VAR=VAN(I)
      DO 70 JJ=1,6
      N=NN(JJ)
      WRITE(6,72) N
72  FORMAT(' ', I2, '//')
      ALPHA=1.0
      DO 19 K=1,110
      S=0.0
      DO 20 II=1,N
      X(II)=(II-N/2.0)
      Q(II)=(II-(N+1.0)/2.0)
      IF(II.NE.1) GO TO 99
      E2=(X0+(VAR-ALPHA*VAR)*SQ)/(1.414*VAR*ALPHA)
      E1=(X(II)+(VAR-ALPHA*VAR)*SQ)/(1.414*VAR*ALPHA)
      GO TO 100
99  IF(II.NE.N) GO TO 101
      E2=E1
      E1=(XF+(VAR-ALPHA*VAR)*SQ)/(1.414*VAR*ALPHA)
      GO TO 100
101 E2=E1
      E1=(X(II)+(VAR-ALPHA*VAR)*SQ)/(1.414*VAR*ALPHA)
100 R1=DERF(E1)-DERF(E2)
      R2=Q(II)*R1
      S=S+R2
20  CONTINUE
      Y(JJ,K)=S/2.0
      X3(K)=ALPHA
      IF(K.EQ.1) GO TO 33
      PER(K)=(1.0-(Y(JJ,K)/VAR)/((ALPHA-1.0)*SQ))*100.0
      GO TO 34
33  PER(1)=0.0
34  ALPHA=ALPHA+.1
19  CONTINUE
      WRITE(6,75) (X3(L), Y(JJ,L), PER(L), L=1,110,3)
75  FORMAT(' ', 3F15.7)
70  CONTINUE
9   CONTINUE
      DO 46 K=1,110
      F5(K)=Y(1,K)
      F6(K)=Y(2,K)
      F7(K)=Y(3,K)
      F8(K)=Y(4,K)
      F9(K)=Y(5,K)
46  F10(K)=Y(6,K)
      CALL DRAW(110,X3,F5,1,0,LABEL,ITITLE,2.0,2.0,0,0,2,2,6
1,6,1, LAST)
      CALL DRAW(110,X3,F6,2,0,LABEL,ITITLE,2.0,2.5,0,0,2,2,6
1,7,1, LAST)
      CALL DRAW(110,X3,F7,2,0,LABEL,ITITLE,3.0,5.0,0,0,2,2,6
1,7,1, LAST)
      CALL DRAW(110,X3,F8,2,0,LABEL,ITITLE,3.0,5.0,0,0,2,2,6
1,7,1, LAST)
      CALL DRAW(110,X3,F9,2,0,LABEL,ITITLE,3.0,5.0,0,0,2,2,6
1,7,1, LAST)

```



```

CALL DRAW(110,X3,F10,3,0,LABEL,ITITLE,3.0,5.0,0,0,2,2,
16,7,1, LAST)
STOP
END

```

```

C      DYNAMIC RANG OF N.A.R. RADIOMETER
      IMPLICIT REAL*8(A-H,O-Z)
      REAL*4 X3,F5,F6,F7,F8,F9,F10
      REAL LABEL/4H      /
      REAL*8 ITITLE(12)/'SWETT      ',11*'      '/
      DIMENSION Q(34),X(34),X3(250),F5(250),F6(250),F7(250)
      X0=-10.0E 10
      XF=10.0E 10
      READ(5,99)N
99  FORMAT(I2)
      WRITE(6,88)N
88  FORMAT(' ',I2)
      S=.0
      VVAR=.1
      DO 8 L=1,250
      VAR=DSQRT(VVAR)
      DO 1 I=1,N
      X(I)=(I-N/2.)/VAR
      Q(I)=(I-(N+1.)/2.)/VAR
      IF(I.NE.1) GO TO 5
      E2=X0/1.414
      E1=X(I)/1.414
      GO TO 6
5  IF(I.NE.N) GO TO 3
      E2=E1
      E1=XF/1.414
      GO TO 6
3  E2=E1
      E1=X(I)/1.414
6  R1=DERF(E1)-DERF(E2)
      R=Q(I)**2*R1
      S=S+R
1  CONTINUE
      QARR=VVAR*S
      F5(L)=QARR
      X3(L)=VVAR
      VVAR=VVAR+.1
      S=.0
8  CCNTINUE
      DO 87 K=1,180
      F6(K)=F5(K+40)
87  F7(K)=F6(K)/F5(K)
      WRITE(6,82)(X3(L),F5(L),F6(L),F7(L),L=1,180,3)
82. FORMAT(' ',4F15.9)
      CALL DRAW(180,X3,F5,1,0,LABEL,ITITLE,3.0,3.0,0,0,2,2,6
1,7,1, LAST)
      CALL DRAW(180,X3,F6,2,0,LABEL,ITITLE,3.0,5.0,0,0,2,2,6
1,7,1, LAST)
      CALL DRAW(180,X3,F7,3,0,LABEL,ITITLE,3.0,5.0,0,0,2,2,6
1,7,1, LAST)
      STOP
      END

```



## LIST OF REFERENCES

1. Kraus, J.D. Radio Astronomy, p. 236-293, McGraw-Hill, 1966.
2. Zink, D., "Electronic Processing in the Vertical Temperature Profile Radiometer," National Telemetry Conference Record, p. 194-202, 1971.
3. Fryberger, D., Uretz, E.F., "Some Considerations Concerning the Measurement of the Atmospheric Temperature Field by Electromagnetic Means," IRE Transactions on Military Electronics, p. 279-295, October 1961.
4. Haroules, G., Brown, W.E., "A 60 GHz Multifrequency Radiometric Sensor for Detecting Clear Air Turbulence in the Troposphere," IEEE Transactions on Aerospace and Electronic Systems, p. 712-723, September 1969.
5. Kazel, S., "Terrain Mapping Using Sidelooking Radiometry," National Aerospace Electronic Conference Record, p. 76-83, 1971.
6. Ball, H.W., Harris, H.G., Hiatt, J., "Absolute Radiometer for the Flow Field of a Hypervelocity Projectile," IEEE Transactions on Aerospace and Electronic Systems, p. 285-296, March 1967.
7. King, D.D., "Passive Detection," Chapter 39 in Radar Handbook, M.I. Skolnik, Editor, McGraw-Hill, 1970.
8. Papoulis, A. Probability, Random Variables, and Stochastic Processes, p. 369-381, 484, McGraw-Hill, 1965.
9. Ryzhik, I.M., Gradstein, I.S., Tables of Integrals, Series and Products, p. 1, Academic Press, 1965.
10. Ohlson, J.E., "Efficiency of Radiometers using Digital Integration," Radio Science, Volume 6, Number 3, p. 341-345, March 1971.
11. Division of Engineering and Applied Physics Harvard University Report 496, Numerical Operations on Random Functions, by W.C. Kellog, April 1966.
12. Davenport, W.B., Root, W.L., An Introduction to the Theory of Random Signals and Noise, p. 80, McGraw-Hill, 1958.



13. Gold, B., Rader, C.M., Digital Processing of Signals, p. 101, 21, McGraw-Hill, 1969.
14. Batelaan, P.D., Goldstein, R.M., Stelzried, C.T., "Noise-Adding Radiometer for Use in the DSN," JPL Space Programs Summary 37-65, Volume II.
15. Ragazzini, J.R., Franklin, G.F., Sampled-Data Control Systems, p. 78, McGraw-Hill, 1958.



# INITIAL DISTRIBUTION LIST

	No. Copies
1. Library, Code 0212 Naval Postgraduate School Monterey, California 93940	2
2. Associate Professor J.E. Ohlson, Code 52 OL Department of Electrical Engineering Naval Postgraduate School Monterey, California 93940	2
3. Professor C.F. Klammer, Jr., Code 52KL Department of Electrical Engineering Naval Postgraduate School Monterey, California 93940	1
4. Defense Documentation Center Cameron Station Alexandria, Virginia 22314	2
5. Director Escuela de Operaciones Navales Correo Naval Valparaiso, Chile S.A.	1
6. LT. Jorge Swett Escuela de Operaciones Navales Correo Naval Valparaiso, Chile S.A.	4



## DOCUMENT CONTROL DATA - R &amp; D

(Security classification of title, body of abstract and indexing annotation must be entered when the overall report is classified)

## ORIGINATING ACTIVITY (Corporate author)

Naval Postgraduate School  
Monterey, California 93940

## 2a. REPORT SECURITY CLASSIFICATION

Unclassified

## 2b. GROUP

## REPORT TITLE

Performance Analysis of Digital Radiometers

## DESCRIPTIVE NOTES (Type of report and, inclusive dates)

Engineer's Thesis; March 1973

## AUTHOR(S) (First name, middle initial, last name)

Jorge Eduardo Swett

## REPORT DATE

March 1973

## 7a. TOTAL NO. OF PAGES

158

## 7b. NO. OF REFS

15

## CONTRACT OR GRANT NO.

## PROJECT NO.

## 9a. ORIGINATOR'S REPORT NUMBER(S)

## 9b. OTHER REPORT NO(S) (Any other numbers that may be assigned this report)

## DISTRIBUTION STATEMENT

Approved for public release; distribution unlimited.

## SUPPLEMENTARY NOTES

## 12. SPONSORING MILITARY ACTIVITY

Naval Postgraduate School  
Monterey, California 93940

## ABSTRACT

This work investigates the effects of digital processing in radiometers. It deals mainly with two digital versions of a total power radiometer. The first consists of RF, Mixer and IF sections followed by an analog to digital converter. All further processing is done in a digital computer. The second version consists of RF, Mixer and IF sections followed by a square law detector, RC filter and analog to digital converter. From this point on the processing is done by a digital computer. A figure of merit is defined based on the performance of an analog total power radiometer. Exact results are obtained for the figure of merit of the first digital version. For the second, an approximate solution is obtained. The effects of saturation and finite step size of the quantizer were taken into consideration for the above results. The performance of digital balanced-Dicke and noise-adding radiometers is investigated using the above results. The effects of digital filtering on the performance of a radiometer is considered.



KEY WORDS	LINK A		LINK B		LINK C	
	ROLE	WT	ROLE	WT	ROLE	WT
Radiometer						
Quantization						
Sampling						
Digital Filtering						



5 DEC 73

22399

Thesis  
S9356 Swett  
c.1

143993

Performance analysis of  
digital radiometers.

5 DEC 73

22399

Thesis

S9356 Swett

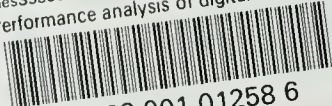
c.1

Performance analysis of  
digital radiometers.

143993

thesS9356

Performance analysis of digital radiomet



3 2768 001 01258 6

DUDLEY KNOX LIBRARY